Editorial

Robotic resection of large anterior mediastinal masses

Nelly Chow^, Nestor Villamizar^

Division of Cardiothoracic Surgery, Department of Surgery, Leonard M. Miller School of Medicine, University of Miami, Miami, FL, USA

Correspondence to: Nestor Villamizar, MD. Division of Cardiothoracic Surgery, Department of Surgery, Leonard M. Miller School of Medicine, University of Miami, 1600 NW 10th Avenue, Miami, FL 33136, USA. Email: nvillamizar@med.miami.edu.

Comment on: Alqudah O, Purmessur R, Hogan J, *et al.* Robotic resection of anterior mediastinal masses >10 cm: a case series. Mediastinum 2023;7:29.

Keywords: Robotic thymectomy; minimally invasive; thoracic oncology

Received: 16 May 2023; Accepted: 05 July 2023; Published online: 19 July 2023.

doi: 10.21037/med-23-17

View this article at: https://dx.doi.org/10.21037/med-23-17

From a surgical standpoint, the 21st century has been largely marked by the advancement of robotic surgery. Robotic surgery is more aptly described as computer-assisted operating with advantages of high definition 3-dimensional visualization, wristed instruments with seven degrees of motion tailored for precise and safe tissue handling, and improved ergonomics for the surgeon. Ashton *et al.* were the first to report successful robotic thymectomy for myasthenia gravis in a 28-year-old patient in 2003 (1). Since then, thoracic surgeons continue to apply this technology to increasingly complex thoracic surgeries. However, there has been a slower adoption for thymic malignancies due to concerns over tumor manipulation, capsular disruption, and incomplete resection (2).

Surgical treatment with complete resection is the standard of care in the management of thymic tumors. It is widely accepted that a complete R0 resection is the most important long-term prognostic factor for thymoma (3). Thymectomy via sternotomy was considered the predominant approach given the thymus' anatomic location in the anterior mediastinum. In 2015, the European Society of Medical Oncology (ESMO) published practice guidelines that recognized minimally invasive techniques as an option for presumed Masaoka-Koga stage I/II tumors "*in the hands of appropriately trained surgeons*" (4). In particular, the authors stated that "*robotic resection seems to provide a better visualization of the tumor when compared to VATS* (*video-assisted thoracoscopic surgery*)". For early stage thymic tumors, video-assisted and robotic-assisted thoracoscopic surgery seem to be oncologically equivalent to open trans-sternal surgery and even superior with regards to postoperative length of stay, complication rate, and reduced pain (4).

Historically, anterior mediastinal tumors >5 cm were considered inappropriate for minimally invasive surgery due to possible risk of incomplete resection or capsular disruption (5). However, a number of case series have demonstrated that tumor size should not be prohibitive to the benefits of minimally invasive surgery (2). Our case report, titled "*A 9 cm robotic thymectomy and pericardial repair case report*", demonstrates a successful *en bloc* resection of a large thymoma involving the right upper lobe lung and pericardium using the robotics platform. Our case highlights the feasibility of minimally invasive techniques even with large thymomas invading adjacent structures. Our patient was subsequently discharged home on postoperative day 3 with minimal pain and narcotic requirement due to our enhanced recovery protocol (6).

"*Robotic resection of anterior mediastinal masses >10 cm: a case series*" by Alqudah *et al.* challenges the conventional size limit of 5 cm tumors by demonstrating that thymomas >10 cm could achieve a R0 resection with robotic assistance (7). Case series have demonstrated that in expert hands, the robotic approach is not only safe, but also the oncologic equivalent to open surgery for large mediastinal

^ ORCID: Nelly Chow, 0000-0002-5591-0250; Nestor Villamizar, 0000-0002-5851-5109.

tumors. It should be strongly emphasized that the type of approach should not compromise achieving a R0 resection. Inexperienced surgeons should not attempt a complex thymectomy robotically if there is risk of capsule disruption or performing an incomplete resection. The International Thymic Malignancy Interest Group (ITMIG) established a set of principles for minimally invasive thymectomy to avoid compromising oncologic outcomes (8). Thymomas must be always removed together with the surrounding normal thymus and fat in order to obtain adequate safety margins. A "no-touch" technique should be utilized. The perithymic and pericardial fat is used for grasping and tractioning the tumor in order to avoid rupture of the tumor capsule and the risk of pleural implantation. Ultimately, there should be no hesitation to convert to an open approach in order to perform the appropriate oncologic operation.

Acknowledgments

Funding: None.

Footnote

Provenance and Peer Review: This article was commissioned by the editorial office, *Mediastinum*. The article did not undergo external peer review.

Conflicts of Interest: Both authors have completed the ICMJE uniform disclosure form (available at https://med.amegroups.com/article/view/10.21037/med-23-17/coif). NV serves as an unpaid editorial board member of *Mediastinum* from August 2022 to July 2024. NV also reports that Ziosoft paid for his registration and traveling expenses to AATS Conference in Los Angeles in 2023. The other author has no conflicts of interest to declare.

Ethical Statement: The authors are accountable for all aspects of the work in ensuring that questions related to the accuracy or integrity of any part of the work are appropriately investigated and resolved.

doi: 10.21037/med-23-17

Cite this article as: Chow N, Villamizar N. Robotic resection of large anterior mediastinal masses. Mediastinum 2023;7:21.

References

1. Ashton RC Jr, McGinnis KM, Connery CP, et al. Totally endoscopic robotic thymectomy for myasthenia gravis. Ann Thorac Surg 2003;75:569-71.
2. Friedant AJ, Handorf EA, Su S, et al. Minimally Invasive versus Open Thymectomy for Thymic Malignancies: Systematic Review and Meta-Analysis. J Thorac Oncol 2016;11:30-8.
3. Safieddine N, Liu G, Cuningham K, et al. Prognostic factors for cure, recurrence and long-term survival after surgical resection of thymoma. J Thorac Oncol 2014;9:1018-22.
4. Ruffini E, Filosso PL, Guerrera F, et al. Optimal surgical approach to thymic malignancies: New trends challenging old dogmas. Lung Cancer 2018;118:161-70.
5. Fiorelli A, Mazzella A, Cascone R, et al. Bilateral thoracoscopic extended thymectomy versus sternotomy. Asian Cardiovasc Thorac Ann 2016;24:555-61.
6. Kodia K, Nguyen DM, Villamizar NR. A 9 cm robotic thymectomy and pericardial repair case report. Mediastinum 2020;4:38.
7. Alqudah O, Purmessur R, Hogan J, et al. Robotic resection of anterior mediastinal masses >10 cm: a case series. Mediastinum 2023;7:29.
8. Toker A, Sonett J, Zielinski M, et al. Standard terms, definitions, and policies for minimally invasive resection of thymoma. J Thorac Oncol 2011;6:S1739-42.

Editorial

Redefining dogma and repealing of false rules—finding the true limits of medicine and surgery

Paul L. Linsky^

Division of Cardiothoracic Surgery, Department of Surgery, Medical College of Wisconsin, Milwaukee, WI, USA

Correspondence to: Paul L. Linsky, MD. Division of Cardiothoracic Surgery, Department of Surgery, HUB 5th Floor, 8701 Watertown Plank Rd., Milwaukee, WI 53226, USA. Email: plinsky@mcw.edu.

Comment on: Alqudah O, Purmessur R, Hogan J, *et al.* Robotic resection of anterior mediastinal masses >10 cm: a case series. Mediastinum 2023;7:29.

Keywords: Mediastinum; robotic; innovation; dogma; mediastinal mass

Received: 07 July 2023; Accepted: 07 August 2023; Published online: 27 August 2023.

doi: 10.21037/med-23-27

View this article at: https://dx.doi.org/10.21037/med-23-27

The field of medicine is made of rules that have been handed down by one generation of practitioners to the next. In its infancy, medicine was an apprenticeship where individual experience was passed on with little or no scientific understanding. As medicine matured, the scientific method and evidence-based medicine became paramount and essential in progressing care and bringing more reproducible results to patients and practitioners alike. The lessons learned became tenets that guided the practice of physicians into the current era. This code of order is often created by members in our specialties who are doing research that define the standard of care for the conditions we encounter. As those who have chosen to enter the field, physicians are taught these tenets and, for the most part, are expected to follow them.

However, at its core, medicine's primary aim is to bend the laws of nature. Medicine takes the principles and power of the natural order to fight against it. Surgery is the zenith of that precept. That fight produces the advancements that have propelled medicine and surgery to what we now have in the 21st century. In all disciplines of medicine, especially surgery, those who have balked the current beliefs to advance the science are elevated as leaders and heroes. Every year brings new advancements in scientific understanding, technology, and, consequently, medical care. It will always be a body in motion trying to solve the next problem or overcome the next hurdle. From time to time, the hurdle is an incorrect rule or false dogma.

The idea of only using minimally invasive techniques to resect mediastinal lesions less than 5 cm has been echoed by many but is not based on any real data (1). In Dr. Alqudah and his colleagues' work, they yet again show us that subjective rules toward the acceptable use of robotics in large mediastinal masses is simply that—subjective (2). Considered originally to be a contraindication, the successful robotic resection of these 10 cm or larger anterior mediastinal masses described in this case series gives further evidence that the original perception of only using minimally invasive techniques for masses 5 cm or less is clearly a doctrine that must be changed and discarded. As cited in their paper, others have found similar results. Burt *et al.*, in using the database of the International Thymic Malignancy Interest Group, looked for determinants of complete resection comparing minimally invasive and open thymectomy (3). They found that size was not a risk factor for positive margins in minimally invasive thymectomy. Using the National Cancer Database, comparing open to minimally invasive thymectomy for stage I to III thymoma, Yang *et al.*, also showed no difference in margins with size, but the data did show an increased use in smaller tumors, as one would expect (1).

The answer of what size one can use a robotic approach

^ ORCID: 0000-0002-3577-8686.

will likely never be answered with a true randomized trial. However, through periodic reviews of large databases, we will see an increase in the usage of robotics for the removal of larger masses everywhere, but especially in the mediastinum. Few would argue the benefits of minimally invasive approaches for these patients. The clear advantage of improved visualization and the instruments in robotics will continue to push the minimally invasive surgical treatments to more and more indications. We have seen this with lung resections, as groups are performing double sleeves all robotically (4,5). Rules regarding the size of masses will clearly be the first to go.

In the end, the decision to operate will not be defined by size. With the continued advancement of technology and the push for individualized care, numbers will no longer be absolute. Over time, most of the other contraindications will become relative and may disappear altogether. The limit will be what surgeons can do and what the patient can handle. Every patient will be viewed with a fresh set of eyes, looking only at what can be done, not being limited by the rules and dogma of past days.

Acknowledgments

Funding: None.

Footnote

Provenance and Peer Review: This article was commissioned by the editorial office, *Mediastinum*. The article did not undergo external peer review.

Conflicts of Interest: The author has completed the ICMJE uniform disclosure form (available at https://med.amegroups.com/article/view/10.21037/med-23-27/coif). The author has no conflicts of interest to declare.

Ethical Statement: The author is accountable for all aspects of the work in ensuring that questions related to the accuracy or integrity of any part of the work are appropriately investigated and resolved.

References

1. Yang CJ, Hurd J, Shah SA, et al. A national analysis of open versus minimally invasive thymectomy for stage I to III thymoma. J Thorac Cardiovasc Surg 2020;160:555-67.e15.
2. Alqudah O, Purmessur R, Hogan J, et al. Robotic resection of anterior mediastinal masses >10 cm: a case series. Mediastinum 2023;7:29.
3. Burt BM, Yao X, Shrager J, et al. Determinants of Complete Resection of Thymoma by Minimally Invasive and Open Thymectomy: Analysis of an International Registry. J Thorac Oncol 2017;12:129-36.
4. Pan X, Gu C, Yang J, et al. Robotic double-sleeve resection of lung cancer: technical aspects. Eur J Cardiothorac Surg 2018;54:183-4.
5. Qiu T, Zhao Y, Xuan Y, et al. Robotic-assisted double-sleeve lobectomy. J Thorac Dis 2017;9:E21-5.

doi: 10.21037/med-23-27
Cite this article as: Linsky PL. Redefining dogma and repealing of false rules—finding the true limits of medicine and surgery. Mediastinum 2023;7:22.

Editorial

Size should not be an absolute contraindication: the case for robotic resection of ever larger anterior mediastinal masses

Matthew M. Rochefort^

Division of Thoracic Surgery, Department of Surgery, Brigham and Women's Hospital, Boston, MA, USA

Correspondence to: Matthew M. Rochefort, MD. Division of Thoracic Surgery, Department of Surgery, Brigham and Women's Hospital, 75 Francis Street, Boston, MA 02115, USA. Email: mrochefort@bwh.harvard.edu.

Comment on: Alqudah O, Purmessur R, Hogan J, *et al.* Robotic resection of anterior mediastinal masses >10 cm: a case series. Mediastinum 2023;7:29.

Keywords: Robot; thymoma; anterior mediastinal mass

Received: 17 July 2023; Accepted: 14 August 2023; Published online: 31 August 2023.

doi: 10.21037/med-23-29

View this article at: https://dx.doi.org/10.21037/med-23-29

Anterior mediastinal masses represent a heterogenous collection of histologic pathologies, but the one most likely to involve the care of a thoracic surgeon, is that of a thymic epithelial neoplasm, either thymoma or thymic carcinoma (1). Common evaluation of thymomas for surgical resection include obtaining a high quality chest computed tomography (CT) scan, to assess for tumor size, presence and extent of involvement of adjacent structures and assessment for evidence of distant metastatic spread (2). Findings that are concerning for risk of invasion include tumor size greater than 5 cm, tumors with broad contact with the pericardium or adjacent lung, and interdigitation between or incasement of the great vessels (1).

The goal of surgical resection for a thymoma is complete removal of the thymic mass, the remainder of the thymus, which may harbor invisible trans-capsular spread, and *en-bloc* resection of all involved adjacent, non-vital structures (2). Non-vital structures include pericardium, lung, unilateral phrenic nerve, brachiocephalic vein and the superior vena cava. The additional resection of these adjacent structures is in hopes of creating a microscopically negative resection (R0) (3), as this has been found to be the main factor associated with long term survival following thymoma resection (4). Furthermore, it is imperative to minimize manipulation of the tumor itself, as disruption of the tumor capsule can result in pleural and chest wall implants, tumor recurrence, and negatively impacted overall survival (5).

Transsternal thymectomy has long been considered the gold standard for resection of the thymus as it provides excellent exposure to the anterior mediastinum, including both phrenic nerves and all of the great vessels, and provides an oncologically sound operation while minimizing the possibility of pleural drop metastasis (1,6-8). This surgical technique, however, involves the division of the long sternal bone and the inherent associated morbidities associated with wound infections and sternal wound dehiscence. Therefore, the advent of video assisted surgery, brought the possibility for minimally invasive procedures in the anterior mediastinum and avoidance of division of the sternum. These operations were associated with shorter operative times, less blood loss, and shorter hospital stays than their open counterparts (9). They were also technically challenging in the anatomically confined anterior mediastinum and were therefore limited to fairly small and early-stage thymic tumors, without involvement of the phrenic nerve or venous invasion (2,5). Enthusiasm for minimally invasive procedures was tempered by the realization of what can be done safely and with the same or better oncologic outcomes as the contemporary open operation.

The advent of the da Vinci robotic surgical platform helped to overcome some of the technical challenges of video assisted surgery. The robotic platform has benefits in

^ ORCID: 0009-0001-1046-4701.

the approach to complex surgical procedures in relatively small anatomic spaces, especially the pelvis and the mediastinum, and its adaptability to the mediastinum is demonstrated by a short learning curve (10). The three-dimensional visualization, ×10 magnification, surgeon control of the camera, 7 degrees of freedom wristed instruments, and tremor filtration all make the robotic system ideally suited to the limited space in the anterior mediastinum (11,12). The anterior mediastinum can be approach from either the right or the left chest at the discretion of the operating surgeon. The author prefers to utilize the side of predominant laterality of the tumor, and for tumors in the midline the right chest as it affords more room and maneuverability with the absence of the heart, however this does male visualization of the contralateral phenic nerve more challenging. Following resection, the specimen must be placed into an endoscopic specimen bag in order to be removed, to minimize capsule disruption within the pleural cavity and decrease the potential for pleural drop metastastasis (13). Comparisons between the open and the robotic surgical approach are often still limited to small tumors, less than 4 or 5 cm, and without involvement of the pericardium or surrounding vessels (14). In these comparisons the robotic approach resulted in fewer complications, shorter hospital stay, and faster recovery of physical and social functioning in comparison to open thymectomy (14). Additionally, in two propensity matched studies comparing robotic to open thymectomy, the robotic group had less blood loss, fewer post-operative complications, shorter hospital length of stay, and no difference in overall survival or recurrence (6,10). Size of a lesion that can be removed minimally invasively is still somewhat controversial, with some contemporary publications listing size greater than 8 cm as an absolute contraindication to attempting robotic assisted thymectomy (6).

In the recent edition of *Mediastinum*, a case series of 4 patients operated on via a robotic assisted approach for very large anterior mediastinal masses was presented (15). All four of these patients had tumors that exceeded 10 cm in at least one dimension, and all were successfully resected via a minimally invasive robotic assisted approach. They therefore concluded that size should not preclude attempt at resection of an anterior mediastinal mass via a robotic minimally invasive approach. Other factors that would affect the complexity of the operation were mentioned for consideration of a minimally invasive approach, such as pericardial, great vessel, and lung involvement.

Tumor size does not always in and of itself correlate to the complexity of a given operation, and the decision to perform a surgery minimally invasively should be made on an individual case by case basis. If the surgeon feels that a minimally invasive approach is unlikely to lead to a complete resection or that it will violate any other tenet of oncologic surgical resection, than conversion to open thymectomy should be performed. However, as the field of robotic surgery continues to evolve and individual surgeons comfort level with the technology increases, the limits of its application will continue to be stretched and larger and more complicated tumors will be resected safely and with similar long-term outcomes to open surgery.

Acknowledgments

Funding: None.

Footnote

Provenance and Peer Review: This article was commissioned by the editorial office, *Mediastinum*. The article did not undergo external peer review.

Conflicts of Interest: The author has completed the ICMJE uniform disclosure form (available at https://med.amegroups.com/article/view/10.21037/med-23-29/coif). The author has no conflicts of interest to declare.

Ethical Statement: The author is accountable for all aspects of the work in ensuring that questions related to the accuracy or integrity of any part of the work are appropriately investigated and resolved.

References

1. Limmer KK, Kernstine KH. Minimally invasive and robotic-assisted thymus resection. Thorac Surg Clin 2011;21:69-83, vii.

2. Koppitz H, Rockstroh JK, Schüller H, et al. State-of-the-art classification and multimodality treatment of malignant thymoma. Cancer Treat Rev 2012;38:540-8.
3. Friedant AJ, Handorf EA, Su S, et al. Minimally Invasive versus Open Thymectomy for Thymic Malignancies: Systematic Review and Meta-Analysis. J Thorac Oncol 2016;11:30-8.
4. Rea F, Marulli G, Girardi R, et al. Long-term survival and prognostic factors in thymic epithelial tumours. Eur J Cardiothorac Surg 2004;26:412-8.
5. Demmy TL, Krasna MJ, Detterbeck FC, et al. Multicenter VATS experience with mediastinal tumors. Ann Thorac Surg 1998;66:187-92.
6. Kang CH, Hwang Y, Lee HJ, et al. Robotic Thymectomy in Anterior Mediastinal Mass: Propensity Score Matching Study With Transsternal Thymectomy. Ann Thorac Surg 2016;102:895-901.
7. Savitt MA, Gao G, Furnary AP, et al. Application of robotic-assisted techniques to the surgical evaluation and treatment of the anterior mediastinum. Ann Thorac Surg 2005;79:450-5; discussion 455.
8. Li WW, van Boven WJ, Annema JT, et al. Management of large mediastinal masses: surgical and anesthesiological considerations. J Thorac Dis 2016;8:E175-84.
9. Hwang SK, Park SI, Kim YH, et al. Clinical results of surgical resection of mediastinal teratoma: efficacy of video-assisted thoracic surgery. Surg Endosc 2016;30:4065-8.
10. Seong YW, Kang CH, Choi JW, et al. Early clinical outcomes of robot-assisted surgery for anterior mediastinal mass: its superiority over a conventional sternotomy approach evaluated by propensity score matching. Eur J Cardiothorac Surg 2014;45:e68-73; discussion e73.
11. Chen K, Zhang X, Jin R, et al. Robot-assisted thoracoscopic surgery for mediastinal masses: a single-institution experience. J Thorac Dis 2020;12:105-13.
12. Bodner J, Wykypiel H, Greiner A, et al. Early experience with robot-assisted surgery for mediastinal masses. Ann Thorac Surg 2004;78:259-65; discussion 265-6.
13. Su KW, Luketich JD, Sarkaria IS. Robotic-assisted minimally invasive thymectomy for myasthenia gravis with thymoma. JTCVS Tech 2022;13:270-4.
14. Balduyck B, Hendriks JM, Lauwers P, et al. Quality of life after anterior mediastinal mass resection: a prospective study comparing open with robotic-assisted thoracoscopic resection. Eur J Cardiothorac Surg 2011;39:543-8.
15. Alqudah O, Purmessur R, Hogan J, et al. Robotic resection of anterior mediastinal masses >10 cm: a case series. Mediastinum 2023;7:29.

doi: 10.21037/med-23-29
Cite this article as: Rochefort MM. Size should not be an absolute contraindication: the case for robotic resection of ever larger anterior mediastinal masses. Mediastinum 2023;7:23.

Original Article

Giant middle mediastinal lesions: when tumor size correlates with mesenchymal origin—a retrospective single-center analysis

Stéphane Collaud[1,2], Theresa Stork[1,2], Hafsa Kaman[1,2], Sebastian Bauer[3], Christoph Pöttgen[4], Hans-Ulrich Schildhaus[5], Bastian Schmack[6], Clemens Aigner[1]

[1]Department of Thoracic Surgery, Ruhrlandklinik, University of Duisburg-Essen, Essen, Germany; [2]Lung Clinic, Department of Thoracic Surgery, Hospital Cologne-Merheim, University Witten Herdecke, Cologne, Germany; [3]Department of Oncology, University Hospital Essen, University of Duisburg-Essen, Essen, Germany; [4]Department of Radiation Oncology, University Hospital Essen, University of Duisburg-Essen, Essen, Germany; [5]Institute of Pathology, University Hospital Essen, University of Duisburg-Essen, Essen, Germany; [6]Department of Cardiac Surgery, University Hospital Essen, University of Duisburg-Essen, Essen, Germany

Contributions: (I) Conception and design: S Collaud, C Aigner; (II) Administrative support: All authors; (III) Provision of study materials or patients: All authors; (IV) Collection and assembly of data: S Collaud, T Stork, H Kaman; (V) Data analysis and interpretation: S Collaud, T Stork, H Kaman, C Aigner; (VI) Manuscript writing: All authors; (VII) Final approval of manuscript: All authors.

Correspondence to: Stéphane Collaud, MD. Department of Thoracic Surgery, Ruhrlandklinik, University of Duisburg-Essen, Essen, Germany; Lung Clinic, Department of Thoracic Surgery, Hospital Cologne-Merheim, University Witten Herdecke, Ostmerheimer Str. 200, 51109 Cologne, Germany. Email: CollaudS@kliniken-koeln.de.

Background: The International Thymic Malignancy Interest Group (ITMIG) proposed an internationally accepted division of the mediastinum into three compartments based on computed tomography (CT): anterior (prevascular), middle (visceral) and posterior (paravertebral) compartment. There is no generally accepted definition for the term "giant" when applied to middle mediastinal lesions. We defined the term "giant" and described our surgical experience in treating patients with giant lesions of the middle mediastinum.

Methods: CT imaging of patients operated in our center from January 2016 to August 2021 for mediastinal lesions was reviewed. Lesions were categorized to one of the ITMIG-defined compartments. Lesion size at diagnosis was measured at its largest diameter on axial CT imaging. Giant middle mediastinal lesions were defined as lesions having a size ≥90th percentile of our middle mediastinal lesion cohort. Patients with giant middle mediastinal lesions were further analyzed.

Results: Thirty-six patients (23%) had lesions located in the middle mediastinal compartment. Most common diagnoses were mediastinal cysts (n=10, 28%), metastatic lesions (n=6, 17%), lymphomas (n=5, 14%), and sarcomas (n=3, 8%). Ninetieth percentile lesion size was 73 mm. As per definition, four patients had giant middle mediastinal lesions. All these four lesions were of mesenchymal origin including oesophageal leiomyoma, synovial sarcoma, leiomyosarcoma and undifferentiated round cell sarcoma. Resection was performed through posterolateral thoracotomy or sternotomy, with or without cardiopulmonary bypass.

Conclusions: The term "giant" could be defined as a mass larger or equal to 73 mm. This definition selected specifically lesions with mesenchymal origin and may therefore guide diagnostic algorithm and patient management.

Keywords: Giant; middle mediastinum; surgery; mesenchymal tumors; sarcoma

Received: 16 October 2022; Accepted: 02 August 2023; Published online: 15 August 2023.
doi: 10.21037/med-22-49
View this article at: https://dx.doi.org/10.21037/med-22-49

Introduction

Many different classifications are available to divide the mediastinum (1,2). One of the most accepted classifications is a computed tomography (CT)-based classification, proposed by the International Thymic Malignancy Interest Group (ITMIG) in 2014 (3). This classification divides the mediastinum into three compartments: a prevascular or anterior compartment, a visceral or middle compartment and a paravertebral or posterior compartment (3). Middle or visceral compartment is limited superiorly by the thoracic inlet, inferiorly by the diaphragm, anteriorly by the anterior aspect of the pericardium and posteriorly by an imaginary vertical line located one centimeter posterior to the anterior margin of the thoracic vertebral bodies (3). The middle mediastinal compartment contains the trachea/carina, oesophagus, mediastinal lymph nodes, heart, aorta, superior vena cava, intrapericardial pulmonary arteries and thoracic duct (3). Most common abnormalities located in the middle mediastinum are lymphadenopathy, foregut duplication cysts (bronchogenic, oesophageal) and pericardial cysts. Tracheal, oesophageal and cardiac tumors as well as vascular lesions (aortic aneurysm) may also be encountered in the middle compartment (2).

There is no common definition for giant lesions in general or more specifically for giant lesions of the middle mediastinal compartment. Based on the common familiar definition, the adjective "giant" implies an extremely large size, when compared to similar persons or things. Interestingly, giant lesions may describe specific tumor entities within an organ or a compartment. Focusing on pulmonary malignant lesions, primary pulmonary sarcomas are commonly giant in size compared to primary lung cancer (4).

Here, we defined the term "giant" in the context of a large middle mediastinal lesion and explore the usefulness of such a definition. Our surgical experience in treating patients with giant lesions of the middle mediastinum was described. We present this article in accordance with the STROBE reporting checklist (available at https://med.amegroups.com/article/view/10.21037/med-22-49/rc).

Highlight box

Key findings

- All giant middle mediastinal tumors—defined as ≥73 mm on axial CT imaging—were of mesenchymal origin in our cohort.

What is known and what is new?

- The prevalence for middle mediastinal tumors is low and best management is unclear.
- The definition "giant" could capture exclusively mesenchymal tumors.

What is the implication, and what should change now?

- Our definition for giant middle mediastinal tumor had a diagnostic impact and could select all patients with tumors of mesenchymal origin.

Methods

We performed a retrospective cross-sectional study, including all consecutive patients who underwent surgery (surgical biopsy or resection) for mediastinal lesions from January 2016 to August 2021 in our center. The study was conducted in accordance with the Declaration of Helsinki (as revised in 2013). The study was approved by institutional ethics board of University Duisburg-Essen (No. 21-10261-BO) and informed patient consent was waived due to the retrospective analysis.

CT imaging was reviewed by three authors (Kaman H), including two senior surgeons (Collaud S, Stork T) to select patients with isolated lesions located to the middle mediastinal compartment as defined by the three-compartment ITMIG classification (3). Authors were blinded to clinical data as the CT were evaluated. Patients with generalized lymph nodes enlargement (e.g., sarcoidosis) or isolated lymph node enlargement in the context of lung cancer were excluded. In case of large lesions overarching other compartments, lesions were categorized in the compartment of origin, based on the "center method" and "structure displacement tool" described elsewhere (3).

Statistical analysis

Patients' clinical data were retrieved from electronic charts in our institutional database. It included, operation reports, imaging reports, and pathology report. In patients with suspected sarcoma, histology examination was routinely performed by a dedicated sarcoma pathologist. Lesion size was measured at its largest diameter on axial CT imaging at diagnosis. Distribution curve of lesion size showed a normal distribution. Giant middle mediastinal lesions were therefore defined as middle mediastinal lesions having a size equal or above the 90th percentile of our middle mediastinal lesion cohort. The 90th percentile was selected as it routinely defines upper outliers in different contexts (5-7). Patients with giant middle mediastinal lesions were further described.

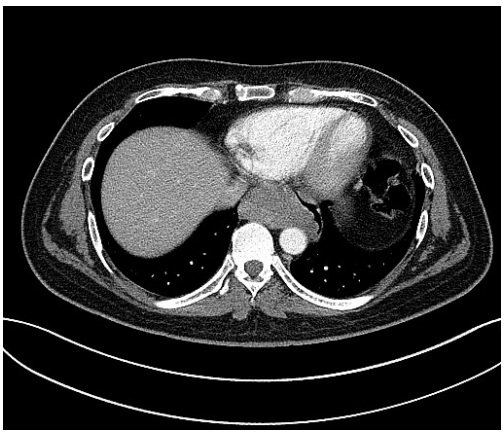

Figure 1 CT shows a 73 mm oesophageal leiomyoma. CT, computed tomography.

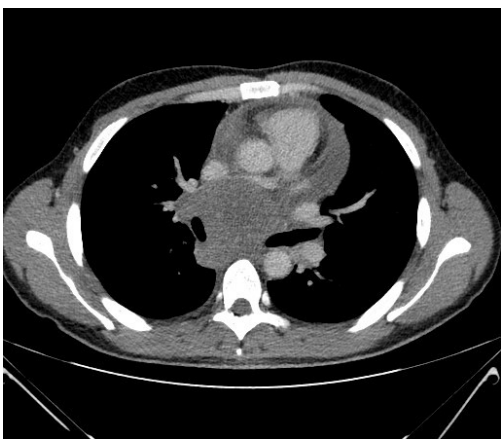

Figure 2 CT shows an 84 mm synovial sarcoma located anteriorly and inferiorly to the tracheal carina, compressing the right pulmonary artery. CT, computed tomography.

Results

One hundred and fifty-seven patients with mediastinal lesions were operated on between January 2016 and August 2021. Thirty-six patients (23%) had lesions located in the middle mediastinal compartment.

Most common diagnoses were mediastinal cysts (n=10, 28%), metastatic lesions (n=6, 17%), lymphomas (n=5, 14%), and sarcomas (n=3, 8%). Other lesions included hemangiomas (n=2, 6%), ectopic thyroids (n=2, 6%), Langerhans cell sarcoma (n=1, 3%), leiomyoma (n=1, 3%), lymphangioma (n=1, 3%), parasitic infection (n=1, 3%), ganglioneuroma (n=1, 3%), thymoma recurrence (n=1, 3%), vagus nerve schwannoma (n=1, 3%) and seminoma (n=1, 3%). Median lesion size was 53 mm (range, 10 to 120 mm). Ninetieth percentile lesion size was 73 mm. As per our definition, four patients had giant middle mediastinal lesions. Patients' treatment and outcome are described below. For patients with sarcoma, treatment decision was made on a case-by-case basis during our multidisciplinary tumorboard specialized for sarcomas.

Patient 1

Patient 1 was a 41-year-old man with a history of primary cerebral diffuse large B-cell lymphoma diagnosed 1 year earlier and treated with chemotherapy. At early follow-up CT imaging, a 73 mm tumor located in the subcarinal space was diagnosed (*Figure 1*).

It showed high fludeoxyglucose (FDG) activity on positron emission tomography-CT (PET/CT). A lymphoma recurrence was suspected and oesophgao-gastro-duodenoscopy (OGD) followed by endoscopic ultrasound (EUS) were performed. It described a tumor located at 32 cm from the incisors and originating from the submucosal plane. EUS-fine-needle aspiration (FNA) was performed but could not establish a diagnosis. A surgical biopsy via video-assisted thoracoscopic surgery (VATS) was performed. Histopathological examination revealed a leiomyoma of the oesophagus. A posterolateral thoracotomy was performed in the 7th intercostal space and the leiomyoma was freed from the oesophagus in its muscular layer. Enucleation was possible without oesophageal resection. Final histopathological examination confirmed the diagnosis of leiomyoma, measuring 82 mm. After an uneventful postoperative stay, the patient was discharged on postoperative day 7.

Patient 2

Patient 2 was a 33-year-old male who presented with coughing and a sudden decline in exercise capacity. Transthoracic and transoesophageal echocardiography revealed a large lesion of the middle mediastinum. On axial CT imaging, it measured 84 mm and was located anteriorly to the tracheal carina, compressed cephalad the right pulmonary artery and caudally the left atrium and oesophagus (*Figure 2*).

EBUS-TBNA was inconclusive and mediastinoscopy was performed in another hospital. Histopathological examination revealed a synovial sarcoma. Staging was

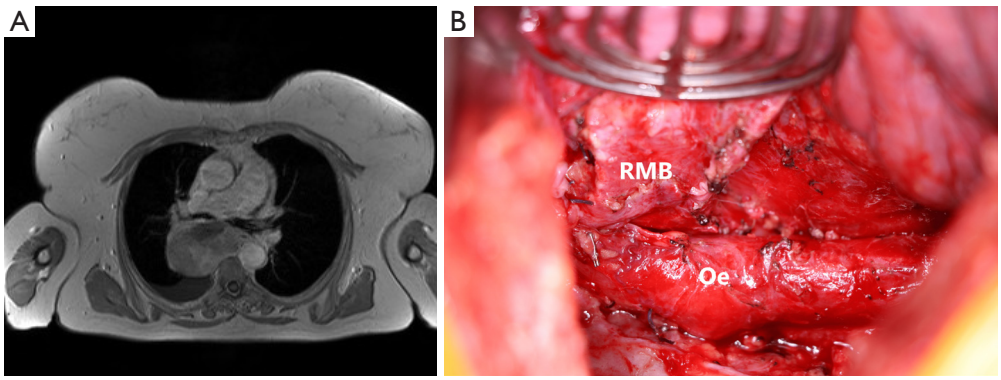

Figure 3 Preoperative imaging and intraoperative situs in a patient with leiomyosarcoma of the middle mediastinum. (A) MRI shows a 90 mm leiomyosarcoma of the middle mediastinum. (B) Intraoperative picture after leiomyosarcoma resection. The RMB and Oe were not infiltrated by the tumor. MRI, magnetic resonance imaging; RMB, right main bronchus; Oe, oesophagus.

completed with CT of the abdomen and did not reveal distant metastases. He underwent 6 cycles of chemotherapy with doxorubicin and ifosfamide. Re-staging chest/abdomen CT showed partial remission. On magnetic resonance imaging (MRI) of the chest/heart, the tumor shrunk down to 2.5 cm × 4 cm × 4 cm and there was no clear evidence of heart invasion.

Posterolateral thoracotomy was performed in the fourth intercostal space. After having freed the tumor from the lung with a lung wedge resection, tumor was sharply freed from the trachea-right main bronchus and superior vena cava. The azygos vein was sacrificed. Dissection was pursued intrapericardially. Evidence of infiltration of bilateral upper and lower veins, left atrium and right atrium at the junction with the inferior vena cava made a complete tumor resection impossible. Debulking was performed. Histopathological assessment confirmed a G2 monophasic synovial sarcoma. Patient was discharged on postoperative day 3. He underwent chemoradiation with 7 cycles of cisplatin and 70.2 Gy. One month later, mediastinal as well as pleuropulmonary progression were identified. Palliative radiotherapy was administered to the pleura (40 Gy) and the mediastinum (40 Gy) followed by maintenance chemotherapy with trofosfamide. Treatment was switched to pazopanib at new progression. The patient died 13 and 8 months after initial diagnosis and surgery, respectively.

Patient 3

Patient 3 was described elsewhere in more details (8).

Briefly, she was a 70-year-old female, who has been suffering from increasing dyspnea for the last 6 months. Axial chest CT imaging showed a 90 mm subcarinal mass with compression of the tracheal carina and oesophagus. An EBUS-TBNA was performed. Cytopathological examination was compatible with a leiomyosarcoma. OGD showed extrinsic oesophageal compression without mucosal infiltration. Staging including FDG PET/CT could exclude distant metastases and a gynaecological evaluation could exclude an extramediastinal primary. Preoperative MRI is shown in *Figure 3A*.

Upfront surgery was favoured over induction chemotherapy. A right posterolateral thoracotomy in the fifth intercostal space was performed. After opening of the mediastinal pleura, the tumor could be freed from the lung, airways, oesophagus and spine. The tumor was removed (*Figure 3B*) and radical mediastinal lymph node dissection was performed.

After an eventful hospital stay, she was discharged on postoperative day 6. Histopathological examination confirmed a completely resected conventional G2 leiomyosarcoma. All 37 mediastinal lymph nodes were free of tumor. She underwent adjuvant chemotherapy with 5 cycles of dacarbazine and doxorubicin followed by 60 Gy of radiation. Follow-up at 10 months did not show evidence of recurrence.

Patient 4

Patient 4 was a 53-year-old male presenting initially with fatigue, sore throat and fever. Later he developed chest pain, weight loss and night sweat. Chest CT revealed a 120 mm tumor on axial imaging, located posterior to the

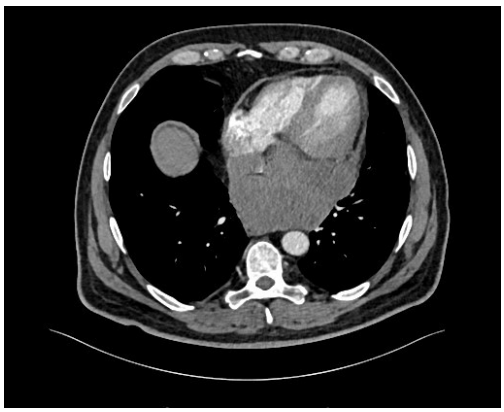

Figure 4 CT shows a 120 mm undifferentiated round cell sarcoma with compression of the inferior vena cava and left atrium. CT, computed tomography.

left atrium (*Figure 4*).

Transoesophageal echocardiography showed compression of the left atrium and ventricle, without hemodynamic relevance. Myocardium was not invaded on heart MRI. Cytopathological examination from EBUS-TBNA showed a round cell sarcoma. He underwent two cycles of doxorubicin and ifosfamide with partial response.

A median sternotomy was performed. The pericardium was opened and intrapericardial adhesions were divided. Right atrium and ventricle were free of tumor. Dissection was continued posteriorly toward the base of the heart. Left atrial invasion by the tumor was suspected. Aorto-bicaval cannulation was performed and cardiopulmonary bypass (CPB) was started. Of note, the inferior vena cava (IVC) was drained from the femoral vein. Tumor resection started at the level of the diaphragmatic pericardium and was continued anteriorly. Left ventriclular infiltration by the tumor was suspected. It was decided to divide the IVC to allow better inspection of the left ventricle. The aorta was crossclamped and cardioplegia was applied. Under full cardiopulmonary bypass the IVC was divided. This maneuver allowed confirmation of left ventricle infiltration. The tumor could be removed without damaging the left ventricle wall. The IVC was reanastomosed and the patient was weaned from CPB. The patient was discharged on postoperative day 7.

Final histopathological assessment confirmed a 4.3 cm undifferentiated round cell sarcoma. The patient underwent additional 4 cycles of doxorubicin and ifosfamide chemotherapy followed by radiation with 66 Gy. Six months postoperative and 9 months after initial diagnosis the patient is well without evidence of tumor progression.

Discussion

Mediastinal lesions are rare and most of them are located in the anterior compartment. In a study including 3,414 healthy individuals who underwent chest CT for medical check-ups, the prevalence of mediastinal tumors was 0.9%, while the prevalence for middle mediastinal tumors was 0.1% (9). Giant middle mediastinal tumors represent a small minority of middle mediastinal tumors, despite the lack of an officially recognized definition for the term "giant". We suggested a definition based on size measured as the largest lesion diameter on axial imaging from chest CT at diagnosis. "Giant" middle mediastinal lesions were lesions equal or larger than the ninetieth percentile lesion size, namely equal or larger than 73 mm. Interestingly, all four patients who had giant middle mediastinal lesions had tumors of mesenchymal origin, despite the extreme rarity of mesenchymal tumors. Indeed, mediastinal sarcomas represent less than 10% of all mediastinal tumors and account for only 1–2% of all soft tissue sarcomas (10). Our definition for "giant" lesion of the middle mediastinum added diagnostic interest since it could capture exclusively mesenchymal tumors. Despite diverging definitions for giant tumors, results from literature research were in line with our results. The case of a giant middle mediastinal schwannoma originating from the left recurrent nerve and measuring 8 cm on axial CT imaging was reported (11). Cases of angiolipoma, fibrolipoma, lipoma as well as synovial sarcoma were also described as giant primary middle mediastinal tumors (12-15). Conclusions on the relation between histologic entity and tumor size could not be drawn from larger series of primary mediastinal sarcomas due to the lack of precise data on tumor size and compartment location (16,17). The reason why all giant middle mediastinal tumors were of mesenchymal origin is unknown. The specific growth of some mesenchymal tumors, following the path of least resistance and therefore becoming symptomatic later in the disease could play a hypothetic role. In any cases, these results should be confirmed prospectively. Surgical treatment for giant middle mediastinal lesions is challenging due to their size and location. Location in close vicinity to vital structures such as heart and great vessels impose a clear frontier to resectability. Complete resection of primary mediastinal sarcoma is uncommon. In a literature review based on 22 articles including 40 patients, median tumor size was

11 cm and resection was complete in 58% (18). Complete resection was the only factor impacting survival in the univariate analysis, with 5-year survival of 63% and 0% in favour of complete resection (P=0.003). In the largest series of primary mediastinal sarcoma including 976 patients from the National Cancer Database, only 48.9% of patients underwent resection, while the most common treatment was radiation and/or chemotherapy (16). Out of surgically resected patients, microscopic complete (R0) resection was obtained only in 33.8% (16). This is very low compared to primary thoracic sarcomas of other locations (4,19). Histopathologic diagnosis is important in guiding multimodality treatment and planning surgical resection. Specific sarcoma entities are commonly treated preoperatively with induction chemotherapy such as Ewing Sarcoma (20). Preoperative imaging work-up with transoesophageal echo, cardiac MRI or CT may not always give reliable information on heart infiltration by the tumor. Knowledge of the histopathologic diagnosis could refine preoperative imaging interpretation. Specific histopathologic tumor entities behave differently regarding structure infiltration. Benign mesenchymal tumors (lipoma, leiomyoma etc.) as well as liposarcoma do not usually invade adjacent structures and middle mediastinal tumor removal is expected without resection of surrounding structures. Rarely, liposarcoma may invade adjacent structures in case of recurrence or previous surgery. On the other hand, synovial sarcoma, round cell sarcoma or Ewing Sarcomas are highly aggressive tumors that do infiltrate neighbouring structures and complete resection requires *en bloc* resection of infiltrated surrounding structures. Complete resection and survival rates were probably highly overrated in this review due to publication bias inherent to reviews based on case reports or small case series, where there is a tendency to report long-term survivors after complete tumor resections and underreport patients with suboptimal outcome (18). Common surgical approach for giant middle mediastinal lesions are posterolateral thoracotomy and sternotomy, with or without CPB. Close cooperation of thoracic and cardiac surgeons may be required in this setting. In leiomyoma of the oesophagus, tumor size and location determine the type of surgery. While enucleation is the procedure of choice for smaller leiomyomas, larger leiomyomas (8–10 cm) of the oesophagus may require oesophageal resection and reconstruction (21).

Our study suffers some limitations mainly based on its relatively small sample size and retrospective nature. A selection bias cannot be excluded since only patients who had surgery were included. Due to the rarity of middle mediastinal tumors or primary mediastinal sarcomas strong conclusion on the best management of these tumors is not possible. Second, the prevalence of sarcoma in our cohort may be overestimated due to a recruitment bias related to our sarcoma centre, recruiting patients from the whole country. Third, there was no tumor of cardiac origin in our cohort, since they would have been directly referred to the cardiac surgery department. A larger (multicenter) study also including patients who did not undergo surgery should be performed to validate our results.

Conclusions

Based on our retrospective data analyses of middle mediastinal lesions, the term “giant” could be defined as a mass larger or equal to 73 mm. This definition had a diagnostic impact since it allowed specifically the selection of tumors with mesenchymal origin. This definition may therefore guide diagnostic algorithm and patient management.

Acknowledgments

Funding: None.

Footnote

Reporting Checklist: The authors have completed the STROBE reporting checklist. Available at https://med.amegroups.com/article/view/10.21037/med-22-49/rc

Data Sharing Statement: Available at https://med.amegroups.com/article/view/10.21037/med-22-49/dss

Peer Review File: Available at https://med.amegroups.com/article/view/10.21037/med-22-49/prf

Conflicts of Interest: All authors have completed the ICMJE uniform disclosure form (available at https://med.amegroups.com/article/view/10.21037/med-22-49/coif). The authors have no conflicts of interest to declare.

Ethical Statement: The authors are accountable for all aspects of the work in ensuring that questions related to the accuracy or integrity of any part of the work are appropriately investigated and resolved. The study was conducted in accordance with the Declaration of Helsinki (as

revised in 2013). The study was approved by institutional ethics board of University Duisburg-Essen (No. 21-10261-BO) and informed patient consent was waived due to the retrospective analysis.

References

1. Fujimoto K, Hara M, Tomiyama N, et al. Proposal for a new mediastinal compartment classification of transverse plane images according to the Japanese Association for Research on the Thymus (JART) General Rules for the Study of Mediastinal Tumors. Oncol Rep 2014;31:565-72.
2. Whitten CR, Khan S, Munneke GJ, et al. A diagnostic approach to mediastinal abnormalities. Radiographics 2007;27:657-71.
3. Carter BW, Tomiyama N, Bhora FY, et al. A modern definition of mediastinal compartments. J Thorac Oncol 2014;9:S97-101.
4. Collaud S, Stork T, Schildhaus HU, et al. Multimodality treatment including surgery for primary pulmonary sarcoma: Size does matter. J Surg Oncol 2020;122:506-14.
5. Ho JC, Fang P, Cardenas CE, et al. Volumetric assessment of apparent diffusion coefficient predicts outcome following chemoradiation for cervical cancer. Radiother Oncol 2019;135:58-64.
6. Li C, Oh SJ, Kim S, et al. Risk factors of survival and surgical treatment for advanced gastric cancer with large tumor size. J Gastrointest Surg 2009;13:881-5.
7. Gamliel A, Ziv-Baran T, Siegel RM, et al. Using weight-for-age percentiles to screen for overweight and obese children and adolescents. Prev Med 2015;81:174-9.
8. Collaud S, Aigner C. A case report of a giant middle mediastinal leiomyosarcoma. Mediastinum 2022;6:38.
9. Kasuga I, Maezawa H, Gamo S, et al. Prevalence of Mediastinal Tumors Using Low-Dose Spiral Computed Tomography in Healthy Population. J Thorac Oncol 2018;13:abstr S605.
10. Suster DI, Suster S. Foreword to the Mediastinal Sarcomas Series. Mediastinum 2020;4:29.
11. Gueldich M, Hentati A, Chakroun A, et al. Giant cystic schwannoma of the middle mediastinum with cervical extension. Libyan J Med 2015;10:27409.
12. Minematsu N, Minato N, Kamohara K, et al. Complete removal of heart-compressing large mediastinal lipoma: a case report. J Cardiothorac Surg 2010;5:48.
13. Liu P, Che WC, Ji HJ, et al. A giant infiltrating angiolipoma of the mediastinum: a case report. J Cardiothorac Surg 2016;11:164.
14. Hsu JS, Kang WY, Liu GC, et al. Giant fibrolipoma in the mediastinum: an unusual case. Ann Thorac Surg 2005;80:e10-2.
15. Rea G, Francesco S, Valente T, et al. Primary mediastinal giant synovial sarcoma: A rare case report. The Egyptian Journal of Radiology & Nuclear Medicine 2014;46:9-12.
16. Engelhardt KE, DeCamp MM, Yang AD, et al. Treatment Approaches and Outcomes for Primary Mediastinal Sarcoma: Analysis of 976 Patients. Ann Thorac Surg 2018;106:333-9.
17. Paquette M, Truong PT, Hart J, et al. Primary sarcoma of the mediastinum: a report of 16 cases referred to the British Columbia Cancer Agency. J Thorac Oncol 2010;5:898-906.
18. Salah S, Salem A. Primary synovial sarcomas of the mediastinum: a systematic review and pooled analysis of the published literature. ISRN Oncol 2014;2014:412527.
19. Collaud S, Stork T, Dirksen U, et al. Surgical Treatment for Primary Chest Wall Sarcoma: A Single-Institution Study. J Surg Res 2021;260:149-54.
20. Zöllner SK, Amatruda JF, Bauer S, et al. Ewing Sarcoma-Diagnosis, Treatment, Clinical Challenges and Future Perspectives. J Clin Med 2021;10:1685.
21. Kandasamy D, Ahamed N, Kannan S, et al. Giant Leiomyoma of the Oesophagus. J Clin Diagn Res 2017;11:PD07-8.

doi: 10.21037/med-22-49

Cite this article as: Collaud S, Stork T, Kaman H, Bauer S, Pöttgen C, Schildhaus HU, Schmack B, Aigner C. Giant middle mediastinal lesions: when tumor size correlates with mesenchymal origin—a retrospective single-center analysis. Mediastinum 2023;7:24.

Review Article

Spindle cell thymoma and its histological mimickers

Annikka Weissferdt

Department of Anatomic Pathology, The University of Texas MD Anderson Cancer Center, Houston, TX, USA

Correspondence to: Annikka Weissferdt, MD, FRCPath. Department of Anatomic Pathology, The University of Texas MD Anderson Cancer Center, 1515 Holcombe Blvd., Unit 085, Houston, TX 77030, USA. Email: aweissferdt@mdanderson.org.

Abstract: Spindle cell thymomas are the most common spindle cell neoplasms of the anterior mediastinum. These tumors belong to the group of thymic epithelial neoplasms and are known for their wide histomorphologic spectrum. This histological heterogeneity is the reason why unequivocal diagnosis can be challenging, especially when dealing with small biopsy material. Conversely, less conventional patterns of the tumor may also pose significant diagnostic problems in resected material and the differential diagnosis often includes other spindle cell neoplasms that are known to arise in the mediastinal cavity. These can be of variable origin and may share overlapping pathological features with spindle cell thymoma. Since spindle cell thymomas are tumors that primarily affect the adult population and predominantly arise from the thymic gland in the anterior mediastinum, this review will focus on the differential diagnosis with other spindle cell neoplasms that share similar demographic characteristics and, for the most part, originate from the anterior mediastinal compartment. These include other epithelial spindle cell tumors of thymic origin (sarcomatoid thymic carcinoma and spindle cell carcinoid tumor), mesenchymal neoplasms [solitary fibrous tumor (SFT), synovial sarcoma, and dedifferentiated liposarcoma] and various other tumors with spindle cell morphology, that may occasionally involve the anterior mediastinum. The clinical, pathological, immunohistochemical and molecular hallmarks of these lesions will be discussed and useful tips for the differential diagnosis with spindle cell thymoma will be provided.

Keywords: Mediastinum; thymoma; spindle cell; sarcoma; thymic carcinoma; thymic carcinoid tumor

Received: 18 October 2022; Accepted: 31 March 2023; Published online: 12 April 2023.

doi: 10.21037/med-22-50

View this article at: https://dx.doi.org/10.21037/med-22-50

Introduction

Mediastinal tumors are uncommon neoplasms that can be derived from virtually any cell lineage, including tumors composed of spindle cells. The frequency of individual types of spindle cell tumors depends to a large degree on the location within the mediastinum; for instance, neurogenic tumors are most commonly found in the posterior mediastinum, while those of thymic or germ cell origin are typically restricted to the anterior mediastinum (1). In the anterior mediastinal compartment, the most common type of spindle cell neoplasm is spindle cell thymoma, a low-grade malignant epithelial tumor of the thymic gland. Spindle cell thymomas are known for their morphologic heterogeneity which can lead to difficulties in the diagnostic process, especially in small biopsy material (2). This histologic diversity is often the reason why other spindle cell tumors are considered in the differential diagnosis. In the anterior mediastinum, tumors with spindle cell morphology that can easily be mistaken with spindle cell thymoma include other epithelial-derived neoplasms, namely spindle cell carcinoid tumor and sarcomatoid thymic carcinoma as well as mesenchymal tumors, primarily solitary fibrous tumor (SFT), synovial sarcoma, and dedifferentiated liposarcoma or tumors with spindle cell morphology of various lineage that are either rare or are more commonly found in other mediastinal compartments. In this review, the differential diagnosis of spindle cell tumors of the anterior mediastinum will be discussed with emphasis on the clinical, histopathological, immunohistochemical and molecular characteristics of these rare neoplasms.

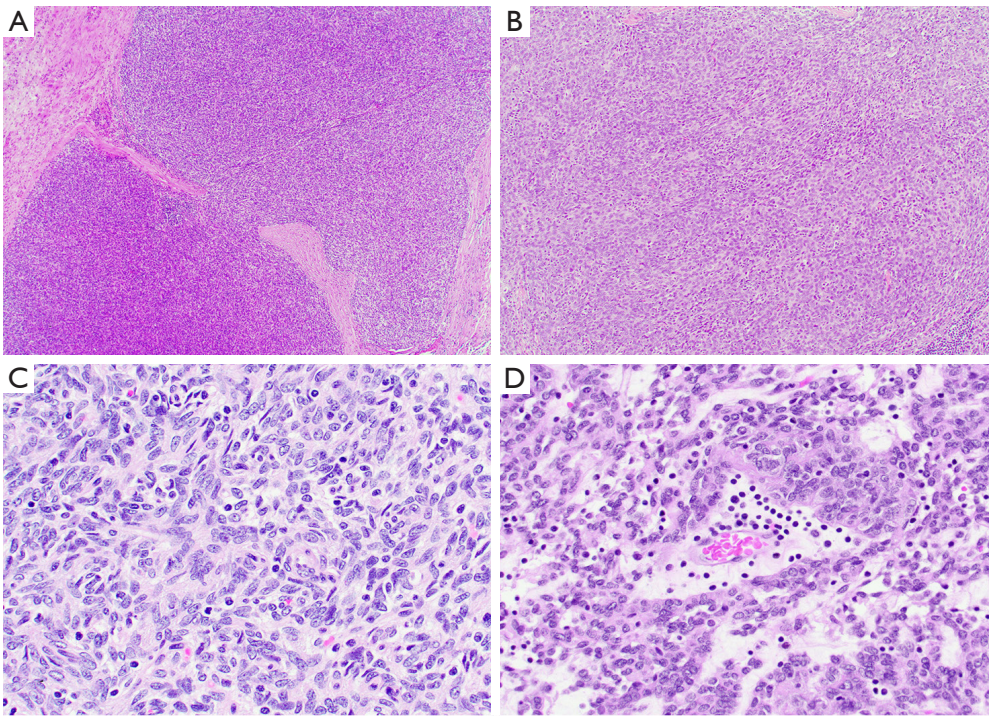

Figure 1 Spindle cell thymoma. (A) Low power view of a spindle cell thymoma showing a lobulated pattern with tumor nodules divided by thick fibrous bands (H&E, ×4); (B) the tumor cells are distributed in a sheet-like arrangement (H&E, ×10); (C) the tumor cells are spindle-shaped, have bland cytologic features and are percolated by scattered small lymphocytes (thymocytes) (H&E, ×20); (D) perivascular spaces, if present, are a good clue to the diagnosis of thymoma (H&E, ×20). H&E, hematoxylin and eosin.

Spindle cell thymoma

Spindle cell thymomas, corresponding to type A thymomas in the World Health Organization classification, are the most common spindle cell tumors of the anterior mediastinum (3). These tumors predominantly affect adult patients in the 5th to 7th decade of life and are typically detected either due to symptoms of mass effect on adjacent anatomic structures, such as chest pain or shortness of breath, or as a result of imaging studies performed for unrelated reasons. Male and female patients are affected equally (2).

Grossly, spindle cell thymomas can be encapsulated, well-circumscribed or infiltrative masses with a firm tan cut surface showing vague lobulation. Cystic changes, hemorrhagic areas and even necrosis may be identified (2). The low power microscopic appearance of the classic type of these tumors is characterized by tumor cells arranged in sheets or storiform patterns that may be divided into lobules by discrete fibrous bands (*Figure 1A,1B*). Individual tumor cells have spindle-shaped nuclei with dispersed chromatin, indistinct nucleoli, and pale eosinophilic cytoplasm. The cytologic features are bland, with no significant nuclear pleomorphism and low or absent mitotic activity. Among these tumor cells, a small number of immature lymphocytes (thymocytes) is dispersed (*Figure 1C*). Perivascular spaces, empty spaces around blood vessels containing proteinaceous fluid and scattered lymphocytes, may be identified but are less often seen than in other types of thymoma (*Figure 1D*). Hassall corpuscles are typically absent. Spindle cell thymomas are notorious for displaying a wide morphological spectrum and familiarity with the different growth patterns is essential in order to avoid misdiagnosis (*Table 1*, *Figure 2A-2H*) (2).

Rare cases of spindle cell thymoma showing mild to moderate nuclear atypia, increased mitotic activity and foci of necrosis but no anaplasia or atypical mitotic figures have recently been assigned as atypical type A thymomas (4). Their clinical significance, however, remains uncertain as they are not associated with more aggressive behavior than conventional spindle cell thymomas and tumor metastasis

Table 1 Morphologic subtypes of spindle cell thymomas

Morphologic subtype	Main histological findings
Classic spindle cell thymoma	Fascicular or storiform patterns; bland spindled/ovoid cells; scant lymphocytes
Micronodular spindle cell thymoma with lymphoid hyperplasia	Multiple tumor nodules composed of bland spindled/ovoid cells; embedded in lymphoid stroma with lymphoid follicles and germinal centers
Adenomatoid spindle cell thymoma	Short spindle-shaped tumor cells arranged in an adenomatoid/microcystic pattern; scant lymphocytes
Ancient (sclerosing) thymoma	Hypocellular spindle cell proliferation distributed in a prominent sclerotic stroma (>85%); calcification; cholesterol clefts; scant lymphocytes
Angiomatoid spindle cell thymoma	Spindle-shaped tumor cells separated by large, cavernous blood-filled spaces; scant lymphocytes
Desmoplastic spindle cell thymoma	Spindle-shaped tumor cells embedded in abundant hyalinized/fibroblastic stroma; scant lymphocytes
Spindle cell thymoma with papillary/ pseudopapillary features	Spindle-shaped tumor cells arranged in papillary/pseudopapillary patterns; scant lymphocytes
Spindle cell thymoma with neuroendocrine pattern	Spindle-shaped tumor cells arranged in organoid nests, ribbons, or rosettes; scant lymphocytes
Spindle cell thymoma with neural pattern	Spindle-shaped tumor cells arranged in whorls (meningothelial pattern) or in alternating hypo- and hypercellular areas with perivascular hyalinization (schwannoma pattern); scant lymphocytes
Spindle cell thymoma with hemangiopericytoma pattern	Spindle-shaped tumor cells with prominent staghorn-like vasculature; scant lymphocytes
Spindle cell thymoma with cystic change	Spindle-shaped tumor cells separated by large cystic/pseudocystic spaces; reactive changes (chronic inflammation, fibrosis, cholesterol clefts, granulomas, etc.)
Atypical (type A) spindle cell thymoma	Spindle-shaped tumor cells with nuclear atypia, increased mitotic activity and foci of necrosis

can occur also in cases devoid of any atypical histologic features (5,6).

The immunohistochemical phenotype of spindle cell thymomas reflects its epithelial origin and is characterized by expression of a range of cytokeratins (AE1/AE3, CAM5.2, CK5/6) as well as p63/p40 (*Figure 3A-3C*) (7). Pax8 is another marker commonly positive in the tumor cells if the polyclonal antibody is used (*Figure 3D*) (8). Recently, a characteristic *GTF2I* mutation was identified in up to 80% of these tumors (9); whilst this is an important new discovery, its use for diagnostic purposes is currently limited as the gene is not yet included in commercial or academic next generation sequencing panels.

Despite their low-grade histopathologic features, spindle cell thymomas are malignant tumors and their prognosis is mostly dependent on the extent of disease at the time of diagnosis. With multimodal therapy, including surgery, chemotherapy and radiotherapy, the 5- and 10-year overall survival rates currently lie in the range of 80–100% (*Table 2*) (3).

Spindle cell carcinoid tumor of the thymus

Spindle cell carcinoid tumors of the thymus are rare tumors of the anterior mediastinum. Like spindle cell thymomas, these tumors originate in the thymic gland and are characterized by a proliferation of monomorphic spindle cells. They are more commonly seen in male patients with a peak incidence in the 5th decade of life (10-12). Approximately 25% of these neoplasms arise in patients with multiple endocrine neoplasia (MEN)-1 syndrome; 50% are functionally active and can induce Cushing syndrome (13). While a subset of patients remains asymptomatic, the majority of patients presents with various symptoms, including chest pain, weight loss, shortness of breath or superior vena cava syndrome (10).

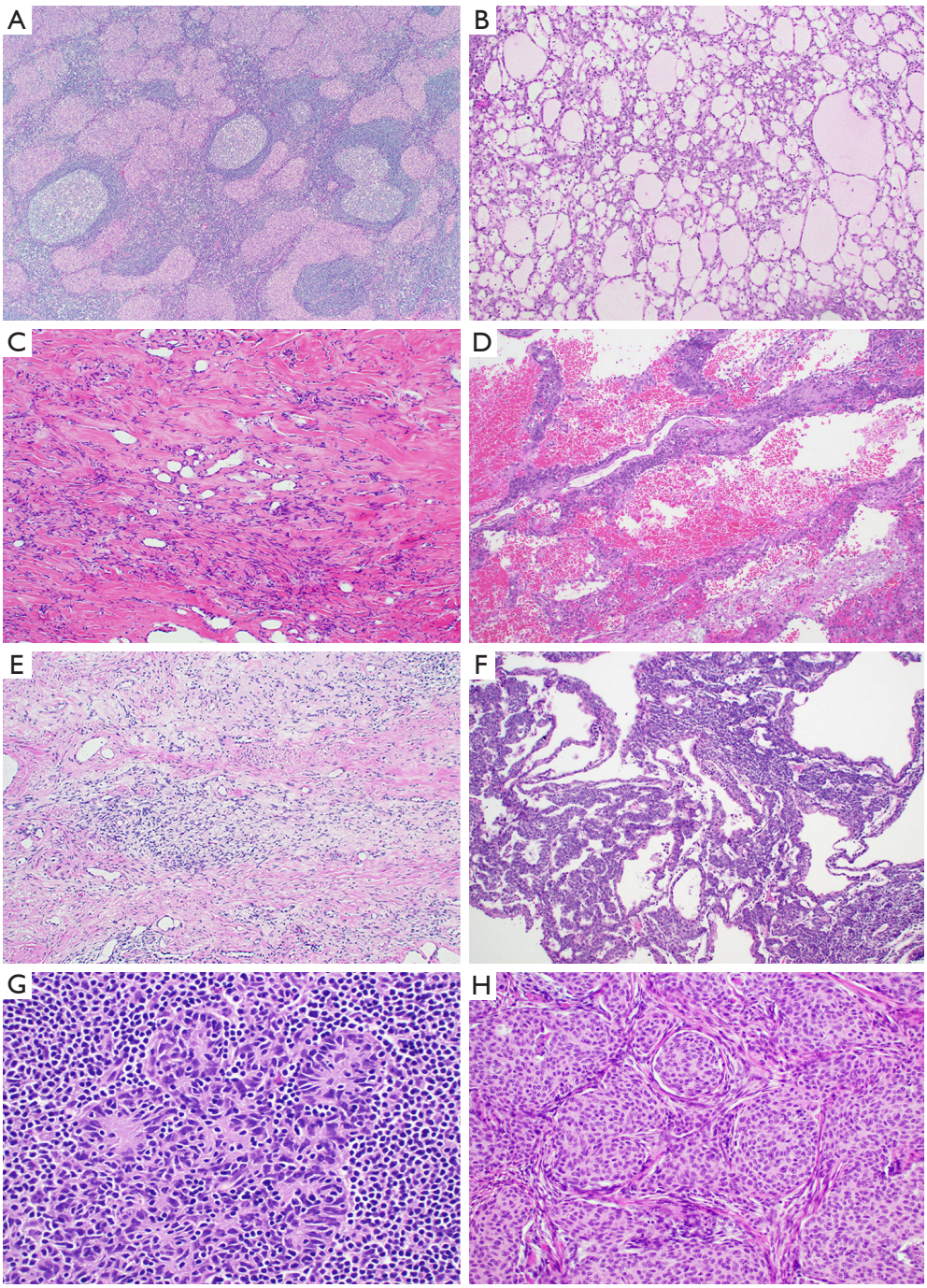

Figure 2 Different variants of spindle cell thymoma include (A) micronodular thymoma with lymphoid hyperplasia (H&E, ×4), (B) adenomatoid spindle cell thymoma (H&E, ×4), (C) ancient (sclerosing) thymoma (H&E, ×10), (D) angiomatoid spindle cell thymoma (H&E, ×10), (E) desmoplastic spindle cell thymoma (H&E, ×10), (F) spindle cell thymoma with papillary/pseudopapillary features (H&E, ×10), (G) spindle cell thymoma with neuroendocrine pattern (H&E, ×20), and (H) spindle cell thymoma with neural (meningothelial) pattern (H&E, ×20). H&E, hematoxylin and eosin.

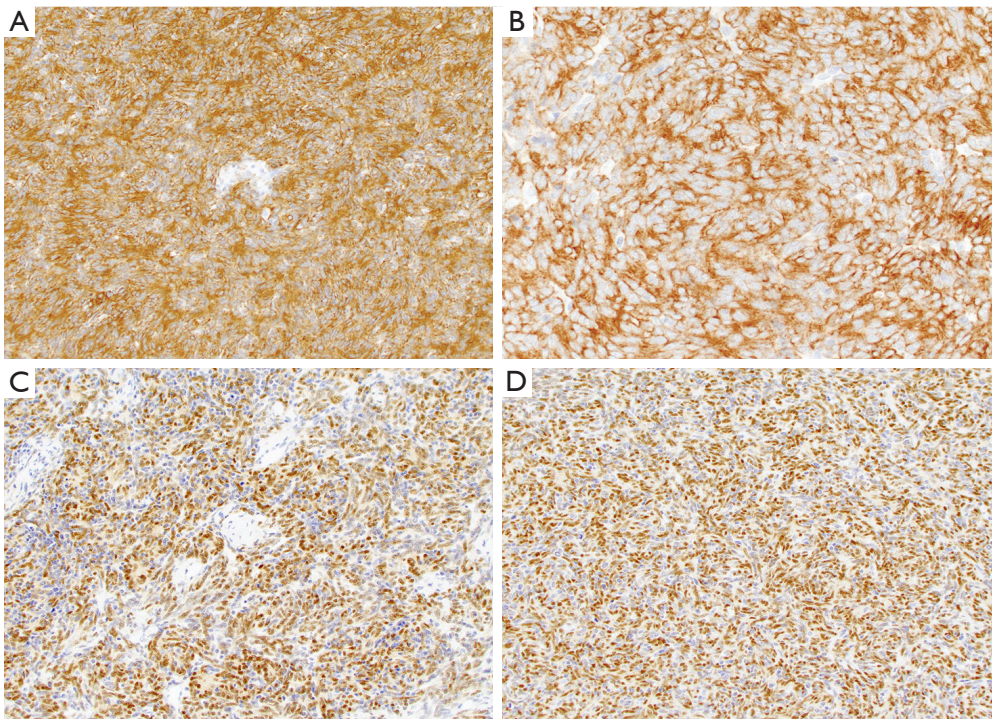

Figure 3 Immunohistochemical phenotype of spindle cell thymoma. Tumor cells with diffuse expression of (A) pancytokeratin (×4), (B) CK5/6 (×10), (C) p40 (×4), and (D) Pax8 (polyclonal) (×10).

Thymic carcinoid tumors are unencapsulated neoplasms that may be well circumscribed or widely infiltrative. The cut surface is firm, gray and homogeneous and typically lacks the characteristic lobulation seen in thymoma. Gross areas of hemorrhage and necrosis are not usually identified (10,14,15). At the microscopic level, these lesions are characterized by an organoid growth pattern consisting of nests, ribbons, cords or rosette-like structures surrounded by delicate fibrovascular septa (*Figure 4A*). The tumor cells are monomorphic, small to medium-sized cells with moderate amounts of cytoplasm, pale eosinophilic cytoplasm, fine chromatin and inconspicuous nucleoli. In contrast to classic thymic carcinoid tumors, in the spindle cell variant, tumor cells have a fusiform shape and are often arranged in a hemangiopericytic growth pattern (*Figure 4B*) (16,17). Cytologic atypia is absent or mild and the mitotic activity is low (up to 3 per 10 high power fields). Necrosis, if present, is minimal (punctuate) (10).

The immunophenotype of these tumors is characterized by reactivity for cytokeratin and various markers associated with neuroendocrine differentiation, including synaptophysin, chromogranin A and CD56 (*Figure 4C*,*4D*) (10,18). The molecular characteristics of thymic neuroendocrine neoplasms are poorly understood and no diagnostic or clinically actionable mutations have been identified (19).

Owing to its location, the prognosis for thymic carcinoid tumors is often poor due to high tumor stage at the time of diagnosis. As a result, the overall survival rate at 5 years is around 50% which is significantly worse than that for spindle cell thymoma (10,20). For this reason, separation of the two entities becomes very important. While both tumors occur in the adult population, thymic carcinoid tumors are more commonly seen in male than in female patients. In addition, these tumors not uncommonly elicit paraneoplastic syndromes. While grossly, both tumors can show similar features, at a histologic level, spindle cell carcinoids typically lack fibrous bands, perivascular spaces and the lymphoid infiltrate that is so characteristic for spindle cell thymomas. On the other hand, spindle cell thymomas may show striking neuroendocrine morphology and immunohistochemical workup becomes indispensable in this setting. By immunohistochemistry, both tumors will express pancytokeratin but while spindle cell thymoma is positive for p63/p40 and negative for neuroendocrine markers the opposite is true for spindle cell carcinoid tumor (*Table 2*).

Table 2 Comparison of spindle cell thymoma and its closest mimickers

Tumor type	Clinical	Histology	IHC	Molecular	Prognosis
Spindle cell thymoma	5th–7th decade; M = F	Heterogeneous; classic type with storiform or diffuse growth; bland spindle/oval cells; scant lymphocytes	CK$^+$, CK5/6$^+$, p63/p40$^+$, Pax8 (polyclonal)$^+$	*GTF2I* mutation	Good
Spindle cell carcinoid tumor	5th decade; M > F	Monotonous spindle cells arranged in organoid patterns	CK$^+$, synaptophysin$^+$, chromogranin$^+$, CD56$^+$	–	Poor
Sarcomatoid thymic carcinoma	6th decade; M > F	Solid or nested proliferation of malignant spindle cells; dense collagenous stroma; ± areas of spindle cell thymoma	CK$^+$, CK5/6$^+$, CK7$^+$, p63/p40$^+$, Pax8 (polyclonal)$^+$, CD5$^{+/-}$, c-kit$^{+/-}$	–	Poor
SFT	6th decade; M = F	Bland spindle cells in patternless pattern; keloid-like stroma; staghorn-like vasculature	CD34$^+$, STAT6$^+$, CK$^-$	*NAB2::STAT6* fusion	Good
Synovial sarcoma	4th decade; M > F	Cellular proliferation of monotonous spindle cells; high mitotic activity; inconspicuous stroma; mast cells; staghorn-like vasculature	TLE1$^+$, SS18-SSX$^+$/SS18_CT$^+$, CK$^{+/-}$	*SYT::SSX* fusion	Poor
Dedifferentiated liposarcoma	5th–6th decade; M = F	Areas of well differentiated liposarcoma and non-lipogenic sarcoma (spindle cell proliferation with variable mitotic activity, nuclear pleomorphism)	MDM2$^+$	*MDM2* amplification	Poor
Angiosarcoma	3rd–4th decade; M = F	Spindle cell proliferation with variable degrees of vasoformation; increased mitotic activity; necrosis	CD31$^+$, CD34$^+$, ERG$^+$, CK$^{+/-}$	–	Poor
Schwannoma	4th–6th decade; M = F	Bland spindle cells with wavy appearance; Antoni A and B areas; hyalinized blood vessels; lymphoid aggregates	S100$^+$, SOX10$^+$	–	Good
Inflammatory myofibroblastic tumor	Children/young adults; M = F	Spindle cells with indistinct cell borders; fascicular growth pattern; mixed chronic inflammatory cell infiltrate; low mitotic activity	SMA$^{+/-}$; ALK$^{+/-}$	*ALK* gene rearrangement	Good
Sarcomatoid mesothelioma	Older adults; M > F	Spindle cells with nuclear atypia, prominent nucleoli, increased mitotic activity	CK$^+$; other mesothelioma markers variable	–	Poor
Intimal sarcoma	5th decade; F > M	Spindle cells with varying degrees of atypia and cellularity; subset with distinct differentiation; heterologous elements possible	Variable	*MDM2* amplification	Poor

SFT, solitary fibrous tumor; M, male; F, female; IHC, immunohistochemistry; CK, cytokeratin; ERG, erythroblast transformation specific related gene; SMA, smooth muscle actin; ALK, anaplastic lymphoma kinase.

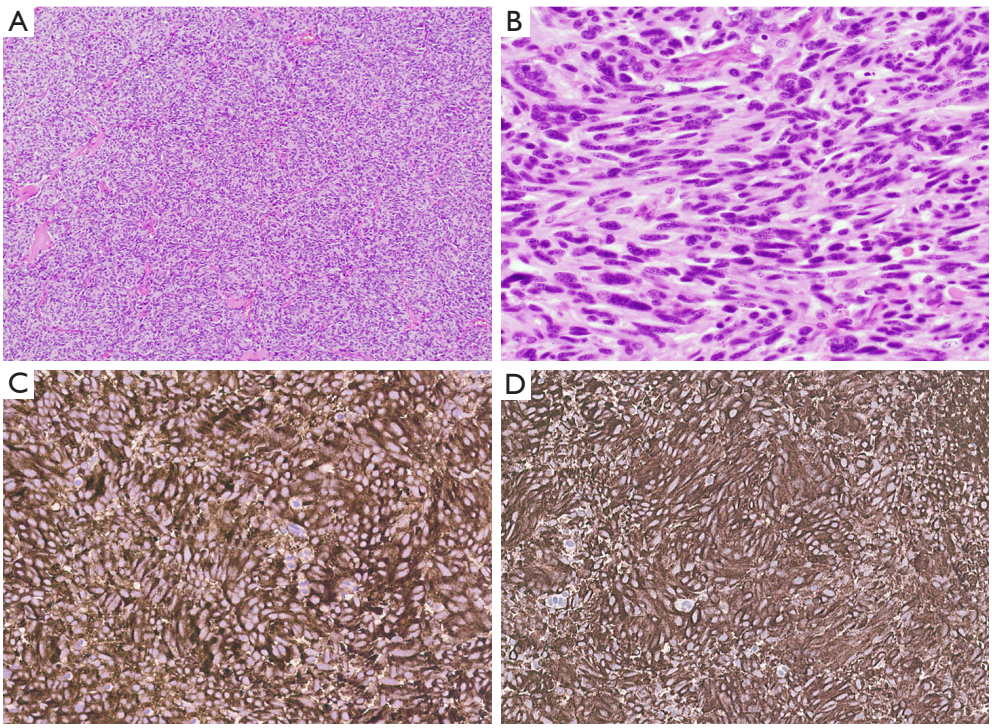

Figure 4 Spindle cell carcinoid tumor of the thymus. (A) Low power view of a thymic spindle cell carcinoid tumor characterized by tumor cells arranged in a nested pattern (H&E, ×4); (B) the tumor cells have fusiform nuclei with a salt-and-pepper chromatin pattern and low to absent mitotic activity (H&E, ×20); the tumor cells show diffuse reactivity with neuroendocrine markers, including (C) synaptophysin (×10) and (D) chromogranin A (×10). H&E, hematoxylin and eosin.

Sarcomatoid thymic carcinoma

Thymic carcinomas composed of spindle-shaped tumor cells are known as spindle cell or sarcomatoid thymic carcinomas. These tumors are epithelial-derived high-grade malignant tumors of the thymic gland; their spindle-shaped nature and origin in the anterior mediastinum is the reason why these tumors must be included in the differential diagnosis of spindle cell thymoma. Sarcomatoid thymic carcinomas occur in older adults with a slight male predominance (21). Chest pain, dyspnea and cough are the most common clinical symptoms.

Gross examination demonstrates well-circumscribed or locally infiltrative tumors with a firm cut surface and with foci of hemorrhage, necrosis and variable cystic change (21). Microscopically, these tumors commonly present as a solid proliferation of highly cellular spindle cells with fascicular or hemangiopericytic growth patterns and cytologically malignant features, including large, hyperchromatic nuclei with prominent nucleoli and frequent mitotic figures (3 to >10 mitoses per 10 high power fields) (*Figure 5A,5B*). The malignant cells are separated by dense collagenous stroma. Areas of hemorrhage, necrosis or cystic degeneration are frequently observed. In some cases, these tumors may display transition from spindle cell thymoma, indicating potential progression from a lower grade malignancy (21,22). Immunohistochemically, sarcomatoid thymic carcinomas are positive for cytokeratin as well as CK5/6, CK7, p63/p40 and polyclonal Pax8 (*Figure 5C,5D*) (8,22). Reactivity of these tumors for markers commonly positive in conventional thymic carcinomas, CD5 and CD117, is more variable in the sarcomatoid type (21,22). Characteristic molecular alterations that could be used for diagnostic or therapeutic purposes have not yet been identified. Contrary to spindle cell thymomas, sarcomatoid thymic carcinomas pursue an aggressive clinical course, with 50% of patients succumbing to the disease between 2 and 5 years after diagnosis according to the largest reported series (21).

The separation of sarcomatoid thymic carcinoma from spindle cell thymoma is primarily based on cytologic features with the former being characterized by nuclear pleomorphism, coarse nuclear chromatin, prominent

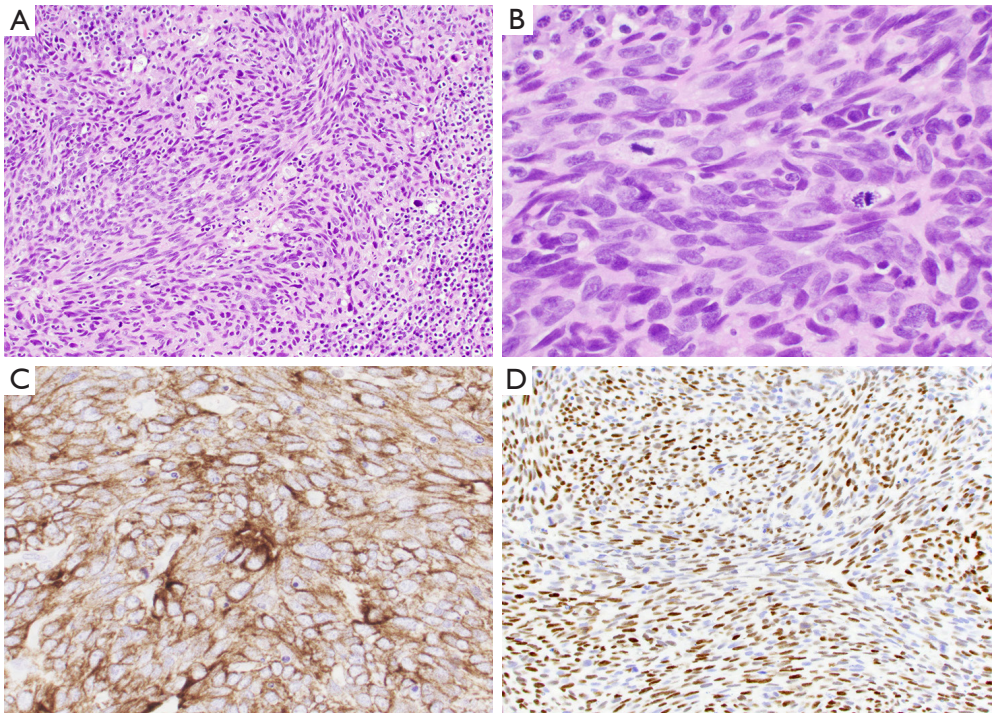

Figure 5 Sarcomatoid thymic carcinoma composed of (A) spindle cells arranged in a fascicular pattern (H&E, ×10); (B) individual tumor cells demonstrate a degree of cytologic atypia and conspicuous mitotic figures (H&E, ×20); by immunohistochemistry, the tumor cells are positive for (C) pancytokeratin (×20) and (D) p40 (×10).

nucleoli, and increased mitotic figures. Contrary to spindle cell thymomas, perivascular spaces and immature lymphocytes are not typically identified in sarcomatoid thymic carcinomas. Immunohistochemical workup is of limited use in this particular context as both neoplasms will show a similar immunophenotype (*Table 2*).

SFT

SFTs are mesenchymal tumors that most commonly arise in the visceral pleura and soft tissues but have also been recognized in the mediastinum, especially in the anterior and superior compartments (1). These tumors typically display low-grade spindle cell features and can occur in the vicinity of the thymic gland, thereby mimicking spindle cell thymomas. Mediastinal SFT are usually seen in the older population with a mean age in the 6th decade and without any specific sex predilection (23,24). Symptoms are related to mass effect of the tumor on neighboring organs and include chest pain, dyspnea and shortness of breath.

Grossly, mediastinal SFT are often large circumscribed but unencapsulated masses that can exceed 15 cm in size and show a tan-gray and firm cut surface (23,24). At microscopic examination, the low power appearance of the tumors is characterized by a "patternless pattern", in which bland spindle-shaped tumor cells are arranged as randomly distributed hypo- and hypercellular areas (*Figure 6A*). Other growth patterns include fascicular, storiform, palisaded or herringbone patterns. Cytologic atypia is typically absent and mitotic activity is low. The stroma is heavily collagenized and often displays a keloid-like or carrot-shred quality (*Figure 6B*). Staghorn-like (hemangiopericytoma-like) vessels are commonly identified in these tumors (23,24). As all SFT are potentially malignant tumors, a four-criteria risk stratification model, which takes into account patient age, tumor size, mitotic activity and necrosis, is currently used to predict the risk of metastasis (25,26).

Immunohistochemically, the tumor cells of SFT show strong expression of CD34 and nuclear reactivity for STAT6 (*Figure 6C,6D*) (27-30). The latter is the result of a characteristic *NAB2*::*STAT6* fusion transcript that has been identified in these tumors (31,32). Complete surgical resection is the treatment of choice for mediastinal SFT, both for primary tumors and recurrent disease (23,24,33-37).

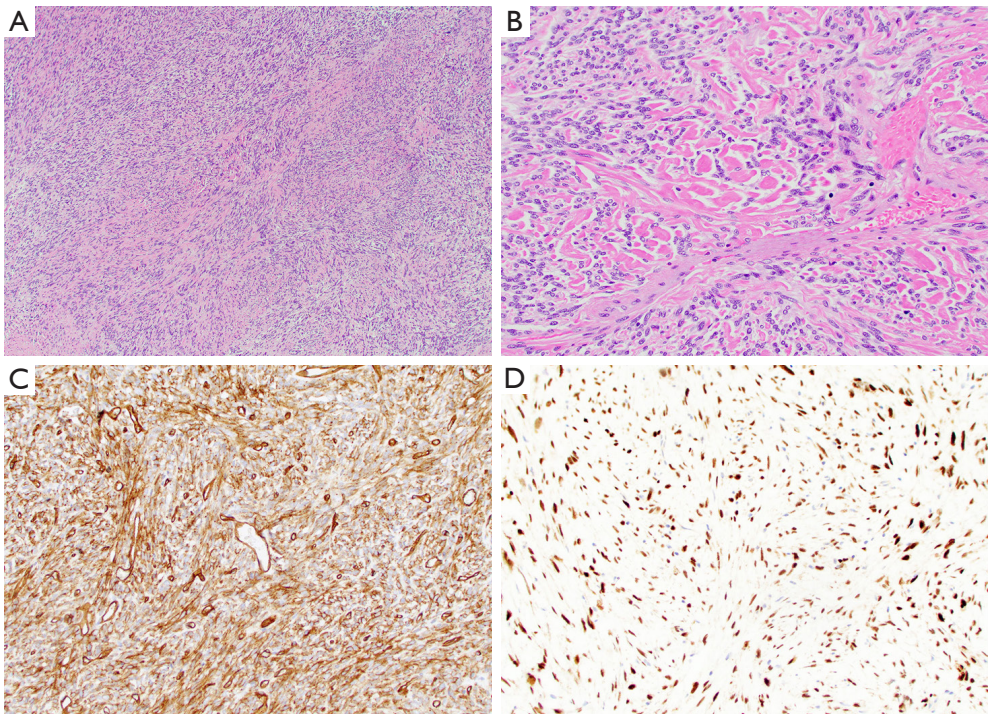

Figure 6 Mediastinal SFT. (A) SFT with a characteristic "patternless pattern" (H&E, ×4); (B) keloid-like collagen is a common finding in these tumors (H&E, ×10); immunohistochemical expression of (C) CD34 (×10) and (D) STAT6 in a mediastinal SFT (×10). SFT, solitary fibrous tumor; H&E, hematoxylin and eosin.

SFTs can easily be mistaken for spindle cell thymomas, especially when displaying more cellular areas. Both tumors are composed of bland tumor cells, however, spindle cell thymomas will also contain a subtle lymphocytic infiltrate, in addition to delicate fibrous bands and perivascular spaces unlike SFT. In addition, immunohistochemical and molecular characteristics may be exploited to distinguish these two entities: while spindle cell thymomas will show strong expression of cytokeratin and p63/p40 and negative staining for STAT6, the opposite is true for SFT. On a molecular level, SFT harbor a *NAB2*::*STAT6* fusion gene which can be used for diagnostic purposes (*Table 2*).

Synovial sarcoma

Synovial sarcoma is an aggressive spindle cell sarcoma that most commonly occurs in the soft tissue of young adults. In the thoracic cavity, most of these tumors involve the chest wall or lung, while the mediastinum is an exceptionally rare primary site accounting for <10% of all thoracic synovial sarcomas (38). Since most mediastinal synovial sarcomas arise in the anterior mediastinal compartment, these tumors may easily be mistaken for spindle cell thymomas. Most mediastinal synovial sarcomas occur in young adult patients with a mean age of 35 years and with a male predominance. Patients present with chest pain, shortness of breath, and pleural effusion or with constitutional symptoms, including fever, weight loss, and weakness (39).

Grossly, mediastinal synovial sarcomas are large tumors (range, 5 to 20 cm). The cut surface shows gray-white to tan tumors with a soft, gelatinous or firm consistency and foci of hemorrhage and necrosis. Variable cystic changes may be observed. Microscopically, synovial sarcomas can display two major growth patterns, monophasic and biphasic types. Most mediastinal synovial sarcomas are of the monophasic type and consist of a monotonous spindle cell proliferation arranged in various growth patterns, including sheets, fascicles, storiform, hemangiopericytic or herringbone patterns (*Figure 7A*) (40). The tumor cells have oval to spindle-shaped nuclei, inconspicuous nucleoli and indistinct eosinophilic cytoplasm. Nuclear pleomorphism is not prominent but mitotic activity can be increased (2 to 12 mitoses/10 high power fields) (*Figure 7B*). The stroma is typically inconspicuous and the reason why the tumors

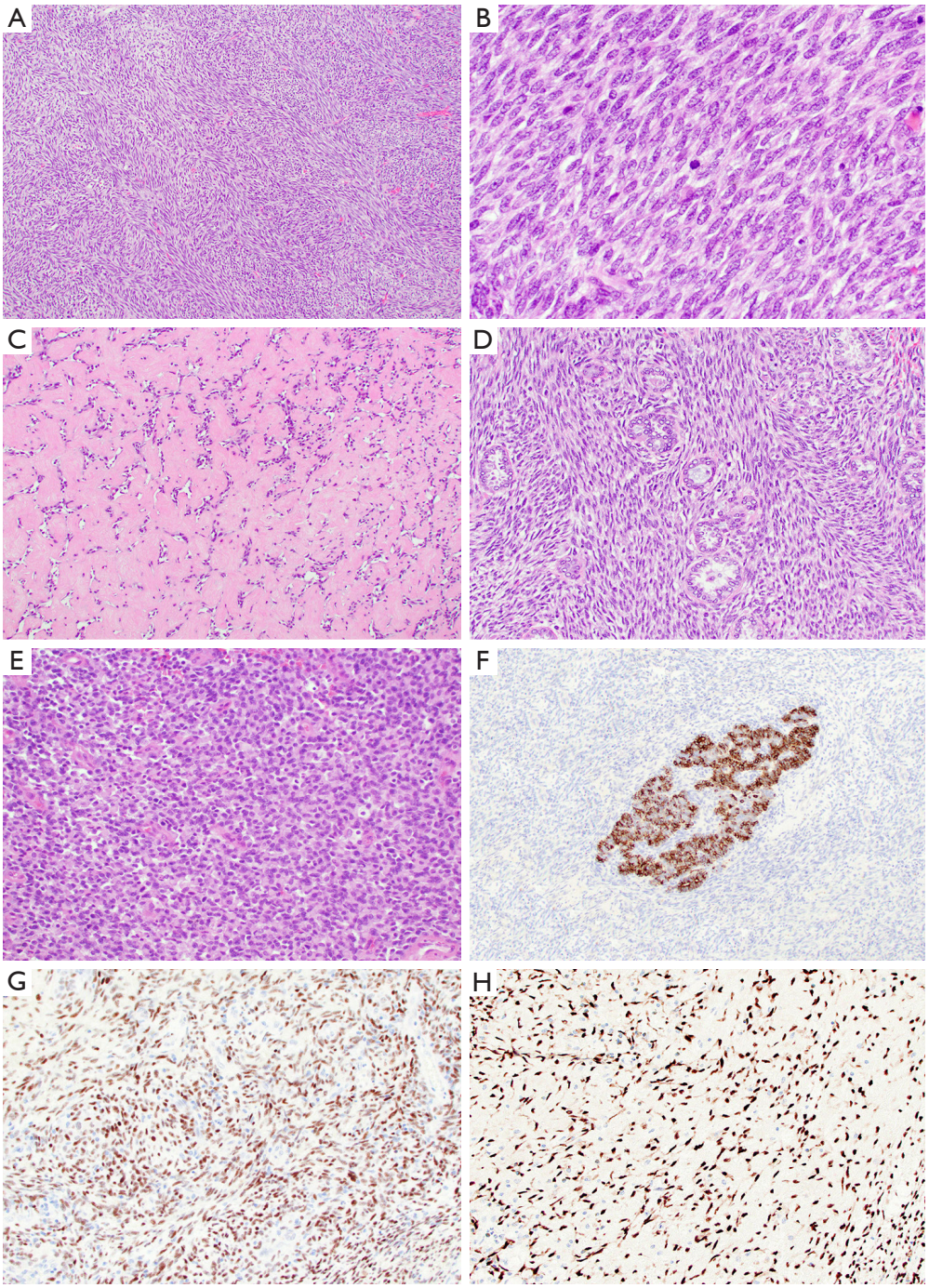

Figure 7 Mediastinal synovial sarcoma. (A) Synovial sarcomas are typically highly cellular spindle cell lesions (H&E, ×4); (B) the tumor cells are monomorphic and mitotically active (H&E, ×20); (C) synovial sarcoma with dense stromal collagen (H&E, ×10); (D) biphasic synovial sarcoma characterized by glandular structures in addition to the spindle cell component (H&E, ×10); (E) poorly differentiated synovial sarcoma demonstrating small round tumor cells with rhabdoid features (H&E, ×10); (F) cytokeratin immunohistochemical expression in a biphasic synovial sarcoma is restricted to the glandular component (×10); novel markers for synovial sarcomas include (G) TLE1 (×10) and (H) SS18-SSX (×10). H&E, hematoxylin and eosin.

appear highly cellular. After treatment, the stroma may become more prominent and consist of thick collagen or myxoid fibroconnective tissue (*Figure 7C*). Other characteristic findings in these tumors are the presence of vessels with a hemangiopericytoma-like or staghorn-like appearance, dystrophic calcification, scattered mast cells and cystic changes (39).

In the biphasic variant, the spindle cells are intermixed with glandular or pseudopapillary structures composed of round, cuboidal or columnar cells with oval nuclei and abundant eosinophilic cytoplasm (*Figure 7D*) (39). In primary mediastinal synovial sarcomas, a third variant is sometimes recognized, the so called poorly differentiated synovial sarcoma. This subtype consists of highly cellular round or oval cells with hyperchromatic nuclei, rhabdoid cytoplasmic features, high mitotic index and necrosis (*Figure 7E*) (39).

More than 90% of synovial sarcomas are characterized by a unique *t(X; 18)(p11.2; q11.2)* translocation resulting in the fusion of the *SYT* gene on chromosome 18 to either one of three closely related genes, *SSX1*, *SSX2*, and *SSX4* on chromosome X (41). Hence, molecular testing for this specific translocation is a valuable aid in the workup of these tumors.

By immunohistochemistry, mediastinal synovial sarcomas are characterized by expression of cytokeratins and epithelial membrane antigen in single cells in the monophasic variant and in the glandular component of biphasic tumors (*Figure 7F*) (39,42,43). More recently, several novel markers have been introduced to identify these tumors. Among these, TLE1 and SS18-SSX are two new antibodies that have been proven useful as a screening tool to identify cases in which molecular genetic testing is likely positive (*Figure 7G,7H*) (44,45). In this context, it has to be noted that TLE1 is only moderately specific for synovial sarcoma and can be expressed in a range of other neoplasms, including potential mimics (46) while SS18-SSX is highly specific but not completely sensitive. In this scenario, a SSX C-terminus antibody can be added to positively identify synovial sarcomas with non-SS18 fusions or if negative, to exclude the diagnosis altogether (45,47).

Surgery is the primary treatment for mediastinal synovial sarcomas and completeness of resection appears to be the main factor influencing patient survival (48). Patients with these tumors have an unfavorable prognosis with a 5-year overall survival rate of 35.7% compared to 50–80% for synovial sarcomas arising in the soft tissues (48-50). Multiple lines of therapy, including chemotherapy and/or radiotherapy are often used for advanced stage disease, tumor progression and incomplete surgical resection (48,49,51,52).

The monophasic variant of synovial sarcoma is the one most prone to be mistaken for spindle cell thymoma. Both tumors are cellular spindle cell lesions with monomorphic appearance. However, while tumor cells may be rather bland in both entities, those in synovial sarcoma are mitotically active. Furthermore, distinct lobulation, lymphocytic infiltrate and perivascular spaces are features seen in spindle cell thymoma but not in synovial sarcoma. If tumor morphology is inconclusive, immunohistochemistry and/or molecular analyses can be performed and will show strong and diffuse staining with cytokeratin and p63/p40 in spindle cell thymoma while synovial sarcomas will be strongly and diffusely positive for TLE1 and SS18-SSX. Likewise, synovial sarcomas will display *SS18*::*SSX* fusion, unlike spindle cell thymoma (*Table 2*).

Dedifferentiated liposarcoma

Primary mediastinal liposarcomas account for less than 1% of all mediastinal tumors and up to a third of these correspond to the dedifferentiated type (53-59). The latter are histologically characterized by areas of a well differentiated liposarcoma admixed with a sarcoma that lacks obvious adipocytic differentiation by morphologic examination. Dedifferentiated liposarcomas, in particular, can mimic spindle cell thymomas since the dedifferentiated component often presents as an undifferentiated spindle cell neoplasm and the well differentiated liposarcoma component may be inconspicuous. These tumors affect adult patients with a mean age at presentation in the 5th to 6th decade and with equal sex distribution (54,57-60). Cough, dyspnea, dysphagia and chest pain are the most common presenting symptoms, usually due to mass effect on neighboring organs, however, some patients may be entirely asymptomatic despite large tumor size (54,57-60).

Mediastinal liposarcomas are typically large lobulated tumors with a size up to 60 cm (54,58,60). Dedifferentiated liposarcomas will show areas grossly resembling mature fatty tissue representing the well differentiated component juxtaposed with firm solid areas representing the non-lipogenic spindle cell sarcoma (*Figure 8A*). Areas of hemorrhage and necrosis may be seen in the latter (54,58,60). The microscopic appearance of the non-lipogenic sarcoma can be highly variable and range from less cellular to highly cellular spindle cell proliferations arranged in solid sheets, whorled or hemangiopericytic patterns (*Figure 8B*). Cytologic

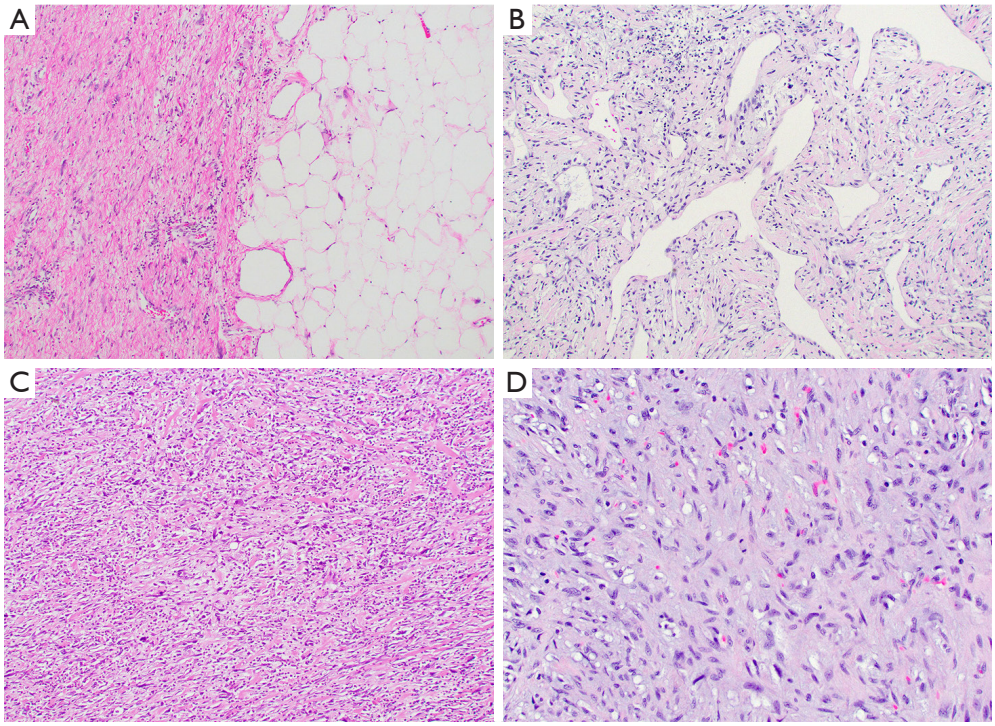

Figure 8 Mediastinal dedifferentiated liposarcoma: (A) a well differentiated liposarcoma component (right) is juxtaposed with dedifferentiated areas (left) (H&E, ×4); (B) the non-lipogenic elements may have a hemangiopericytoma-like growth pattern (H&E, ×10); cytologically, the dedifferentiated tumor may show (C) high-grade (H&E, ×10) or (D) low-grade features (H&E, ×20). H&E, hematoxylin and eosin.

atypia, mitotic activity and presence of hemorrhage or necrosis can vary from tumor to tumor (*Figure 8C,8D*). Likewise, the stroma may range from highly collagenized to myxoid in appearance. The well differentiated component may be inconspicuous or absent and close attention should be paid to the edges of the dedifferentiated elements to identify a rim of background well differentiated liposarcoma composed of mature adipose tissue with variably sized adipocytes, bands of fibrotic stroma and atypical spindle cells that may mimic adipose tissue with reactive changes.

The value of immunohistochemistry for the diagnosis of dedifferentiated liposarcomas remains limited due to an often non-specific immunophenotype. On a molecular level, well differentiated and dedifferentiated liposarcomas are characterized by amplification of the 12q13-15 region, including *MDM2* and *CDK4* which is detectable by immunohistochemistry and fluorescence in situ hybridization (FISH) (61-64).

As a group, mediastinal liposarcomas are characterized by a high rate of recurrence (approximately 30%) and overall mortality of 30–50% and hence the overall prognosis for these patients remains poor. Complete surgical resection is not only the treatment of choice but is also an important prognostic factor associated with better overall survival (59,65).

Dedifferentiated liposarcoma may closely resemble spindle cell thymoma, particularly if the well differentiated component is not recognized or not sampled sufficiently. If morphological details are inconclusive, immunohistochemical workup is indicated and would support a diagnosis of spindle cell thymoma if diffuse keratin reactivity is seen in combination with expression of p63/p40. On the other hand, if these markers return negative and no other specific immunophenotype is recognized, FISH analysis to identify *MDM2* amplification may be indicated and if positive would support a diagnosis of dedifferentiated liposarcoma instead (*Table 2*).

Miscellaneous other spindle cell neoplasms

There are various other benign and malignant spindle cell neoplasms that can be included in the differential diagnosis of spindle cell thymoma. These are either very rare or more commonly encountered in other mediastinal compartments.

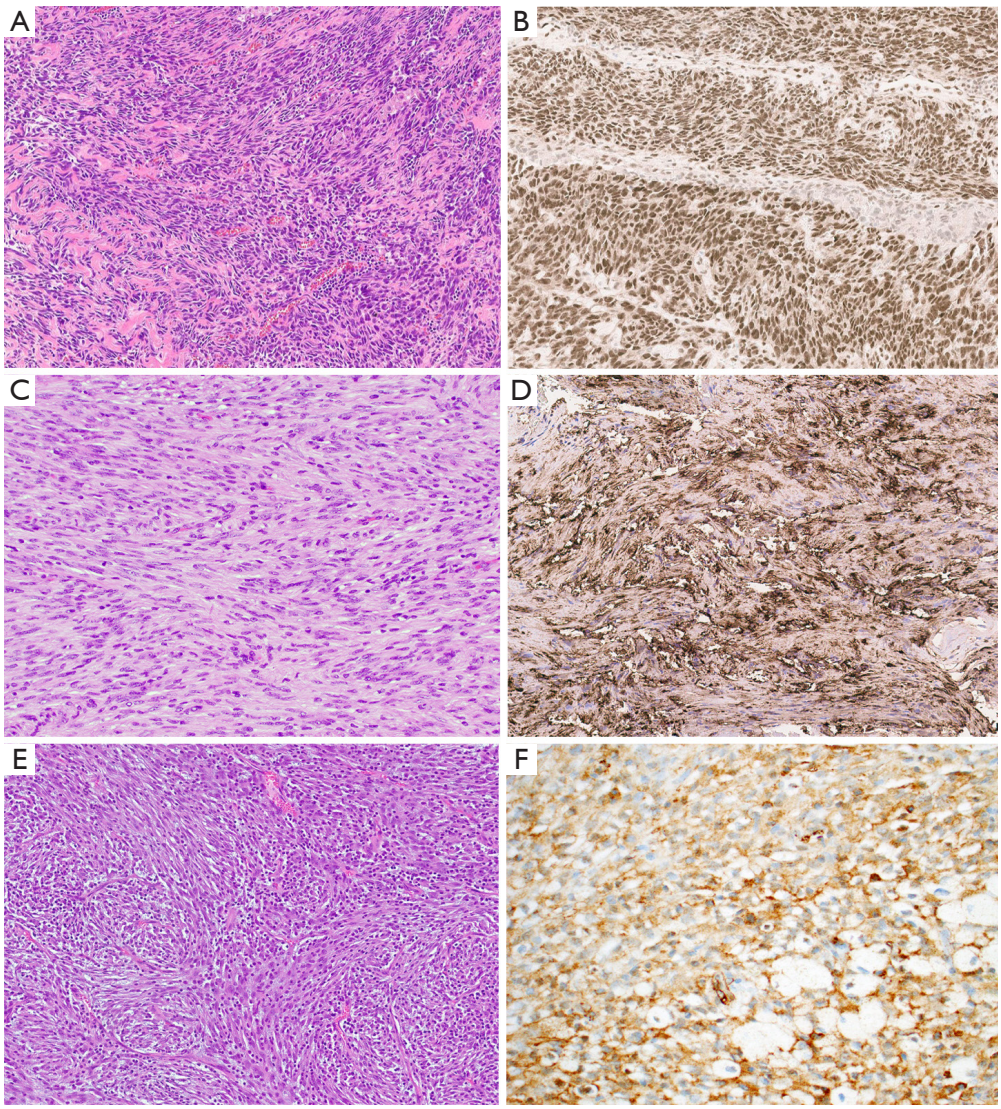

Figure 9 Miscellaneous spindle cell neoplasms of the mediastinum. (A) Mediastinal angiosarcoma presenting as a cellular spindle cell tumor (H&E, ×10); (B) immunohistochemistry for ERG in a mediastinal angiosarcoma (×10); (C) spindle cells with a wavy configuration are characteristic for schwannomas (H&E, ×10); (D) the tumor cells of a schwannoma are diffusely positive for S100 protein (×10); (E) inflammatory myofibroblastic tumor composed of bland spindle cells admixed with an inflammatory cell infiltrate (H&E, ×10); (F) reactivity for smooth muscle antigen in a mediastinal inflammatory myofibroblastic tumor (×10). H&E, hematoxylin and eosin; ERG, erythroblast transformation specific related gene.

Nevertheless, their tumor morphology may show sufficient similarities with that of spindle cell thymoma to be summarized here.

Only few cases of primary angiosarcoma of the mediastinum have been described accounting for less than 1% of mediastinal tumors (66). Many of these tumors are comprised of spindle cells and composed of large, cavernous vascular structures, capillary proliferations, slit-like vascular channels, or solid sheet-like tumor cells (*Figure 9A*). While low-grade tumors display spindle cells with minimal cytologic atypia and retain the capacity to form vascular structures, high-grade tumors may lose their vasoformative properties. In the latter, necrosis is commonly identified and the mitotic activity is often increased (66,67). Expression of vascular immunohistochemical markers, including factor III-related antigen, CD34, CD31, and erythroblast

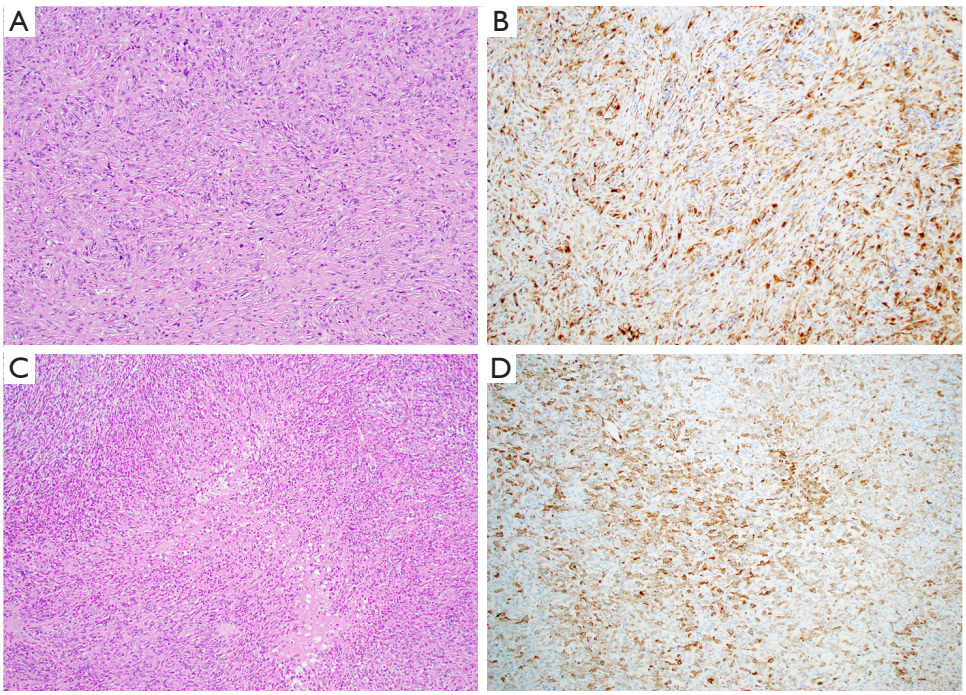

Figure 10 Miscellaneous spindle cell neoplasms of the mediastinum. (A) Sarcomatoid mesothelioma composed of pleomorphic spindle cells arranged in a haphazard pattern (H&E, ×10); (B) the tumor cells of a sarcomatoid mesothelioma are highlighted by a pancytokeratin immunostain (×10); (C) intimal sarcoma characterized by an undifferentiated cellular spindle cell proliferation with central necrosis (H&E, ×10); (D) this particular case displayed variable reactivity with smooth muscle actin by immunohistochemistry (×10). H&E, hematoxylin and eosin.

transformation specific related gene (ERG) is characteristic for these tumors and allows separation from spindle cell thymoma (*Figure 9B*, *Table 2*).

Neurogenic tumors predominantly occur in the posterior mediastinum but can occasionally also arise in the anterior mediastinal compartment (68). Among these, the bland spindle cells of schwannoma are particularly prone to be mistaken for spindle cell thymoma (*Figure 9C*). Careful search for characteristic Antoni A (high cellularity) and Antoni B (low cellularity) areas and hyalinized vessels will likely point to the correct diagnosis; if needed, immunohistochemical analysis will reveal tumor cells positive for S100, SOX10 and neuron-specific enolase (*Figure 9D*, *Table 2*).

Inflammatory myofibroblastic tumors are rare mediastinal lesions, most commonly occurring in young adult patients (69). Due to their composition of bland myofibroblastic spindle cells and diffuse inflammatory cell infiltrate, these tumors may be mistaken for spindle cell thymoma, especially if arising in the anterior mediastinum (*Figure 9E*). Contrary to spindle cell thymoma, these tumors are characterized immunohistochemically by diffuse expression of vimentin and variable reactivity for smooth muscle actin. Approximately 50% of these tumors will be positive for anaplastic lymphoma kinase (ALK) protein which correlates well with *ALK* gene rearrangement in these tumors (*Figure 9F*, *Table 2*) (70).

The spindle cell variant of mesothelioma (sarcomatoid mesothelioma) may rarely involve the anterior mediastinum. This tumor is composed of fusiform tumor cells arranged in fascicular or storiform patterns and may thus resemble spindle cell thymoma. Close attention should be paid to the cytologic characteristics which will usually demonstrate atypical spindle cells with hyperchromatic nuclei, prominent nucleoli and increased mitotic activity (*Figure 10A*) (71). The immunophenotype of these tumors is very limited and reactivity is often limited to pancytokeratin and only variable expression of other mesothelial markers (CK5/6, calretinin, WT-1, etc.) (*Figure 10B*) (72). Contrary to spindle cell thymomas, these tumors are typically negative for p63/p40 (*Table 2*).

Intimal sarcoma typically arises in the pulmonary arteries of the right ventricular outflow tract of the heart but can involve the anterior mediastinum by direct extension. These tumors can show a wide spectrum of differentiation,

ranging from undifferentiated fibroblastic/myofibroblastic tumors to sarcomas with distinct differentiation, such as rhabdomyosarcoma or angiosarcoma among others (*Figure 10C*) (73). These tumors are often hypercellular and will show varying degrees of cytologic atypia, necrosis and mitotic activity which should serve to distinguish them from spindle cell thymoma. In addition, close attention should be paid to the tumor origin as demonstrated on radiologic imaging, gross and microscopic examination. Immunohistochemically, these tumors will show a variable phenotype depending on the tumor subtype (*Figure 10D*); however, these neoplasms are generally negative for cytokeratin, CK5/6 and p63/p40 allowing distinction from spindle cell thymoma. Another diagnostic tool includes amplification of *MDM2* which is a characteristic alteration in the majority of these tumors (*Table 2*) (74).

Acknowledgments

Funding: None.

Footnote

Conflicts of Interest: The author has completed the ICMJE uniform disclosure form (available at https://med.amegroups.com/article/view/10.21037/med-22-50/coif). AW serves as an unpaid editorial board member of *Mediastinum* from October 2021 to September 2023. The author has no other conflicts of interest to declare.

Ethical Statement: The author is accountable for all aspects of the work in ensuring that questions related to the accuracy or integrity of any part of the work are appropriately investigated and resolved.

References

1. Weissferdt A. Mesenchymal Tumors of the Mediastinum. In: Weissferdt A. Diagnostic Thoracic Pathology. 1st ed. Cham: Springer; 2020:972.
2. Weissferdt A, Moran CA. The histomorphologic spectrum of spindle cell thymoma. Hum Pathol 2014;45:437-45.
3. Ströbel P, Badve S, Chan JKC, et al. Type A thymoma. In: World Health Organization. WHO Classification of Tumours Editorial Board. Thoracic Tumours. 5th ed. Lyon: IARC Press; 2021:326-31.
4. Nonaka D, Rosai J. Is there a spectrum of cytologic atypia in type a thymomas analogous to that seen in type B thymomas? A pilot study of 13 cases. Am J Surg Pathol 2012;36:889-94.
5. Vladislav IT, Gökmen-Polar Y, Kesler KA, et al. The role of histology in predicting recurrence of type A thymomas: a clinicopathologic correlation of 23 cases. Mod Pathol 2013;26:1059-64.
6. Moran CA, Kalhor N, Suster S. Invasive spindle cell thymomas (WHO Type A): a clinicopathologic correlation of 41 cases. Am J Clin Pathol 2010;134:793-8.
7. Weissferdt A, Hernandez JC, Kalhor N, et al. Spindle cell thymomas: an immunohistochemical study of 30 cases. Appl Immunohistochem Mol Morphol 2011;19:329-35.
8. Weissferdt A, Moran CA. Pax8 expression in thymic epithelial neoplasms: an immunohistochemical analysis. Am J Surg Pathol 2011;35:1305-10.
9. Radovich M, Pickering CR, Felau I, et al. The Integrated Genomic Landscape of Thymic Epithelial Tumors. Cancer Cell 2018;33:244-58.e10.
10. Moran CA, Suster S. Neuroendocrine carcinomas (carcinoid tumor) of the thymus. A clinicopathologic analysis of 80 cases. Am J Clin Pathol 2000;114:100-10.
11. Gaur P, Leary C, Yao JC. Thymic neuroendocrine tumors: a SEER database analysis of 160 patients. Ann Surg 2010;251:1117-21.
12. Filosso PL, Yao X, Ahmad U, et al. Outcome of primary neuroendocrine tumors of the thymus: a joint analysis of the International Thymic Malignancy Interest Group and the European Society of Thoracic Surgeons databases. J Thorac Cardiovasc Surg 2015;149:103-9.e2.
13. Gibril F, Chen YJ, Schrump DS, et al. Prospective study of thymic carcinoids in patients with multiple endocrine neoplasia type 1. J Clin Endocrinol Metab 2003;88:1066-81.
14. Filosso PL, Yao X, Ruffini E, et al. Comparison of outcomes between neuroendocrine thymic tumours and other subtypes of thymic carcinomas: a joint analysis of the European Society of Thoracic Surgeons and the International Thymic Malignancy Interest Group. Eur J

Cardiothorac Surg 2016;50:766-71.
15. Ose N, Maeda H, Inoue M, et al. Results of treatment for thymic neuroendocrine tumours: multicentre clinicopathological study. Interact Cardiovasc Thorac Surg 2018;26:18-24.
16. Moran CA, Suster S. Spindle-cell neuroendocrine carcinomas of the thymus (spindle-cell thymic carcinoid): a clinicopathologic and immunohistochemical study of seven cases. Mod Pathol 1999;12:587-91.
17. Levine GD, Rosai J. A spindle cell varient of thymic carcinoid tumor. A clinical, histologic, and fine structural study with emphasis on its distinction from spindle cell thymoma. Arch Pathol Lab Med 1976;100:293-300.
18. Herbst WM, Kummer W, Hofmann W, et al. Carcinoid tumors of the thymus. An immunohistochemical study. Cancer 1987;60:2465-70.
19. Modlin IM, Kidd M, Filosso PL, et al. Molecular strategies in the management of bronchopulmonary and thymic neuroendocrine neoplasms. J Thorac Dis 2017;9:S1458-73.
20. Crona J, Björklund P, Welin S, et al. Treatment, prognostic markers and survival in thymic neuroendocrine tumours. a study from a single tertiary referral centre. Lung Cancer 2013;79:289-93.
21. Suster S, Moran CA. Spindle cell thymic carcinoma: clinicopathologic and immunohistochemical study of a distinctive variant of primary thymic epithelial neoplasm. Am J Surg Pathol 1999;23:691-700.
22. Weissferdt A, Moran CA. Thymic carcinoma, part 1: a clinicopathologic and immunohistochemical study of 65 cases. Am J Clin Pathol 2012;138:103-14.
23. Zhang L, Liu X, Li X, et al. Diagnosis and surgical treatment of mediastinal solitary fibrous tumor. Asia Pac J Clin Oncol 2017;13:e473-80.
24. Witkin GB, Rosai J. Solitary fibrous tumor of the mediastinum. A report of 14 cases. Am J Surg Pathol 1989;13:547-57.
25. Demicco EG, Park MS, Araujo DM, et al. Solitary fibrous tumor: a clinicopathological study of 110 cases and proposed risk assessment model. Mod Pathol 2012;25:1298-306.
26. Demicco EG, Wagner MJ, Maki RG, et al. Risk assessment in solitary fibrous tumors: validation and refinement of a risk stratification model. Mod Pathol 2017;30:1433-42.
27. van de Rijn M, Lombard CM, Rouse RV. Expression of CD34 by solitary fibrous tumors of the pleura, mediastinum, and lung. Am J Surg Pathol 1994;18:814-20.
28. Chmielecki J, Crago AM, Rosenberg M, et al. Whole-exome sequencing identifies a recurrent NAB2-STAT6 fusion in solitary fibrous tumors. Nat Genet 2013;45:131-2.
29. Doyle LA, Vivero M, Fletcher CD, et al. Nuclear expression of STAT6 distinguishes solitary fibrous tumor from histologic mimics. Mod Pathol 2014;27:390-5.
30. Yoshida A, Tsuta K, Ohno M, et al. STAT6 immunohistochemistry is helpful in the diagnosis of solitary fibrous tumors. Am J Surg Pathol 2014;38:552-9.
31. Mohajeri A, Tayebwa J, Collin A, et al. Comprehensive genetic analysis identifies a pathognomonic NAB2/STAT6 fusion gene, nonrandom secondary genomic imbalances, and a characteristic gene expression profile in solitary fibrous tumor. Genes Chromosomes Cancer 2013;52:873-86.
32. Robinson DR, Wu YM, Kalyana-Sundaram S, et al. Identification of recurrent NAB2-STAT6 gene fusions in solitary fibrous tumor by integrative sequencing. Nat Genet 2013;45:180-5.
33. Aydemir B, Celik S, Okay T, et al. Intrathoracic giant solitary fibrous tumor. Am J Case Rep 2013;14:91-3.
34. Chu X, Zhang L, Xue Z, et al. Solitary fibrous tumor of the pleura: An analysis of forty patients. J Thorac Dis 2012;4:146-54.
35. Xiang Y, Tu S, Zhang F. Rapid metastasis of mediastinal solitary fibrous tumor: Report a case. Medicine (Baltimore) 2017;96:e9307.
36. Cardillo G, Carbone L, Carleo F, et al. Solitary fibrous tumors of the pleura: an analysis of 110 patients treated in a single institution. Ann Thorac Surg 2009;88:1632-7.
37. Milano MT, Singh DP, Zhang H. Thoracic malignant solitary fibrous tumors: A population-based study of survival. J Thorac Dis 2011;3:99-104.
38. Terra SBSP, Aesif SW, Maleszewski JJ, et al. Mediastinal Synovial Sarcoma: Clinicopathologic Analysis of 21 Cases With Molecular Confirmation. Am J Surg Pathol 2018;42:761-6.
39. Suster S, Moran CA. Primary synovial sarcomas of the mediastinum: a clinicopathologic, immunohistochemical, and ultrastructural study of 15 cases. Am J Surg Pathol 2005;29:569-78.
40. Salah S, Salem A. Primary synovial sarcomas of the mediastinum: a systematic review and pooled analysis of the published literature. ISRN Oncol 2014;2014:412527.
41. Przybyl J, Sciot R, Rutkowski P, et al. Recurrent and novel SS18-SSX fusion transcripts in synovial sarcoma: description of three new cases. Tumour Biol 2012;33:2245-53.

42. Pelmus M, Guillou L, Hostein I, et al. Monophasic fibrous and poorly differentiated synovial sarcoma: immunohistochemical reassessment of 60 t(X;18)(SYT-SSX)-positive cases. Am J Surg Pathol 2002;26:1434-40.
43. Miettinen M, Limon J, Niezabitowski A, et al. Calretinin and other mesothelioma markers in synovial sarcoma: analysis of antigenic similarities and differences with malignant mesothelioma. Am J Surg Pathol 2001;25:610-7.
44. Foo WC, Cruise MW, Wick MR, et al. Immunohistochemical staining for TLE1 distinguishes synovial sarcoma from histologic mimics. Am J Clin Pathol 2011;135:839-44.
45. Zaborowski M, Vargas AC, Pulvers J, et al. When used together SS18-SSX fusion-specific and SSX C-terminus immunohistochemistry are highly specific and sensitive for the diagnosis of synovial sarcoma and can replace FISH or molecular testing in most cases. Histopathology 2020;77:588-600.
46. Kosemehmetoglu K, Vrana JA, Folpe AL. TLE1 expression is not specific for synovial sarcoma: a whole section study of 163 soft tissue and bone neoplasms. Mod Pathol 2009;22:872-8.
47. Baranov E, McBride MJ, Bellizzi AM, et al. A Novel SS18-SSX Fusion-specific Antibody for the Diagnosis of Synovial Sarcoma. Am J Surg Pathol 2020;44:922-33.
48. Syred K, Weissferdt A. Primary mediastinal synovial sarcomas. Mediastinum 2020;4:13.
49. Deshmukh R, Mankin HJ, Singer S. Synovial sarcoma: the importance of size and location for survival. Clin Orthop Relat Res 2004;(419):155-61.
50. Ulmer C, Kettelhack C, Tunn PU, et al. Synovial sarcoma of the extremities. Results of surgical and multimodal therapy. Chirurg 2003;74:370-4.
51. Eilber FC, Brennan MF, Eilber FR, et al. Chemotherapy is associated with improved survival in adult patients with primary extremity synovial sarcoma. Ann Surg 2007;246:105-13.
52. Trassard M, Le Doussal V, Hacène K, et al. Prognostic factors in localized primary synovial sarcoma: a multicenter study of 128 adult patients. J Clin Oncol 2001;19:525-34.
53. Macchiarini P, Ostertag H. Uncommon primary mediastinal tumours. Lancet Oncol 2004;5:107-18.
54. Hahn HP, Fletcher CD. Primary mediastinal liposarcoma: clinicopathologic analysis of 24 cases. Am J Surg Pathol 2007;31:1868-74.
55. Evans HL. Liposarcoma: a study of 55 cases with a reassessment of its classification. Am J Surg Pathol 1979;3:507-23.
56. Kindblom LG, Angervall L, Svendsen P. Liposarcoma a clinicopathologic, radiographic and prognostic study. Acta Pathol Microbiol Scand Suppl 1975;(253):1-71.
57. Boland JM, Colby TV, Folpe AL. Liposarcomas of the mediastinum and thorax: a clinicopathologic and molecular cytogenetic study of 24 cases, emphasizing unusual and diverse histologic features. Am J Surg Pathol 2012;36:1395-403.
58. Ortega P, Suster D, Falconieri G, et al. Liposarcomas of the posterior mediastinum: clinicopathologic study of 18 cases. Mod Pathol 2015;28:721-31.
59. Chen M, Yang J, Zhu L, et al. Primary intrathoracic liposarcoma: a clinicopathologic study and prognostic analysis of 23 cases. J Cardiothorac Surg 2014;9:119.
60. Klimstra DS, Moran CA, Perino G, et al. Liposarcoma of the anterior mediastinum and thymus. A clinicopathologic study of 28 cases. Am J Surg Pathol 1995;19:782-91.
61. Pedeutour F, Suijkerbuijk RF, Forus A, et al. Complex composition and co-amplification of SAS and MDM2 in ring and giant rod marker chromosomes in well-differentiated liposarcoma. Genes Chromosomes Cancer 1994;10:85-94.
62. Pedeutour F, Forus A, Coindre JM, et al. Structure of the supernumerary ring and giant rod chromosomes in adipose tissue tumors. Genes Chromosomes Cancer 1999;24:30-41.
63. Rosai J, Akerman M, Dal Cin P, et al. Combined morphologic and karyotypic study of 59 atypical lipomatous tumors. Evaluation of their relationship and differential diagnosis with other adipose tissue tumors (a report of the CHAMP Study Group). Am J Surg Pathol 1996;20:1182-9.
64. Mandahl N, Höglund M, Mertens F, et al. Cytogenetic aberrations in 188 benign and borderline adipose tissue tumors. Genes Chromosomes Cancer 1994;9:207-15.
65. Wychulis AR, Payne WS, Clagett OT, et al. Surgical treatment of mediastinal tumors: a 40 year experience. J Thorac Cardiovasc Surg 1971;62:379-92.
66. Weissferdt A, Kalhor N, Suster S, et al. Primary angiosarcomas of the anterior mediastinum: a clinicopathologic and immunohistochemical study of 9 cases. Hum Pathol 2010;41:1711-7.
67. Meis-Kindblom JM, Kindblom LG. Angiosarcoma of soft tissue: a study of 80 cases. Am J Surg Pathol 1998;22:683-97.
68. Boland JM, Colby TV, Folpe AL. Intrathoracic peripheral nerve sheath tumors-a clinicopathological study of 75

cases. Hum Pathol 2015;46:419-25.
69. Gorolay V, Jones B. Inflammatory myofibroblastic tumor of mediastinum with esophageal and bronchial invasion: a case report and literature review. Clin Imaging 2017;43:32-5.
70. Coffin CM, Hornick JL, Fletcher CD. Inflammatory myofibroblastic tumor: comparison of clinicopathologic, histologic, and immunohistochemical features including ALK expression in atypical and aggressive cases. Am J Surg Pathol 2007;31:509-20.
71. Attanoos RL, Gibbs AR. Pathology of malignant mesothelioma. Histopathology 1997;30:403-18.
72. Klebe S, Brownlee NA, Mahar A, et al. Sarcomatoid mesothelioma: a clinical-pathologic correlation of 326 cases. Mod Pathol 2010;23:470-9.
73. Huo L, Moran CA, Fuller GN, et al. Pulmonary artery sarcoma: a clinicopathologic and immunohistochemical study of 12 cases. Am J Clin Pathol 2006;125:419-24.
74. Bode-Lesniewska B, Zhao J, Speel EJ, et al. Gains of 12q13-14 and overexpression of mdm2 are frequent findings in intimal sarcomas of the pulmonary artery. Virchows Arch 2001;438:57-65.

doi: 10.21037/med-22-50
Cite this article as: Weissferdt A. Spindle cell thymoma and its histological mimickers. Mediastinum 2023;7:25.

Review Article

Bronchogenic cysts: a narrative review

Daniel J. Gross[1], Laurence M. Briski[2], Eric M. Wherley[1], Dao M. Nguyen[1]

[1]Thoracic Surgery Section, Division of Cardiothoracic Surgery, The DeWitt Daughtry Family Department of Surgery, Miller School of Medicine, University of Miami, Miami, FL, USA; [2]Department of Pathology, University of Miami, Miami, FL, USA

Contributions: (I) Conception and design: DJ Gross, DM Nguyen; (II) Administrative support: DM Nguyen; (III) Provision of study materials or patients: DM Nguyen, LM Briski; (IV) Collection and assembly of data: EM Wherley, DJ Gross, DM Nguyen; (V) Data analysis and interpretation: All authors; (VI) Manuscript writing: All authors; (VII) Final approval of manuscript: All authors.

Correspondence to: Dao M. Nguyen, MD, MSc, FRCSC, FACS. Thoracic Surgery Section, Division of Cardiothoracic Surgery, The DeWitt Daughtry Family Department of Surgery, Miller School of Medicine, University of Miami, 1295 NW 14th Street Suite J, Miami, FL 33136, USA. Email: DNguyen4@med.miami.edu.

Background and Objective: Bronchogenic cysts represent a rare form of cystic malformation of the respiratory tract. Primarily located in the mediastinum if occurring early in gestation as opposed to the thoracic cavity if arising later in development. However, they can arise from any site along the foregut. They exhibit a variety of clinical and radiologic presentations, representing a diagnostic challenge, especially in areas with endemic hydatid disease. Endoscopic drainage has emerged as a diagnostic and potentially therapeutic option but has been complicated by reports of infection. Surgical excision remains the standard of care allowing for symptomatic resolution and definitive diagnosis via pathologic examination; minimally invasive approaches such as robotic and thoracoscopic approaches aiding treatment. Following complete resection, prognosis is excellent with essentially no recurrence.

Methods: A review of the available electronic literature was performed from 1975 through 2022, using PubMed and Google Scholar, with an emphasis on more recent series. We included all retrospective series and case reports. A single author identified the studies, and all authors reviewed the selection until there was a consensus on which studies to include.

Key Content and Findings: The literature consisted of relatively small series, mixed between adult and pediatric patients, and the consensus remains that all symptomatic lesions should be excised via minimally invasive approach where feasible.

Conclusions: Surgical excision of symptomatic bronchogenic cysts remains the gold standard, with endoscopic drainage being reserved for diagnosis or as a temporizing measure in clinically unstable patients.

Keywords: Bronchogenic cyst; robotic surgery; mediastinum; mediastinal cyst

Received: 30 September 2022; Accepted: 07 April 2023; Published online: 20 April 2023.

doi: 10.21037/med-22-46

View this article at: https://dx.doi.org/10.21037/med-22-46

Introduction

Bronchogenic cysts, first described in 1859, are rare congenital cystic malformations of the respiratory tract, with an incidence of 1 per 42,000 to 68,000 hospital admissions in one hospital series (1,2). They comprise 10–15% of mediastinal tumors and between 50–60% of mediastinal cystic lesions (3). Bronchogenic cysts arise from the abnormal budding of the tracheobronchial tree or embryonic ventral lung bud, between the 26th–40th day of gestation (4). Their location is usually a function of their embryological development, with central (mediastinal) cysts arising earlier in development (*Figures 1*,*2*), and more peripheral development suggesting later formation (*Figure 3*) (4,5). Parenchymal bronchogenic cysts are reported to comprise 20–30% of all bronchogenic cysts (5,6). Histologically, bronchogenic cysts are typically unilocular and recapitulate elements of normal bronchial structures. The cyst wall is usually lined by respiratory-type epithelium (i.e., ciliated pseudostratified columnar epithelial cells

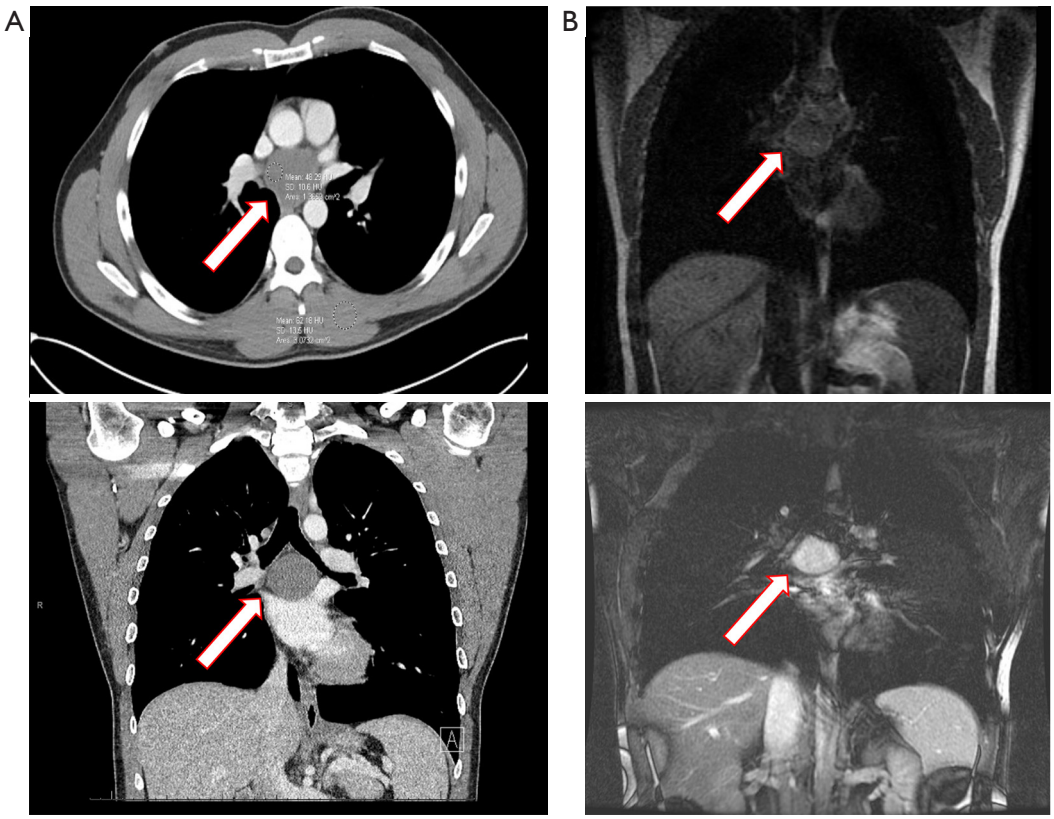

Figure 1 Posterior mediastinal bronchogenic cyst. Subcarinal bronchogenic cyst detected by CT scan of chest with intravenous contrast to investigate complaints of mild dysphagia and nonspecific back pain in a 35-year-old healthy man. (A) Axial and coronal CT images demonstrates a smooth-bordered 4.5 cm cystic lesion in the subcarinal location. The cyst has high density with HU of 48 and thick proteinaceous fluid was drained at the time of robotic thoracoscopic resection. Red bordered arrow marks the cyst. (B) Coronal CT MRIs image delineates the bronchogenic cyst with the MRI image, T1-weighted image shows liquid nature of the cyst contents, demonstrating dark contents consistent with fluid. T2-weighted confirms these findings as illustrated by cyst bright finding. Complete resection was achieved by right robotic thoracoscopic approach, and the cyst was filled with thick proteinaceous fluid. Red bordered arrow marks the cyst. CT, computed tomography; HU, Houndsfield units; MRI, magnetic resonance imaging.

with occasional mucin-filled goblet cells) and is comprised of variable amounts of hyaline cartilage, smooth muscle, and/or seromucinous bronchial glands (*Figure 4*) (7,8). Occasionally, bronchogenic cysts can undergo various histologic changes related to infarction, infection, and/or prior procedure. These changes include acute and chronic inflammation with epithelial denudation, hemorrhage with hemosiderin-laden macrophages, squamous metaplasia, cholesterol clefts, and fibrosis. Bronchogenic cysts typically develop into blind ending fluid-filled structures, though fistulization to adjacent organs and fatal air emboli have been reported (3,9-12). Malignant transformation is very rare but reported in the literature (13,14). The objective of our review is to summarize the historical management of bronchogenic cysts and the impact of evolving technologies including minimally invasive excision and endoscopic drainage. The article is presented in accordance with the Narrative Review reporting checklist (available at https://med.amegroups.com/article/view/10.21037/med-22-46/rc).

Methods

We systematically searched the available electronic literature, PubMed and Google Scholar to identify relevant case series in the adult and pediatric peer reviewed literature focusing on diagnosis and management of bronchogenic cysts. We searched the following terms 'bronchogenic cyst', 'bronchogenic parenchymal cysts',

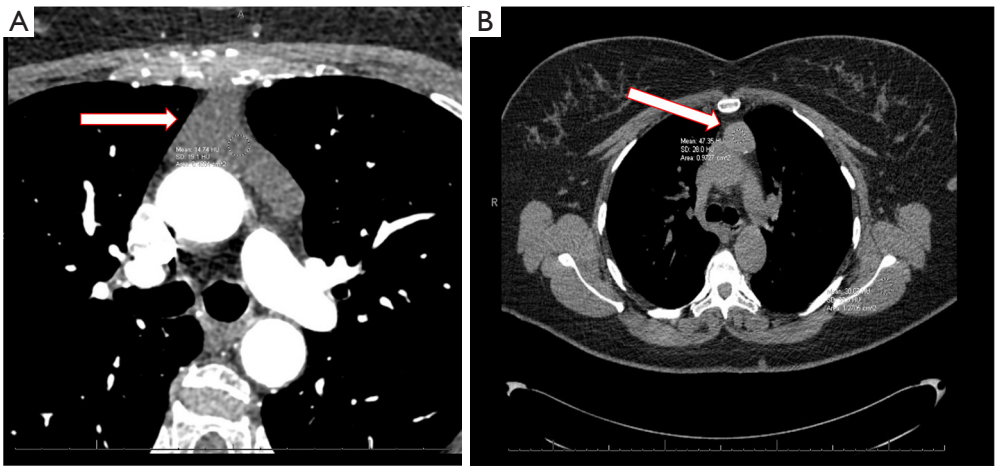

Figure 2 Anterior mediastinal bronchogenic cyst. (A) Incidental finding on cardiac CT scan for coronary artery calcium scoring in a 75-year-old asymptomatic woman. The cyst has low density with HU of 14 and clear fluid was found in the cyst at the time of robotic thoracoscopic resection. Red bordered arrow marks the cyst. (B) Incidental finding of anterior mediastinal cystic lesions by CT scan of the chest for investigation of non-specific chest discomfort in a 45-year-old woman. The cyst content had a high density with HU of 47 and proteinaceous fluid was drained that the time of robotic thoracoscopic resection. Red bordered arrow marks the cyst. CT, computed tomography; HU, Houndsfield units.

'bronchogenic mediastinal cysts', 'drainage bronchogenic cyst', 'pediatric bronchogenic cysts' and 'VATS bronchogenic cyst' (*Table 1*).

Discussion

Clinical presentations

Bronchogenic cysts are frequently incidental findings on ultrasound or chest radiograph in the neonatal period (4). Symptoms in neonates are usually related to mass effect on the involved structure or infection (15). Major bronchus obstruction is rare but has been reported in the setting of a subcarinal cyst (16). More commonly, the presentation mimics centrilobular emphysema secondary to air trapping of the smaller airways (17). The presentation of bronchogenic cysts in the adult population ranges from an asymptomatic incidental finding of computed tomography (CT) of the chest to a clinical presentation of hemoptysis, pneumothorax, pneumonia (bronchogenic cyst in the lung parenchyma) or chest pain, dysphagia, central venous compression due to mass effecting the mediastinum. Imaging diagnosis is typically made using CT scan, demonstrating a smooth mass with sharp borders (occasionally lobulated), with cystic components (3,18). Masses can occasionally appear solid on CT, and in this setting, magnetic resonance imaging (MRI) can serve as an adjunctive role to highlight the cystic nature of these lesions. Fluid-filled cystic lesion demonstrates high T2 intensity without enhancement with contrast, T1 weighted imaging is variable depending upon cystic contents and their relative tissue composition (*Figure 1*) (3). Fiberoptic bronchoscopy with endoscopic bronchial ultrasound (EBUS) has been used to further characterize peri-bronchial cystic masses and can serve a dual therapeutic role by allowing for aspiration in cases of compressive symptoms while providing a pathologic diagnosis, albeit with an increased risk of infection secondary to bacterial contamination of the cyst content by the transbronchial needle (19-22).

Treatment

Surgical excision remains the mainstay of therapy (23-25). Surgery in the neonate can be safely delayed allowing for weight gain. Symptomatic adult patients should undergo resection after immediate stabilization (26). Aspiration is a temporizing measure only for compressive symptoms and should be shortly followed by resection as there is a significant risk of infection following biopsy/aspiration, with very high incidence of short-term recurrence of the lesion, though some series are emerging advocating for drainage as a definitive means of therapy (19-21). Mediastinal bronchogenic cysts resection must ensure complete removal

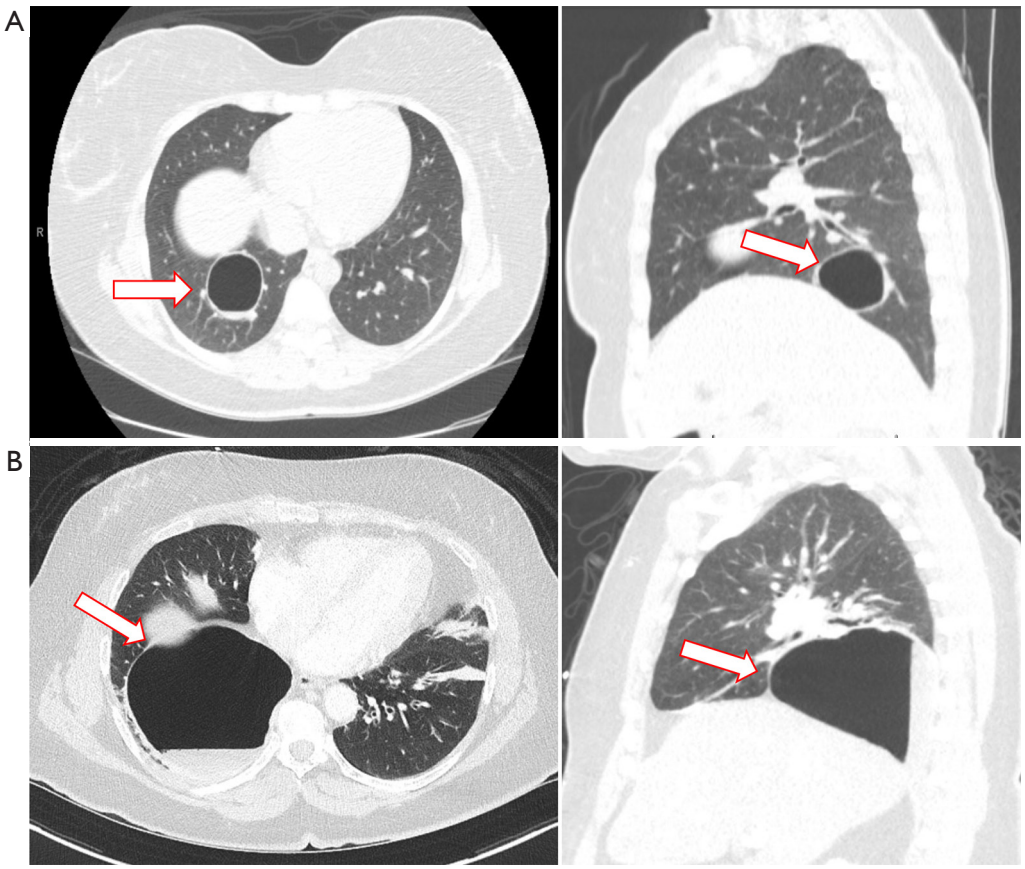

Figure 3 Intraparenchymal bronchogenic cyst. (A) Axial and sagittal images of a chest CT scan with intravenous contrast of a 34-year-old woman demonstrating a large peripherally located cyst in the right lower lobe, adjacent to segmental pulmonary vessels. She had a history an enlarging cystic lesion once complicated by an infection that was treated with a month-course of oral antibiotic. A complete resection was achieved by right robotic thoracoscopy and enucleation of the lung cyst separating the cyst wall from the underlying vessels and bronchus thus avoiding a pulmonary segmentectomy. Pathologic examination determined this lesion being a benign bronchogenic cyst. Red bordered arrow marks the cyst. (B) Axial and sagittal cuts of a CT scan with intravenous contrast of a 63-year-old woman admitted to the hospital with fever/chills and leukocytosis showing a cystic lesion in the right lower lobe with air-fluid level suggestive of an infected intrapulmonary bronchogenic cyst. This was her first presentation of a bronchogenic cyst. The cyst was completely resected by a right robotic thoracoscopy and wedge resection of the cyst. Final pathology report shows: Respiratory-lined cyst with fibrosis, adjacent fibrinopurulent exudate, granulation tissue and reactive mesothelial hyperplasia. Red bordered arrow marks the cyst. CT, computed tomography.

of the epithelium-lined cyst wall via resection or ablation to prevent the accumulation of fluid or recurrence (27,28). In the case of intrapulmonary bronchogenic cysts within lung parenchyma, lobectomy has been the historical gold standard though more recently parenchymal sparing approaches, such as non-anatomic wedge resection or segmentectomy, have been advocated by some surgeons (29). Thoracotomy has traditionally been the standard approach given their location and inflammation of surrounding tissues, with the vast majority of older series being exclusively completed via an open approach (14,26). With the emergence of minimally invasive platforms, resection of bronchogenic cysts either mediastinal or intraparenchymal variants can frequently be performed via thoracoscopic approach (25). Our own institutional experience follows more recent trends of adopting a robotic thoracoscopic platform for resection of these lesions (30,31). There are few long-term sequelae following resection of bronchogenic cysts, although recent literature still reports a combined morbidity and mortality rate of 9.8% in a mixed series comprising bronchogenic and other cystic lesions of the lung (32).

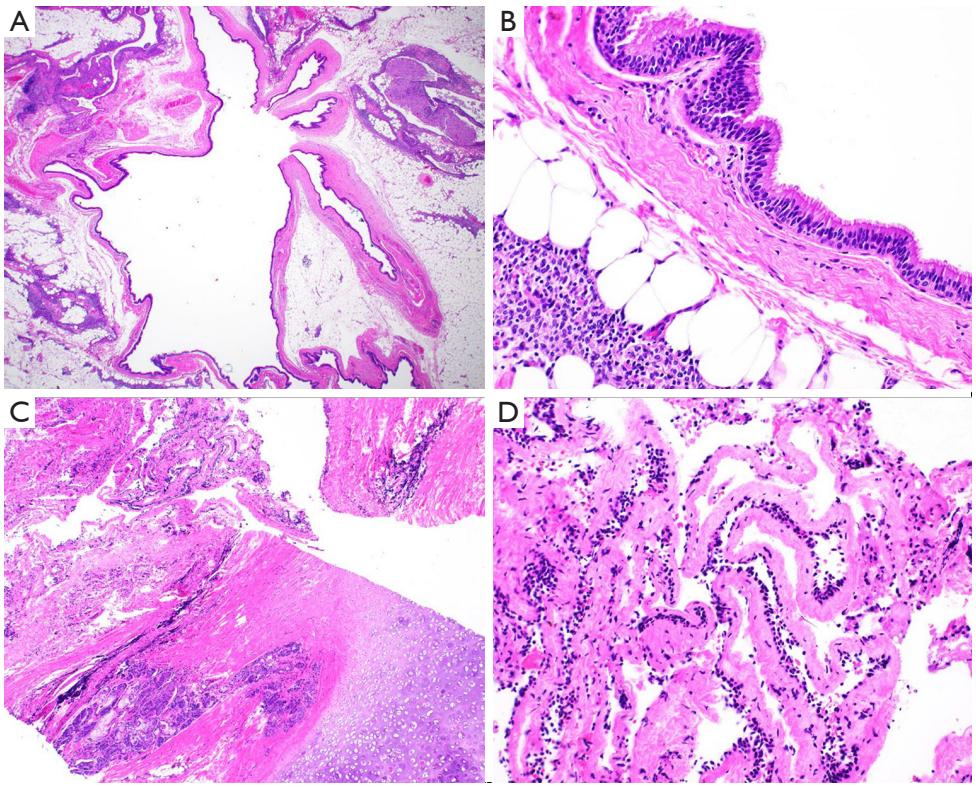

Figure 4 Histologic findings of bronchogenic cysts corresponding with imaging (hemoxylin & eosin stain). (A) Low power magnification (×12.5) reveals a thin-walled cyst with adjacent adipose and thymic tissue. (B) Higher power magnification (×400) demonstrates that the epithelial lining consists of ciliated pseudostratified columnar respiratory-type epithelium. The cyst wall lacks other features typical of a mature bronchogenic cyst. (C) Medium power magnification (×40) corresponding with images shown in *Figure 2A*,*2B* demonstrating an epithelial-lined cyst wall (upper lefthand corner) with adjacent seromucinous glands and mature hyaline cartilage (bottom righthand corner). (D) Higher power magnification (×200) demonstrates that the cyst wall is lined by an attenuated flat-to-cuboidal epithelium.

Table 1 Search strategy summary

Items	Specification
Date of search	7/1/2022–8/29/2022
Databases and other sources searched	PubMed, Google Scholar
Search terms used	'Bronchogenic cyst', 'bronchogenic parenchymal cysts', 'bronchogenic mediastinal cysts', 'drainage bronchogenic cyst', 'pediatric bronchogenic cysts', 'VATS bronchogenic cyst'
Timeframe	1975–2022
Inclusion and exclusion criteria	Inclusion: retrospective studies, meta-analyses, case studies
	Exclusion: thoracic duct cyst, necrotic
Selection process	One author compiled a list of eligible studies followed by review by the entire authorship team to determine suitability

VATS, video assisted thoracoscopic surgery.

Conclusions

Bronchogenic cysts are a relatively rare congenital malformation. Aspiration and EBUS potentially serve as useful adjuncts for compression relief and potential diagnosis but are plagued by high recurrence and risk of infection. The gold standard remains surgical excision with excellent long-term outcomes free of recurrence and low peri-operative morbidity/mortality. Video-assisted thoracoscopic resection has emerged as a viable approach and with the adoption of the robotic platform for minimally invasive thoracic surgery, thoracoscopic resection has become more feasible. The transition from open to video assisted thoracoscopic surgery (VATS) to robotic-assisted thoracoscopy has followed the authors' experience and has been associated with few complications. Therefore, we advocate for minimally invasive resection as a diagnostic and therapeutic procedure in a single setting with relatively few complications in our own institutional experience.

Acknowledgments

Funding: None.

Footnote

Provenance and Peer Review: This article was commissioned by the Guest Editor (Nestor Villamizar) for the series "Mediastinal Cysts" published in *Mediastinum*. The article has undergone external peer review.

Reporting Checklist: The authors have completed the Narrative Review reporting checklist. Available at https://med.amegroups.com/article/view/10.21037/med-22-46/rc

Peer Review File: Available at https://med.amegroups.com/article/view/10.21037/med-22-46/prf

Conflicts of Interest: All authors have completed the ICMJE uniform disclosure form (available at https://med.amegroups.com/article/view/10.21037/med-22-46/coif). The series "Mediastinal Cysts" was commissioned by the editorial office without any funding or sponsorship. The authors have no other conflicts of interest to declare.

Ethical Statement: The authors are accountable for all aspects of the work in ensuring that questions related to the accuracy or integrity of any part of the work are appropriately investigated and resolved.

References

1. Meyer H. Ueber angeborene blasige Missbildung der Lungen, nebst einigen Bemerkungen über Cyanose aus Lungenleiden. Archiv f pathol Anat 1859;16:78-95.
2. Coselli MP, de Ipolyi P, Bloss RS, et al. Bronchogenic cysts above and below the diaphragm: report of eight cases. Ann Thorac Surg 1987;44:491-4.
3. McAdams HP, Kirejczyk WM, Rosado-de-Christenson ML, et al. Bronchogenic cyst: imaging features with clinical and histopathologic correlation. Radiology 2000;217:441-6.
4. Di Lorenzo M, Collin PP, Vaillancourt R, et al. Bronchogenic cysts. J Pediatr Surg 1989;24:988-91.
5. St-Georges R, Deslauriers J, Duranceau A, et al. Clinical spectrum of bronchogenic cysts of the mediastinum and lung in the adult. Ann Thorac Surg 1991;52:6-13.
6. Suen HC, Mathisen DJ, Grillo HC, et al. Surgical management and radiological characteristics of bronchogenic cysts. Ann Thorac Surg 1993;55:476-81.
7. Bailey PV, Tracy T Jr, Connors RH, et al. Congenital bronchopulmonary malformations. Diagnostic and therapeutic considerations. J Thorac Cardiovasc Surg 1990;99:597-603.
8. Limaïem F, Ayadi-Kaddour A, Djilani H, et al. Pulmonary and mediastinal bronchogenic cysts: a clinicopathologic study of 33 cases. Lung 2008;186:55-61.
9. Sarper A, Ayten A, Golbasi I, et al. Bronchogenic cyst. Tex Heart Inst J 2003;30:105-8.
10. Zaugg M, Kaplan V, Widmer U, et al. Fatal air embolism in an airplane passenger with a giant intrapulmonary bronchogenic cyst. Am J Respir Crit Care Med 1998;157:1686-9.
11. Closon M, Vivier E, Breynaert C, et al. Air embolism during an aircraft flight in a passenger with a pulmonary cyst: a favorable outcome with hyperbaric therapy.

Anesthesiology 2004;101:539-42.
12. Pages ON, Rubin S, Baehrel B. Intra-esophageal rupture of a bronchogenic cyst. Interact Cardiovasc Thorac Surg 2005;4:287-8.
13. Whooley J, White A, Soo A. Bronchogenic cyst: a rare case of malignant transformation. BMJ Case Rep 2022;15:e248916.
14. Cuypers P, De Leyn P, Cappelle L, et al. Bronchogenic cysts: a review of 20 cases. Eur J Cardiothorac Surg 1996;10:393-6.
15. Haller JA, Shermeta DW, Donahoo JS, et al. Life-threatening respiratory distress from mediastinal masses in infants. Ann Thorac Surg 1975;19:365-70.
16. Funakoshi Y, Takeda S, Kadota Y, et al. Mediastinal bronchogenic cyst with respiratory distress from airway and vascular compression. Thorac Cardiovasc Surg 2007;55:53-4.
17. Lucaya J, Baert AL, Strife JL. Pediatric Chest Imaging: Chest Imaging in Infants and Children. Heidelberg: Springer Berlin; 2007.
18. Yoon YC, Lee KS, Kim TS, et al. Intrapulmonary bronchogenic cyst: CT and pathologic findings in five adult patients. AJR Am J Roentgenol 2002;179:167-70.
19. Bukamur HS, Alkhankan E, Mezughi HM, et al. The role and safety of endobronchial ultrasound-guided transbronchial needle aspiration in the diagnosis and management of infected bronchogenic mediastinal cysts in adults. Respir Med Case Rep 2018;24:46-9.
20. Onuki T, Kuramochi M, Inagaki M. Mediastinitis of bronchogenic cyst caused by endobronchial ultrasound-guided transbronchial needle aspiration. Respirol Case Rep 2014;2:73-5.
21. Rajmane R, Adams AM, Rajmane O, et al. Cyst Rupture After Endobronchial Ultrasound-guided Transbronchial Needle Aspiration. J Bronchology Interv Pulmonol 2016;23:e20-2.
22. Singh A, Singh S, Malpani A, et al. Treatment of bronchogenic cyst surgical versus transbronchial drainage? J Bronchology Interv Pulmonol 2011;18:359-61.
23. Bolton JW, Shahian DM. Asymptomatic bronchogenic cysts: what is the best management? Ann Thorac Surg 1992;53:1134-7.
24. Martinod E, Pons F, Azorin J, et al. Thoracoscopic excision of mediastinal bronchogenic cysts: results in 20 cases. Ann Thorac Surg 2000;69:1525-8.
25. Weber T, Roth TC, Beshay M, et al. Video-assisted thoracoscopic surgery of mediastinal bronchogenic cysts in adults: a single-center experience. Ann Thorac Surg 2004;78:987-91.
26. Patel SR, Meeker DP, Biscotti CV, et al. Presentation and management of bronchogenic cysts in the adult. Chest 1994;106:79-85.
27. Gharagozloo F, Dausmann MJ, McReynolds SD, et al. Recurrent bronchogenic pseudocyst 24 years after incomplete excision. Report of a case. Chest 1995;108:880-3.
28. Hasegawa T, Murayama F, Endo S, et al. Recurrent bronchogenic cyst 15 years after incomplete excision. Interact Cardiovasc Thorac Surg 2003;2:685-7.
29. Mestan H, Ceylan KC, Kaya ŞÖ. Surgery outcomes of the bronchogenic cysts. Eur Respir J 2019;54:PA1094.
30. Caterino U, Amore D, Cicalese M, et al. Anterior bronchogenic mediastinal cyst as priority procedure for robotic thoracic surgery. J Thorac Dis 2017;9:E674-6.
31. Xu S, Liu B, Wang X, et al. Robotic thoracic surgery of the anterior superior mediastinal bronchogenic cyst. Ann Transl Med 2015;3:57.
32. Makhija Z, Moir CR, Allen MS, et al. Surgical management of congenital cystic lung malformations in older patients. Ann Thorac Surg 2011;91:1568-73; discussion 1573.

doi: 10.21037/med-22-46
Cite this article as: Gross DJ, Briski LM, Wherley EM, Nguyen DM. Bronchogenic cysts: a narrative review. Mediastinum 2023;7:26.

Review Article

Multimodality imaging of mediastinal masses and mimics

John Matthew Archer, Jitesh Ahuja, Chad D. Strange, Girish S. Shroff, Gregory W. Gladish, Bradley S. Sabloff, Mylene T. Truong^

Department of Thoracic Imaging, University of Texas MD Anderson Cancer Center, Houston, TX, USA

Contributions: (I) Conception and design: All authors; (II) Administrative support: All authors; (III) Provision of study materials or patients: All authors; (IV) Collection and assembly of data: All authors; (V) Data analysis and interpretation: All authors; (VI) Manuscript writing: All authors; (VII) Final approval of manuscript: All authors.

Correspondence to: Mylene T. Truong, MD. Department of Thoracic Imaging, University of Texas MD Anderson Cancer Center, 1400 Pressler Street, Unit 1478, Houston, TX 77030-4008, USA. Email: mtruong@mdanderson.org.

Abstract: A wide variety of neoplastic and nonneoplastic conditions occur in the mediastinum. Imaging plays a central role in the evaluation of mediastinal pathologies and their mimics. Localization of a mediastinal lesion to a compartment and characterization of morphology, density/signal intensity, enhancement, and mass effect on neighboring structures can help narrow the differentials. The International Thymic Malignancy Interest Group (ITMIG) established a cross-sectional imaging-derived and anatomy-based classification system for mediastinal compartments, comprising the prevascular (anterior), visceral (middle), and paravertebral (posterior) compartments. Cross-sectional imaging is integral in the evaluation of mediastinal lesions. Computed tomography (CT) and magnetic resonance imaging (MRI) are useful to characterize mediastinal lesions detected on radiography. Advantages of CT include its widespread availability, fast acquisition time, relatively low cost, and ability to detect calcium. Advantages of MRI include the lack of radiation exposure, superior soft tissue contrast resolution to detect invasion of the mass across tissue planes, including the chest wall and diaphragm, involvement of neurovascular structures, and the potential for dynamic sequences during free-breathing or cinematic cardiac gating to assess motion of the mass relative to adjacent structures. MRI is superior to CT in the differentiation of cystic from solid lesions and in the detection of fat to differentiate thymic hyperplasia from thymic malignancy.

Keywords: Mediastinal compartments; mediastinal mass; computed tomography (CT); magnetic resonance imaging (MRI)

Received: 15 November 2022; Accepted: 28 April 2023; Published online: 08 May 2023.
doi: 10.21037/med-22-53
View this article at: https://dx.doi.org/10.21037/med-22-53

Introduction

A wide variety of neoplastic and nonneoplastic conditions occur in the mediastinum. While many mediastinal masses are incidentally detected on imaging, some are associated with nonspecific symptoms such as shortness of breath and chest discomfort. Cross-sectional imaging plays a central role in the evaluation of mediastinal pathologies and their mimics. Improvements in computed tomography (CT) and magnetic resonance imaging (MRI) have resulted in greater lesion characterization allowing radiologists to suggest limited differentials or specific diagnoses.

Mediastinal compartments classification

Several mediastinal classification systems have been developed, which historically were based on nonanatomic

^ ORCID: 0000-0001-9795-529X.

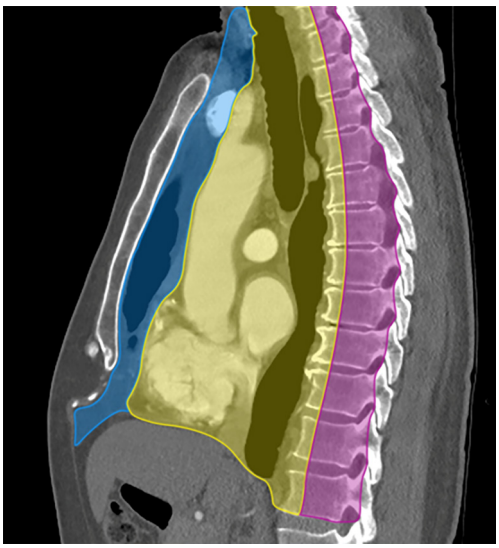

Figure 1 ITMIG classification of mediastinal compartments bound superiorly by the thoracic inlet and inferiorly by the diaphragm. Sagittal CT with intravenous contrast shows the prevascular compartment (blue), bound anteriorly by the sternum and posteriorly by the anterior aspect of the parietal pericardium, and contains the thymus, fat, lymph nodes, and the left brachiocephalic vein. The visceral compartment (yellow) is bound anteriorly by the posterior boundaries of the prevascular compartment, and posteriorly by a vertical line 1 cm posterior to the anterior margin of each thoracic vertebral body, and contains the trachea, esophagus, lymph nodes, and vascular structures including the heart, thoracic aorta, superior vena cava, intrapericardial pulmonary arteries, and the thoracic duct. The paravertebral compartment (pink) is bound anteriorly by the posterior boundaries of the visceral compartment, and posterolaterally by a vertical line against the posterior margin of the chest wall at the lateral margin of the transverse process of the thoracic spine. ITMIG, International Thymic Malignancy Interest Group; CT, computed tomography.

divisions on the lateral chest radiographs. The International Thymic Malignancy Interest Group (ITMIG) established a cross-sectional imaging-derived and anatomy-based classification system for mediastinal compartments (1). The ITMIG classification system includes prevascular (anterior), visceral (middle), and paravertebral (posterior) compartments (2). Localization of a mediastinal lesion to a compartment can help narrow differentials (*Figure 1*).

Prevascular compartment

The contents of the prevascular compartment include the thymus, lymph nodes, fat, and the left brachiocephalic vein. The prevascular compartment is bound superiorly by the thoracic inlet, inferiorly by the diaphragm, anteriorly by the sternum, laterally by the parietal mediastinal pleura, and posteriorly by the anterior aspect of the pericardium (2).

Visceral compartment

The contents of the visceral compartment include the trachea, carina, esophagus, lymph nodes, and vascular structures such as the heart, thoracic aorta, superior vena cava (SVC), intrapericardial pulmonary arteries, and thoracic duct. The visceral compartment is bound superiorly by the thoracic inlet, inferiorly by the diaphragm, anteriorly by the posterior boundary of the prevascular compartment, and posteriorly by a vertical line connecting each thoracic vertebral body 1 cm posterior to its anterior margin (2).

Paravertebral compartment

The contents of the paravertebral compartment include the thoracic spine and the paravertebral soft tissues. The paravertebral compartment is bound superiorly by the thoracic inlet, inferiorly by the diaphragm, anteriorly by the posterior boundary of the visceral compartment, and posterolaterally by a vertical line at the lateral margin of the transverse processes along the posterior margin of the chest wall (2).

Imaging evaluation

Chest radiography can detect a mediastinal mass with the loss of normal mediastinal borders (referred to as the silhouette sign) (*Figure 2*). The American College of Radiology Appropriateness Criteria Imaging of Mediastinal Masses recommends either CT or MRI as the next imaging study of patients with indeterminate mediastinal mass detected on radiography (3). CT and MRI can characterize size, location, morphology, margins, density/intensity, enhancement, and invasion of neighboring structures (4). Advantages of CT include its widespread availability, fast acquisition time, relatively low cost, and detection of calcium (5). Advantages of MRI include lack of radiation exposure, superior soft tissue contrast resolution to detect invasion of the mass across tissue planes, including the chest wall and diaphragm, involvement of neurovascular structures, and potential for dynamic sequences during free-

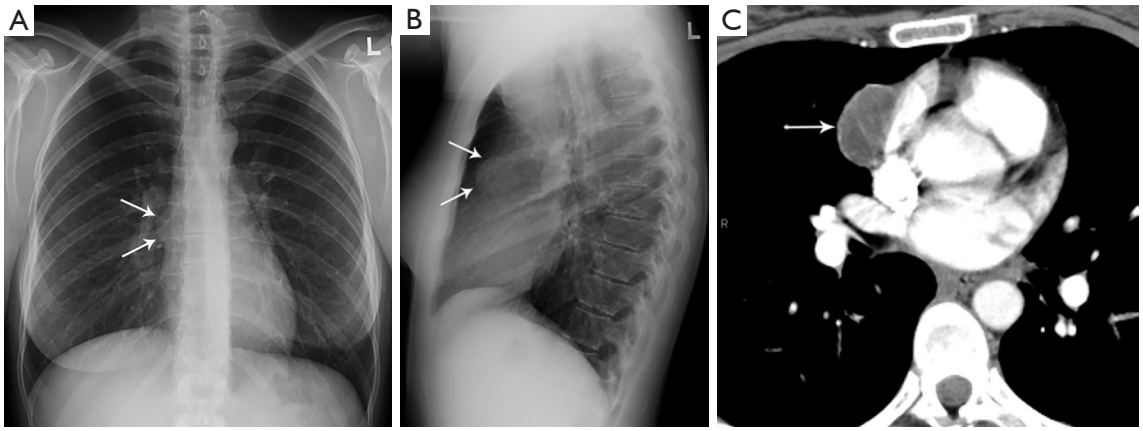

Figure 2 Pericardial cyst. (A,B) Frontal and lateral chest radiograph shows subtle contour abnormality (arrows) with loss of the silhouette of part of the right mediastinal border termed the "silhouette sign". (C) CT shows low attenuation consistent with pericardial cyst (arrow). CT, computed tomography.

breathing or cinematic cardiac gating to assess motion of the mass relative to adjacent structures (3). MRI is superior to CT in the differentiation of cystic from solid lesions and in detection of fat to differentiate thymic hyperplasia from thymic malignancy.

Cystic lesions

Cystic lesions represent 15% to 20% of mediastinal masses (6). Cystic lesions occur in all three mediastinal compartments. CT features that distinguish benign cysts include an imperceptible or thin wall with no significant enhancement, homogenous attenuation, water attenuation [between 0 and 10 Hounsfield units (HU)], and no invasion of mediastinal structures (7). However, some benign mediastinal cysts can have attenuation values of up to 100 HU and therefore mimic solid lesions on CT, leading to unnecessary surgical resection, including thymectomy (8).

When CT features are indeterminate, further imaging evaluation with MRI can provide diagnostic information (9). Cysts on MRI typically are hypointense on T1-weighted images, hyperintense on T2-weighted images and do not show contrast enhancement. However, cysts with blood products can be hypointense on T2-weighted MRI.

Pericardial cyst

Pericardial cysts are most commonly located in the anterior cardiophrenic angles, right more common than left (10). However, these lesions can arise anywhere along the pericardial lining and can be remote from the cardiophrenic angles (10) (*Figure 3*). Approximately one-third of pericardial cysts are associated with symptoms including chest pain, dyspnea, or persistent cough (10). Pedunculated pericardial cysts can appear to be mobile when imaged at different times (11). On radiography pericardial cysts appear as smooth, round masses at the cardiophrenic angle. On CT, these lesions demonstrate water attenuation and an imperceptible wall.

Bronchogenic cyst

Bronchogenic cysts develop from abnormal budding of the primitive ventral foregut, which gives rise to the tracheobronchial tree (12). Bronchogenic cysts contain mucoid material and a respiratory epithelium lining (13).

In one series of 66 patients, 58% were symptomatic at presentation with the most common symptoms being pain, dyspnea, respiratory infection, wheezing, and cough (14). Although these lesions most commonly are located in the mediastinum, approximately 15% of bronchogenic cysts are extramediastinal, located in the lung parenchyma or rarely in the diaphragm or pleura (14).

These lesions have variable appearances on CT and MRI, depending on their contents. On CT, characteristic findings include sharp margins with soft-tissue or water attenuation (14). On MRI, these lesions can demonstrate variable signal intensity on T1-weighted sequences depending on the composition on their contents, with approximately 50% hyperintense relative to skeletal muscle (14). On T2-

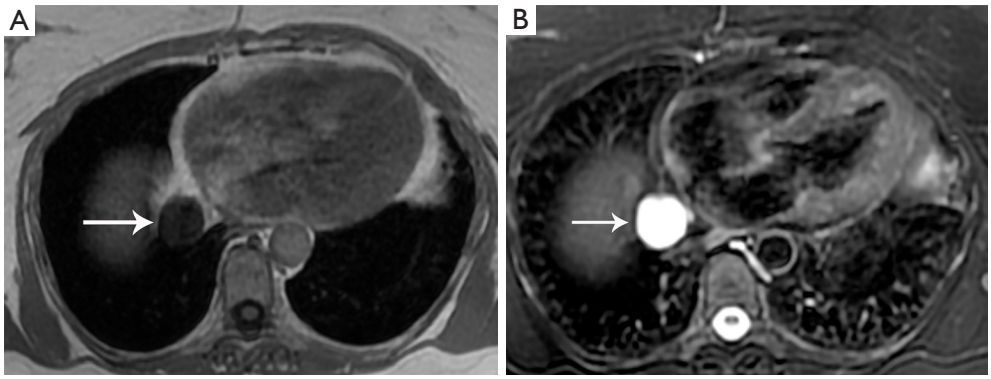

Figure 3 Pericardial cyst. (A,B) MRI images show typical low signal intensity on T1-weighted (A) and high signal intensity on T2-weighted (B) images of fluid (arrow) in the pericardial cyst. MRI, magnetic resonance imaging.

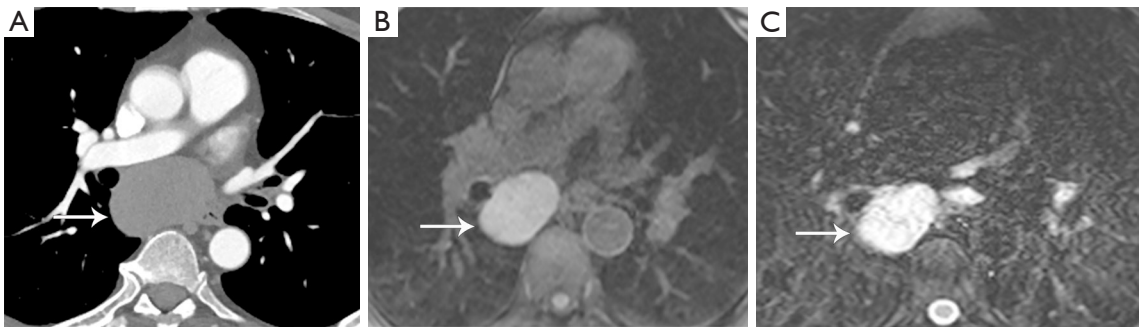

Figure 4 Esophageal duplication cyst. (A) Contrast enhanced CT shows lesion (arrow) in the right subcarinal region with heterogeneous attenuation and could be cystic or solid. When CT is indeterminate, MRI is useful to differentiate fluid from solid mediastinal lesions. (B,C) MRI images show the visceral mediastinal lesion (arrow) with intermediate signal intensity on T1-weighted (B) and high signal intensity on T2-weighted (C) MRI images. The intermediate signal intensity on T1-weighted images can be seen with cysts with proteinaceous material. CT, computed tomography; MRI, magnetic resonance imaging.

weighted sequences, bronchogenic cysts are isointense to hyperintense relative to cerebrospinal fluid (13,14).

Duplication cyst

Esophageal duplication cysts are the second most common benign esophageal lesion, with a wall comprised of smooth muscle and a mucosal lining (12,15). Ectopic gastric mucosa may be present within these lesions, which can result in hemorrhage or ulceration (2). Esophageal duplication cysts are typically located adjacent to or within the esophageal wall and can have thick walls (7). Similar to other mediastinal cystic lesions, the CT and MRI appearance can be variable depending on the cyst contents. Proteinaceous or hemorrhagic contents can cause these lesions to have hyperintense signal on T1-weighted sequences and soft-tissue attenuation on CT (*Figure 4*).

Fat-containing lesions

Fat-containing mediastinal lesions include both benign and malignant processes, such as mature teratoma, thymolipoma, thymic hyperplasia, lipoma, liposarcoma, and fat necrosis. On CT, fat-containing mediastinal lesions demonstrate macroscopic fat measuring between –40 and –120 HU. On MRI, areas of macroscopic fat demonstrate hyperintense signal on T1-weighted images and loss of signal of signal on T1-weighted fat saturated images. In-phase and opposed-phase gradient echo sequences can be helpful identifying intravoxel fat. When fat and soft tissue are present in the same voxel, as typically present with thymic hyperplasia or the normal thymus, there is a homogeneous decrease in signal intensity on opposed-phase images compared to in-phase images. When this signal drop is not clearly visible to the naked eye, quantitative calculation of signal drop in

chemical shift MRI can be useful. This can be measured with the Chemical Shift Ratio (CSR) or the more recent Signal Intensity Index (SII) (16). The CSR is dependent on the signal intensity of paraspinal musculature and its formula is: CSR = (tSIop/mSIop)/(tSIin/mSIin). On the other hand, SII does not depend on muscle signal intensity and is calculated as: SIIthy = [(tSIin – tSIop)/(tSIin)] × 100% (17), where t = thymus, SI = signal intensity, m = muscle, op = opposed phase, in = in phase.

Figure 5 Mature teratoma. Contrast enhanced CT shows large right mediastinal mass with heterogeneous attenuation, including calcifications (long arrow) and fat (short arrows). There is mass effect on the right atrium. CT, computed tomography.

Mature teratoma

Mature teratomas are benign mediastinal germ cell tumors, typically containing fat, fluid, calcification, and soft tissue (18). In a series of 66 mediastinal mature teratomas evaluated with CT, soft tissue was observed in 100%, fluid in 88%, fat in 76%, and calcifications in 53% (19) (*Figure 5*). Mature teratomas are more common in young patients, accounting for approximately 25% of anterior mediastinal masses in ages 10 to 19 and less than 5% over age 50 (20).

At CT, mature teratomas characteristically have a well-defined, lobulated, smooth margin with a heterogenous appearance (21). Common MRI findings include areas of hyperintense signal on T2-weighted sequences (consistent with fluid), and areas of hyperintense signal on T1-weighted sequences that are hypointense on fat-suppressed sequences (19).

Fat necrosis

Mediastinal fat necrosis is a rare, self-limiting process that can occur following trauma, interventional procedures, or surgery. On CT, characteristic findings include fat attenuation surrounded by a rim of soft tissue, with areas of fat stranding (22). On positron emission tomography (PET)/CT, fat necrosis can show focal avid uptake of [18F]-fluoro-2-deoxy-D-glucose (FDG) (23) (*Figure 6*). The CT and PET findings can present a diagnostic dilemma, as they can mimic nodal metastases. Partial or complete resolution of

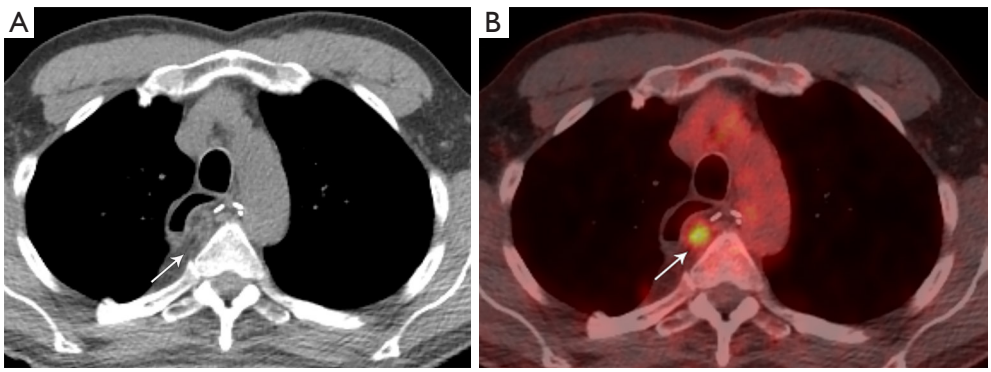

Figure 6 Fat necrosis. (A) CT shows oval lesion (arrow) posterior to the gastric pull-through in a patient treated for esophageal cancer. The lesion shows predominant fat attenuation demarcated by a soft tissue rim, typical of fat necrosis. (B) FDG PET/CT shows the fat necrosis (arrow) is FDG avid due to the inflammatory component and can be misinterpreted as tumor recurrence. CT, computed tomography; FDG, fluoro-2-deoxy-D-glucose; PET, positron emission tomography.

Figure 7 Hemangioma. CT shows large left mediastinal mass with focus of calcification (arrow) consistent with phlebolith interspersed with soft tissue and fat. CT, computed tomography.

FDG uptake is expected on follow-up PET/CT (23).

Spontaneous necrosis of the juxtapericardial mediastinal fat is an uncommon condition, typically presenting as a well-circumscribed fatty lesion with adjacent inflammatory changes along the cardiophrenic angle in patients presenting with acute chest pain (24). This condition is typically self-limiting and treatment consists of supportive therapy such as nonsteroidal anti-inflammatory drugs.

Enhancing lesions

Hemangioma

Mediastinal hemangiomas are uncommon benign vascular tumors, accounting for less than 0.5% of mediastinal masses (25). These lesions are most commonly located in the prevascular and paravertebral compartments (25,26). Histologically, hemangiomas are composed of vascular spaces with various stromal tissues, including fat, myxoid and fibrous tissues (27). On CT, these lesions are well circumscribed, with smooth or lobulated margins and heterogeneous attenuation. Similar to extramediastinal hemangiomas, one pattern of enhancement is the discontinuous peripheral nodular enhancement with progressive fill-in on delayed phases on both CT and MRI (28). On MRI, hemangiomas are hyperintense on T2-weighted sequences. Calcified phleboliths may be present. Although uncommon, fat may be interspersed throughout these lesions (25,29) (*Figure* 7).

Esophageal leiomyoma

Although leiomyomas are the most common benign neoplasm of the esophagus, esophageal carcinoma is approximately 50 times more common (15,30). While small tumors are typically asymptomatic, larger tumors can be associated with symptoms including epigastric discomfort, dysphagia, regurgitation, and gastrointestinal hemorrhage (30). These tumors occur most commonly in the middle and distal portions of the esophagus and multiple tumors are found in 3% to 10% of patients (30). On CT, leiomyomas are typically isoattenuating or hypoattenuating relative to smooth muscle on nonenhanced CT, with homogeneous enhancement following contrast administration (15,31). Calcifications may be present, and can be helpful in distinguishing them from other benign and malignant esophageal tumors (31). On MRI, leiomyomas are typically slightly hyperintense on T2-weighted sequences (15,31,32). Minimal or no FDG uptake is usually seen on PET (15,31).

Carney triad

The association of gastrointestinal leiomyosarcoma, extra-adrenal paraganglioma, and pulmonary chondromas was first described in 1977 by J. Aidan Carney (33). Carney triad is a rare condition caused by the down-regulation of succinate dehydrogenase (34). Although termed a triad, adrenocortical tumors and esophageal leiomyoma have been associated with this condition more recently (35).

Tumors originating from chromaffin cells are located in 90% of cases in the adrenal gland and called pheochromocytomas, while in the remaining 10% of cases have an extra-adrenal origin (paraganglionic cells scattered throughout the body) and are termed paragangliomas (36). In the anterior mediastinum, paragangliomas arise from the parasympathetic paraganglia, usually the aortic body chemoreceptors located in the aorticopulmonary window, and are termed aorticopulmonary paragangliomas or aortic body tumors. In the posterior mediastinum, paragangliomas arise from the sympathetic chain along the neck of the ribs in the paravertebral sulci. Mediastinal paragangliomas have indistinguishable imaging characteristics to paragangliomas elsewhere in the body. On CT, paragangliomas may show calcifications, areas of low attenuation that can reflect hemorrhage or cystic degeneration, and intense enhancement following the administration of contrast (36) (*Figure 8*). On MRI, paragangliomas are typically hyperintense on T2-weighted sequences and have a characteristic "salt-and-pepper" pattern cause by areas of signal void related to high velocity flow in intratumoral vessels (36). However, many paragangliomas, especially

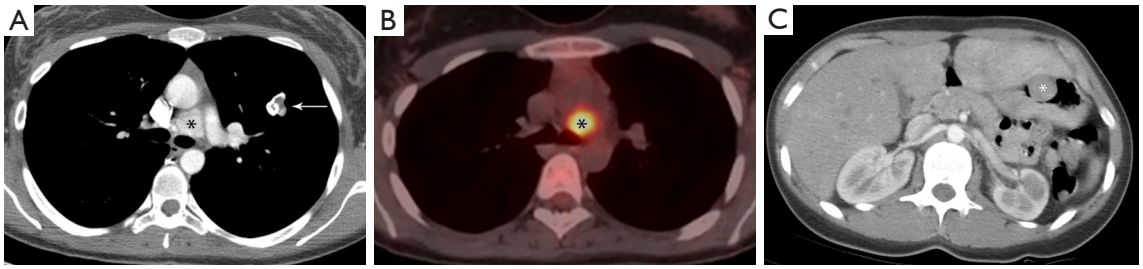

Figure 8 Carney's triad. (A) Contrast enhanced CT shows enhancement of the left paratracheal mediastinal soft tissue mass (asterisk) due to paraganglioma and a solid lung nodule in the left upper lobe with coarse calcification (arrow) consistent with chondroma. (B) FDG PET/CT shows increased FDG uptake of the paraganglioma (asterisk). (C) Contrast-enhanced CT abdomen shows round well-circumscribed soft tissue nodule (asterisk) in the anterior wall of the stomach consistent with gastrointestinal stromal tumor. CT, computed tomography; FDG, fluoro-2-deoxy-D-glucose; PET, positron emission tomography.

small ones, may not exhibit the "salt and pepper pattern" on MRI. PET/CT with 68-Ga DOTATATE is increasingly used for the diagnosis and follow-up of paragangliomas. PET/CT with ^{18}F-FDG has been shown to better detect metastatic disease/recurrent disease in comparison to 123-Iodine metaiodobenzylguanidine (MIBG) and CT/MRI (37).

Gastrointestinal stromal tumors (GIST) are the most common mesenchymal malignancy of the gastrointestinal tract (38). GISTs were previously referred to as gastrointestinal smooth muscle tumor: leiomyoma if benign, and leiomyosarcoma if malignant (38). While the stomach is the most common site of involvement, GISTs can occur from the distal esophagus to the anus (38). In the esophagus, the most common benign neoplasm is leiomyoma, far more common than GISTs. These lesions can present with gastrointestinal hemorrhage or pain. Distant metastases are present in greater than 50% of patients, with the peritoneum and liver being the most common sites of spread (39). While thoracic metastases are relatively uncommon, occurring in approximately 10% of patients, the most common sites of involvement are the lungs, intrathoracic lymph nodes, bones, and pleura (39). On CT, GISTs typical imaging characteristics include large, exophytic, heterogeneously enhancing masses with areas of hypo-enhancement corresponding to necrosis, hemorrhage, or cystic degeneration (40). On MRI, small GISTs (≤5 cm) appeared as round tumors with strong and homogeneous arterial enhancement and a persistent enhancement pattern. Large GISTs (>5 cm) appeared as lobulated tumors with mild heterogeneous gradual enhancement, and they frequently exhibited intratumoral cystic change. The presence of intratumoral cysts or a low apparent diffusion coefficient (ADC) value is suggestive of a high-risk GIST (41).

The final component of Carney's triad is pulmonary chondromas, composed of hyaline cartilage surrounded by a thin fibrous pseudocapsule (42). On CT, pulmonary chondromas typically appears as round nodules with smooth margins, and a variable amount of calcification (43). On MRI, calcifications within the lesions appear as foci of low signal intensity (44).

Ectopic parathyroid adenoma

The parathyroid glands are typically located along the posterior border of the thyroid gland. Parathyroid glands located above or below the thyroid gland in the neck or mediastinum are considered ectopic (45). The inferior parathyroid glands are more commonly ectopic, located in the mediastinum in approximately 4% to 5% of the population (45). Patients can present with incidentally detected hypercalcemia (46). Symptoms of hypercalcemia can include muscle pain, lethargy, nausea, constipation, and confusion.

Parathyroid adenomas are typically oval or rounded with smooth margins, occasionally cystic (47). There are multiple options for imaging of parathyroid adenomas, including CT, MRI, and single photon emission computed tomography (SPECT) using technetium-99m (99mTc) sestamibi. Many centers utilize pre-contrast and post-contrast CT (with arterial and delayed phases) for the detection of parathyroid adenoma. The primary purpose of the pre-contrast CT is to distinguish high-attenuation thyroid tissue from arterially enhancing parathyroid adenoma (which should be low attenuation on pre-contrast images) (47) (*Figure 9*). Rapid washout of contrast material is expected from the arterial

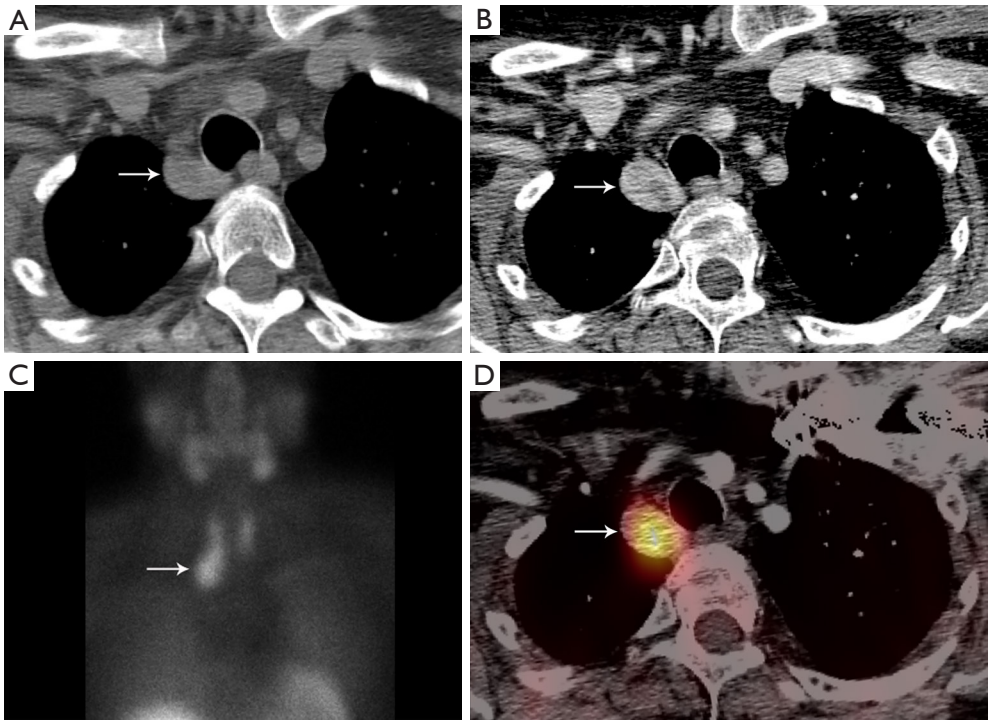

Figure 9 Ectopic parathyroid adenoma. (A,B) Pre- and post-contrast enhanced CT show right paratracheal solid lesion (arrow) with heterogeneous enhancement. The pre-contrast CT is useful to differentiate high attenuation thyroid tissue from low attenuation parathyroid tissue. (C,D) Technetium-99m sestamibi parathyroid scintigraphy and SPECT/CT show the right parathyroid adenoma is sestamibi avid (arrow). CT, computed tomography; SPECT, single photon emission computed tomography.

to delayed phases (47). High-temporal-resolution dynamic contrast enhanced (DCE) MRI allows differentiation of the parathyroid glands from lymph nodes and thyroid tissue due to their faster arterial enhancement and earlier contrast washout, with a mean parathyroid maximal enhancement of 13 seconds earlier than thyroid tissue and 29 seconds earlier than lymph nodes using this technique (48). MRI has the benefit of making the diagnosis without subjecting the patient to ionizing radiation exposure.

Although the majority of parathyroid adenomas occur in isolation, several genetic syndromes have been associated with parathyroid neoplasia, including multiple endocrine neoplasia (MEN) types 1 and 2A. MEN 1 and 2A are autosomal dominant conditions (49). Hyperparathyroidism in these conditions is typically multiglandular (49). The classic components of MEN 1 include parathyroid tumors, pancreatic islet cell tumors, and pituitary tumors. Additional associations in MEN 1 include facial angiofibromas, adrenal cortical tumors, lipomas, and carcinoid tumors (49). MEN 2A is characterized by medullary thyroid carcinoma, pheochromocytomas, and parathyroid hyperplasia or tumors.

Paravertebral lesions

The paravertebral compartment of the mediastinum includes the spine and paravertebral soft tissues. When a mass is detected in the paravertebral region on CT, the most likely diagnosis is a neurogenic lesion. There are two broad categories of neurogenic neoplasms: peripheral nerve sheath tumors such as schwannoma or neurofibroma which present as round or dumbbell lesions and the sympathetic ganglion neoplasms such as ganglioneuroma (*Figure 10*), ganglioneuroblastoma and neuroblastoma which present as

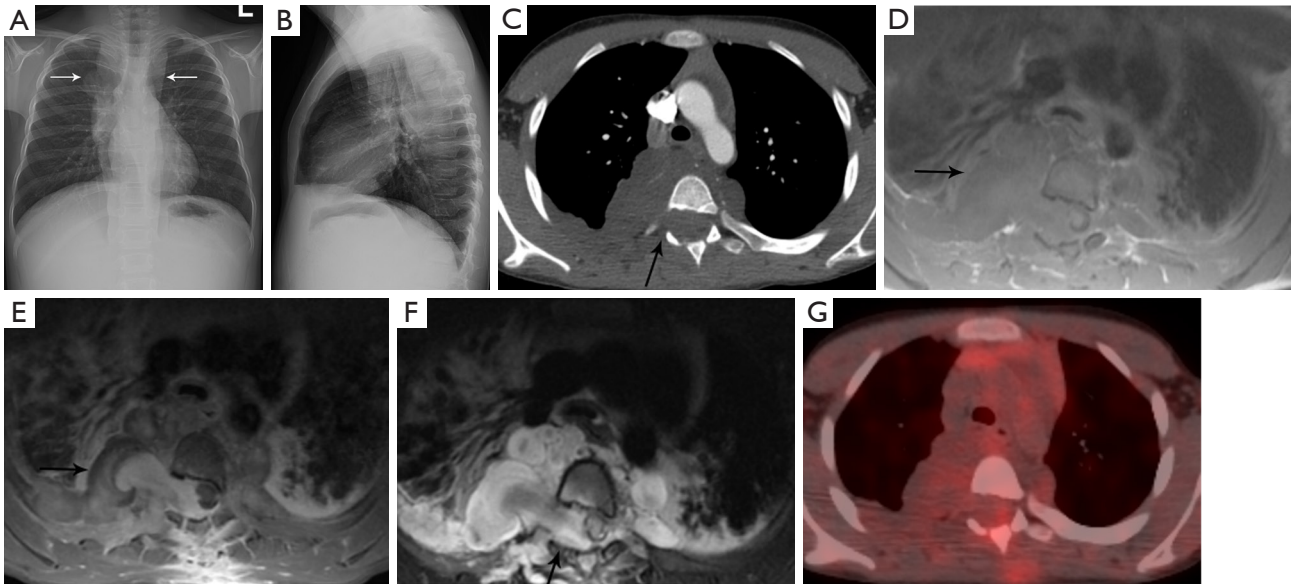

Figure 10 Ganglioneuroma. (A,B) PA and lateral chest radiographs show elongated bilateral posterior mediastinal lesion (arrows) extending from the neck down to below the diaphragm. (C) Axial contrast enhanced CT shows bilateral paraspinal masses with low attenuation and enlargement of the right neural foramen of T4 (arrow) with extension into the spinal canal. (D) Axial T1-weighted MRI shows the mass (arrow) is heterogeneous with iso- to hyperintense signal. Extension into the spinal canal displaces and the spinal cord to the left with abnormal signal intensity within the cord due to cord compression and edema. (E) Axial T1-weighted post-contrast MRI shows the mass (arrow) enhances heterogeneously. (F) Axial T2-weighted MRI shows the mass (arrow) is heterogeneously hyperintense. (G) Fused PET/CT shows the ganglioneuroma is not FDG avid. Biopsy confirmed ganglioneuroma. PA, posterior anterior; CT, computed tomography; MRI, magnetic resonance imaging; PET, positron emission tomography; FDG, fluoro-2-deoxy-D-glucose.

elongated masses involving 3 or more vertebral levels. Other less common neoplasms in the differential include lymphoma, bone tumors, and metastases. Nonneoplastic entities include spinal infections, cystic lesions (meningocele and neurenteric cyst), pancreatic pseudocyst and extramedullary hematopoiesis.

Accounting for 70% of mediastinal neurogenic tumors, peripheral nerve sheath tumors arise from spinal or proximal intercostal nerves, less commonly from the vagus, recurrent laryngeal, or phrenic nerves (50). Peripheral nerve sheath neoplasms can show communication with the spinal canal. Areas of heterogeneity may be due to cystic changes or hemorrhage and are more common in schwannomas than in neurofibromas (*Figure 11*) (50). Neurogenic tumors can erode adjacent ribs or vertebrae and enlarge the neural foramina. MRI is useful to show the extent of intraspinal/extradural extension. The "fascicular sign" is seen in some schwannomas and refers to multiple hypointense, small, ring-like structures corresponding to fascicular bundles. The "target sign" is more commonly seen in neurofibromas than in schwannomas and refers to the central low signal intensity surrounded by peripheral high signal intensity. FDG PET/CT is useful to differentiate malignant peripheral nerve sheath tumors from benign neurofibromas, with sensitivity of 95% and specificity of 72% (51). It is important to be aware that some schwannomas may demonstrate intense FDG avidity (52).

Additional imaging considerations for mediastinal lesions

Mediastinal lesions can exert mass effect on the critical

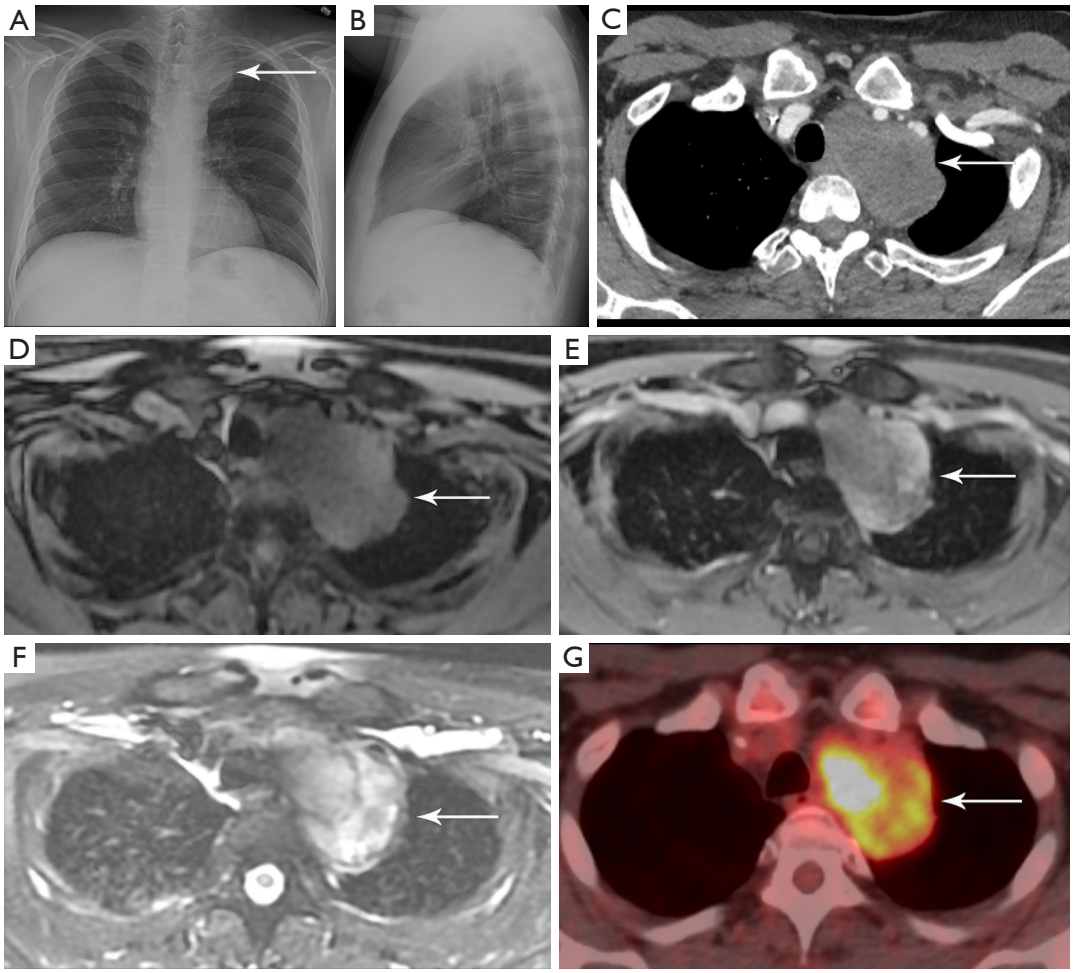

Figure 11 Schwannoma. (A,B) PA and lateral chest radiographs show a left mediastinal mass (arrow) in the upper thorax. (C) Axial contrast enhanced CT shows the mass (arrow) is solid with heterogeneous attenuation. (D) Axial T1-weighted MRI shows the mass (arrow) is isointense to muscle. (E) Axial T1-weighted post-contrast MRI shows the mass (arrow) enhances heterogeneously. (F) Axial T2-weighted MRI shows the mass (arrow) is heterogeneously hyperintense with cystic areas. (G) Fused PET/CT shows the mass (arrow) is FDG avid. Biopsy confirmed schwannoma. PA, posterior anterior; CT, computed tomography; MRI, magnetic resonance imaging; PET, positron emission tomography; FDG, fluoro-2-deoxy-D-glucose.

vascular structures. Masses in the prevascular and visceral compartments can compress and obstruct the SVC. Patients with SVC obstruction may present with upper body edema, distended neck veins, dyspnea, cough, hoarseness, syncope, headaches, and dizziness (53). Cerebral edema and narrowing of the respiratory tract due to edema are rare, but potentially serious effects (53). The most common malignancies associated with SVC syndrome include lung cancer, lymphoma, metastatic cancer, germ-cell tumors, and thymomas (53). The imaging modality of choice is contrast enhanced CT (*Figure 12*). Symptoms may improve with treatment or as collateral circulation develops.

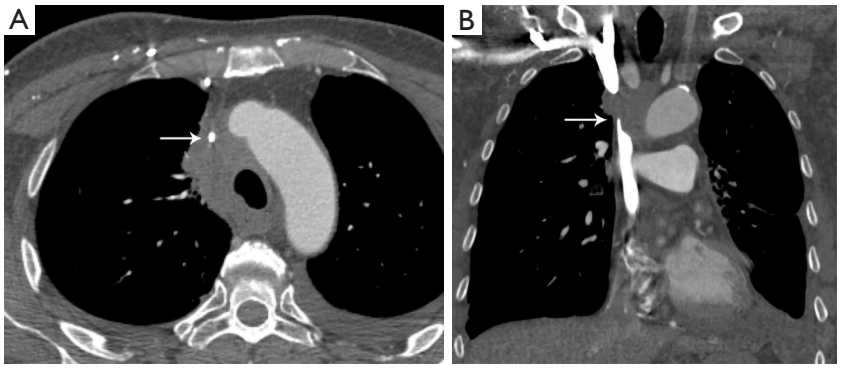

Figure 12 SVC obstruction. (A) Axial contrast enhanced CT shows mediastinal adenopathy due to lung cancer narrowing the SVC (arrow) with multiple collaterals in the right anterior chest wall. (B) Coronal contrast enhanced CT shows the SVC is patent below the level of obstruction due to the adenopathy (arrow). SVC, superior vena cava; CT, computed tomography.

Conclusions

Cross-sectional imaging with CT and MRI is indispensable in the evaluation of mediastinal pathologies. Localization of a mediastinal lesion to a compartment and characterization of morphology, density/intensity, enhancement, and mass effect on neighboring structures can help narrow differentials.

Acknowledgments

The authors wish to thank Chastity A. Holmes, Executive Assistant in the Department of Thoracic Imaging at the University of Texas M.D. Anderson Cancer Center, for her invaluable help in manuscript preparation and Kelly M. Kage, Medical Illustrator in the Division of Diagnostic Imaging at the University of Texas M.D. Anderson Cancer Center for her skillful expertise in preparation of the figures for publication.
Funding: None.

Footnote

Peer Review File: Available at https://med.amegroups.com/article/view/10.21037/med-22-53/prf

Conflicts of Interest: All authors have completed the ICMJE uniform disclosure form (available at https://med.amegroups.com/article/view/10.21037/med-22-53/coif). The authors have no conflicts of interest to declare.

Ethical Statement: The authors are accountable for all aspects of the work in ensuring that questions related to the accuracy or integrity of any part of the work are appropriately investigated and resolved.

References

1. Carter BW, Tomiyama N, Bhora FY, et al. A modern definition of mediastinal compartments. J Thorac Oncol 2014;9:S97-101.
2. Carter BW, Benveniste MF, Madan R, et al. ITMIG Classification of Mediastinal Compartments and Multidisciplinary Approach to Mediastinal Masses. Radiographics 2017;37:413-36.
3. Expert Panel on Thoracic Imaging; Ackman JB, Chung JH, et al. ACR Appropriateness Criteria® Imaging of Mediastinal Masses. J Am Coll Radiol 2021;18:S37-S51.
4. Carter BW, Okumura M, Detterbeck FC, et al. Approaching the patient with an anterior mediastinal mass: a guide for radiologists. J Thorac Oncol 2014;9:S110-8.
5. Heeger AP, Ackman JB. Added Value of Magnetic Resonance Imaging for the Evaluation of Mediastinal Lesions. Radiol Clin North Am 2021;59:251-77.

6. Oldham HN Jr. Mediastinal tumors and cysts. Ann Thorac Surg 1971;11:246-75.
7. Jeung MY, Gasser B, Gangi A, et al. Imaging of cystic masses of the mediastinum. Radiographics 2002;22 Spec No:S79-93.
8. Ackman JB, Verzosa S, Kovach AE, et al. High rate of unnecessary thymectomy and its cause. Can computed tomography distinguish thymoma, lymphoma, thymic hyperplasia, and thymic cysts? Eur J Radiol 2015;84:524-33.
9. Madan R, Ratanaprasatporn L, Ratanaprasatporn L, et al. Cystic mediastinal masses and the role of MRI. Clin Imaging 2018;50:68-77.
10. Feigin DS, Fenoglio JJ, McAllister HA, et al. Pericardial cysts. A radiologic-pathologic correlation and review. Radiology 1977;125:15-20.
11. Cramer JA, Mann H, Layfield LJ. AIRP Best Cases in Radiologic-Pathologic Correlation: Migrating Pericardial Cyst. RadioGraphics 2014;34:373-6.
12. Berrocal T, Madrid C, Novo S, et al. Congenital anomalies of the tracheobronchial tree, lung, and mediastinum: embryology, radiology, and pathology. Radiographics 2004;24:e17.
13. Goitein O, Truong MT, Bekker E, et al. Potential Pitfalls in Imaging of the Mediastinum. Radiol Clin North Am 2021;59:279-90.
14. McAdams HP, Kirejczyk WM, Rosado-de-Christenson ML, et al. Bronchogenic cyst: imaging features with clinical and histopathologic correlation. Radiology 2000;217:441-6.
15. Lewis RB, Mehrotra AK, Rodriguez P, et al. From the radiologic pathology archives: esophageal neoplasms: radiologic-pathologic correlation. Radiographics 2013;33:1083-108.
16. Priola AM, Priola SM, Ciccone G, et al. Differentiation of rebound and lymphoid thymic hyperplasia from anterior mediastinal tumors with dual-echo chemical-shift MR imaging in adulthood: reliability of the chemical-shift ratio and signal intensity index. Radiology 2015;274:238-49.
17. Raptis CA, McWilliams SR, Ratkowski KL, et al. Mediastinal and Pleural MR Imaging: Practical Approach for Daily Practice. Radiographics 2018;38:37-55.
18. Walker CM. Muller's imaging of the chest. 2nd edition. ed. Philadelphia, PA: Elsevier; 2018.
19. Moeller KH, Rosado-de-Christenson ML, Templeton PA. Mediastinal mature teratoma: imaging features. AJR Am J Roentgenol 1997;169:985-90.
20. Carter BW, Marom EM, Detterbeck FC. Approaching the patient with an anterior mediastinal mass: a guide for clinicians. J Thorac Oncol 2014;9:S102-9.
21. Gaerte SC, Meyer CA, Winer-Muram HT, et al. Fat-containing lesions of the chest. Radiographics 2002;22 Spec No:S61-78.
22. Shroff GS, Ahuja J, Strange CD, et al. Pitfalls in Oncologic Imaging of the Pericardium on CT and PET/CT. Semin Ultrasound CT MR 2022;43:194-203.
23. Kashyap R, Lau E, George A, et al. High FDG activity in focal fat necrosis: a pitfall in interpretation of posttreatment PET/CT in patients with non-Hodgkin lymphoma. Eur J Nucl Med Mol Imaging 2013;40:1330-6.
24. Gayer G. Mediastinal (Epipericardial) Fat Necrosis: An Overlooked and Little Known Cause of Acute Chest Pain Mimicking Acute Coronary Syndrome. Semin Ultrasound CT MR 2017;38:629-33.
25. McAdams HP, Rosado-de-Christenson ML, Moran CA. Mediastinal hemangioma: radiographic and CT features in 14 patients. Radiology 1994;193:399-402.
26. Yamazaki A, Miyamoto H, Saito Y, et al. Cavernous hemangioma of the anterior mediastinum: case report and 50-year review of Japanese cases. Jpn J Thorac Cardiovasc Surg 2006;54:221-4.
27. Cheung YC, Ng SH, Wan YL, et al. Dynamic CT features of mediastinal hemangioma: more information for evaluation. Clin Imaging 2000;24:276-8.
28. Li SM, Hsu HH, Lee SC, et al. Mediastinal hemangioma presenting with a characteristic feature on dynamic computed tomography images. J Thorac Dis 2017;9:E412-5.
29. Agarwal PP, Seely JM, Matzinger FR. Case 130: mediastinal hemangioma. Radiology 2008;246:634-7.
30. Mutrie CJ, Donahue DM, Wain JC, et al. Esophageal leiomyoma: a 40-year experience. Ann Thorac Surg 2005;79:1122-5.
31. Lichtenberger JP 3rd, Zeman MN, Dulberger AR, et al. Esophageal Neoplasms: Radiologic-Pathologic Correlation. Radiol Clin North Am 2021;59:205-17.
32. Yang PS, Lee KS, Lee SJ, et al. Esophageal leiomyoma: radiologic findings in 12 patients. Korean J Radiol 2001;2:132-7.
33. Carney JA, Sheps SG, Go VL, et al. The triad of gastric leiomyosarcoma, functioning extra-adrenal paraganglioma and pulmonary chondroma. N Engl J Med 1977;296:1517-8.
34. Settas N, Faucz FR, Stratakis CA. Succinate dehydrogenase (SDH) deficiency, Carney triad and the epigenome. Mol Cell Endocrinol 2018;469:107-11.
35. Benesch M, Wardelmann E, Ferrari A, et al.

Gastrointestinal stromal tumors (GIST) in children and adolescents: A comprehensive review of the current literature. Pediatr Blood Cancer 2009;53:1171-9.
36. Ocazionez D, Shroff GS, Vargas D, et al. Imaging of Intrathoracic Paragangliomas. Semin Ultrasound CT MR 2017;38:584-93.
37. Timmers HJ, Chen CC, Carrasquillo JA, et al. Staging and functional characterization of pheochromocytoma and paraganglioma by 18F-fluorodeoxyglucose (18F-FDG) positron emission tomography. J Natl Cancer Inst 2012;104:700-8.
38. Miettinen M, Lasota J. Gastrointestinal stromal tumors. Gastroenterol Clin North Am 2013;42:399-415.
39. Shinagare AB, Ip IK, Lacson R, et al. Gastrointestinal stromal tumor: optimizing the use of cross-sectional chest imaging during follow-up. Radiology 2015;274:395-404.
40. Hong X, Choi H, Loyer EM, et al. Gastrointestinal stromal tumor: role of CT in diagnosis and in response evaluation and surveillance after treatment with imatinib. Radiographics 2006;26:481-95.
41. Yu MH, Lee JM, Baek JH, et al. MRI features of gastrointestinal stromal tumors. AJR Am J Roentgenol 2014;203:980-91.
42. Chatzopoulos K, Johnson TF, Boland JM. Clinical, Radiologic, and Pathologic Characteristics of Pulmonary Hamartomas With Uncommon Presentation. Am J Clin Pathol 2021;155:903-11.
43. McGahan JP. Carney syndrome: usefulness of computed tomography in demonstrating pulmonary chondromas. J Comput Assist Tomogr 1983;7:137-9.
44. Sodhi KS, Ciet P, Vasanawala S, et al. Practical protocol for lung magnetic resonance imaging and common clinical indications. Pediatr Radiol 2022;52:295-311.
45. Eslamy HK, Ziessman HA. Parathyroid scintigraphy in patients with primary hyperparathyroidism: 99mTc sestamibi SPECT and SPECT/CT. Radiographics 2008;28:1461-76.
46. Cabral FC, Trotman-Dickenson B, Madan R. Hypervascular mediastinal masses: action points for radiologists. Eur J Radiol 2015;84:489-98.
47. Hoang JK, Sung WK, Bahl M, et al. How to perform parathyroid 4D CT: tips and traps for technique and interpretation. Radiology 2014;270:15-24.
48. Nael K, Hur J, Bauer A, et al. Dynamic 4D MRI for Characterization of Parathyroid Adenomas: Multiparametric Analysis. AJNR Am J Neuroradiol 2015;36:2147-52.
49. Scarsbrook AF, Thakker RV, Wass JA, et al. Multiple endocrine neoplasia: spectrum of radiologic appearances and discussion of a multitechnique imaging approach. Radiographics 2006;26:433-51.
50. Strollo DC, Rosado-de-Christenson ML, Jett JR. Primary mediastinal tumors: part II. Tumors of the middle and posterior mediastinum. Chest 1997;112:1344-57.
51. Bredella MA, Torriani M, Hornicek F, et al. Value of PET in the assessment of patients with neurofibromatosis type 1. AJR Am J Roentgenol 2007;189:928-35.
52. Broski SM, Johnson GB, Howe BM, et al. Evaluation of (18)F-FDG PET and MRI in differentiating benign and malignant peripheral nerve sheath tumors. Skeletal Radiol 2016;45:1097-105.
53. Wilson LD, Detterbeck FC, Yahalom J. Clinical practice. Superior vena cava syndrome with malignant causes. N Engl J Med 2007;356:1862-9.

doi: 10.21037/med-22-53
Cite this article as: Archer JM, Ahuja J, Strange CD, Shroff GS, Gladish GW, Sabloff BS, Truong MT. Multimodality imaging of mediastinal masses and mimics. Mediastinum 2023;7:27.

Review Article

Imaging evaluation of thymic tumors

Chad D. Strange[1]^, Mylene T. Truong[1]^, Jitesh Ahuja[1], Taylor A. Strange[2], Smita Patel[3], Edith M. Marom[4]

[1]Department of Thoracic Imaging, University of Texas MD Anderson Cancer Center, Houston, TX, USA; [2]University of Texas Medical Branch, Galveston, TX, USA; [3]Division of Cardiothoracic Radiology, University of Michigan, Ann Arbor, MI, USA; [4]Department of Diagnostic Radiology, Chaim Sheba Medical Center, Affiliated with the Tel Aviv University, Tel Hashomer, Israel

Contributions: (I) Conception and design: All authors; (II) Administrative support: All authors; (III) Provision of study materials or patients: All authors; (IV) Collection and assembly of data: All authors; (V) Data analysis and interpretation: All authors; (VI) Manuscript writing: All authors; (VII) Final approval of manuscript: All authors.

Correspondence to: Chad D. Strange, MD. Department of Thoracic Imaging, University of Texas MD Anderson Cancer Center, 1515 Holcombe Blvd., Houston, TX 77030-4008, USA. Email: CDStrange@mdanderson.org.

Abstract: An integral part of managing patients with thymoma and thymic carcinoma is imaging. At diagnosis and staging, imaging helps demonstrate the extent of local invasion and distant metastases which allows the proper stratification of patients for therapy. For decades, the predominant staging system for thymic tumors was the Masaoka-Koga staging system. More recently, however, the International Association for the Study of Lung Cancer, the International Thymic Malignancies Interest Group (ITMIG), the European Society of Thoracic Surgeons, the Chinese Alliance for Research on Thymomas, and the Japanese Association of Research on Thymus partnered together to develop a tumor-node-metastasis (TNM) staging system specifically for thymic tumors based on a retrospective database of nearly 10,000 patients. The TNM 8th edition defines specific criteria for thymic tumors. Imaging also serves to assess treatment response and detect recurrent disease after various treatment modalities. The Response Evaluation Criteria in Solid Tumors (RECIST) version 1.1 is currently used to assess response to treatment. ITMIG recommends certain modifications to RECIST version 1.1, however, in thymic tumors due to unique patterns of spread. While there is often overlap, computed tomography (CT), magnetic resonance imaging (MRI), and positron emission tomography/computed tomography (PET/CT) characteristics can help differentiate thymoma and thymic carcinoma, with newer CT and MRI techniques under evaluation showing encouraging potential.

Keywords: Thymoma; thymic carcinoma; computed tomography (CT); magnetic resonance imaging (MRI); positron emission tomography/computed tomography (PET/CT)

Received: 01 December 2022; Accepted: 19 May 2023; Published online: 06 June 2023.
doi: 10.21037/med-22-58
View this article at: https://dx.doi.org/10.21037/med-22-58

Introduction

Imaging plays a critical role in the management of patients with thymoma and thymic carcinoma. Imaging is integral in diagnosis and staging, detection of locally invasive and distant metastases, stratification of patients for therapy, and prognosis evaluation. Imaging also serves to assess treatment response and detect recurrent disease after various treatment modalities. This is particularly important since patients with resected recurrent disease have similar outcomes as patients who do not have recurrent disease (1-3).

Routine imaging modalities

The most performed imaging examination is the routine

^ ORCID: Chad D. Strange, 0000-0002-8675-3956; Mylene T. Truong, 0000-0001-9795-529X.

chest radiograph which can be the first modality suggesting a thymic lesion. Thymic tumors may result in added soft tissue projecting over normal anatomic structures resulting in thickening of the anterior junction line or the "silhouette sign". Normally air in the lungs delineates the soft tissue structures that abut the lung, such as the heart and mediastinum. Clear delineation of anatomic structures can be limited when a mass is present as soft tissue now abuts normal structure instead of air. This inability to distinguish one structure from another results in obscuration, or the "silhouette sign". Lateral radiographs help confirm the presence of thymic tumors as they better demonstrate the prevascular space which is readily seen behind the sternum and is normally lucent. A mass in the prevascular space can form a convex contour abnormality when outlined by adjacent lung (*Figure 1*). Small prevascular lesions may not be radiographically apparent, however. Given the low sensitivity and specificity of radiographs, cross-sectional imaging is essential in the assessment of thymic tumors.

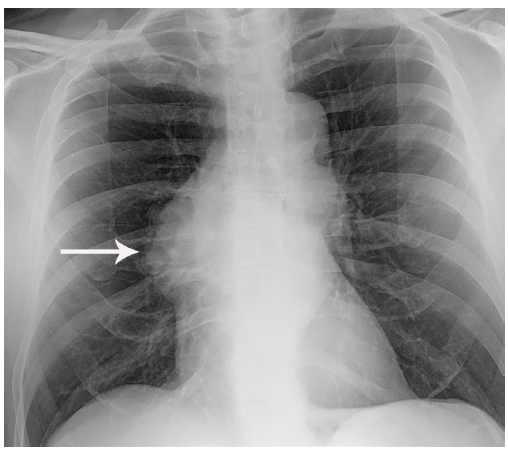

Figure 1 Thymoma. Frontal chest radiograph shows right mediastinal contour abnormality (arrow) that results in loss of the silhouette of the upper right heart border.

Computed tomography (CT) with contrast is the imaging modality of choice to evaluate thymic tumors due to its high spatial and temporal resolution, ease of access, and convenience. CT can reliably discern location, size/shape, morphology, margins, density, enhancement, and relationship to, or invasion of, adjacent structures (4) (*Figure 2*). Overall, CT is equal or superior to magnetic resonance imaging (MRI) in the evaluation of mediastinal masses with the caveat that MRI better evaluates thymic cysts or cystic components of tumors (5) (*Figure 3*).

MRI is not routinely utilized in thymic tumor evaluation, although, there are specific scenarios where MRI adds value, such as the differentiation of solid and cystic lesions and the evaluation of cystic or necrotic components of a mass, enhancing septations within a cyst, and the extent of local invasion (*Figure 4*). Chemical shift imaging can additionally be utilized to detect microscopic or intravoxel fat, which can differentiate thymic neoplasm from hyperplasia (6,7). Finally, MRI can be performed in patients who cannot receive iodinated CT or to avoid radiation exposure.

The role of fluorodeoxyglucose (FDG) positron emission tomography (PET)/computed tomography (CT)

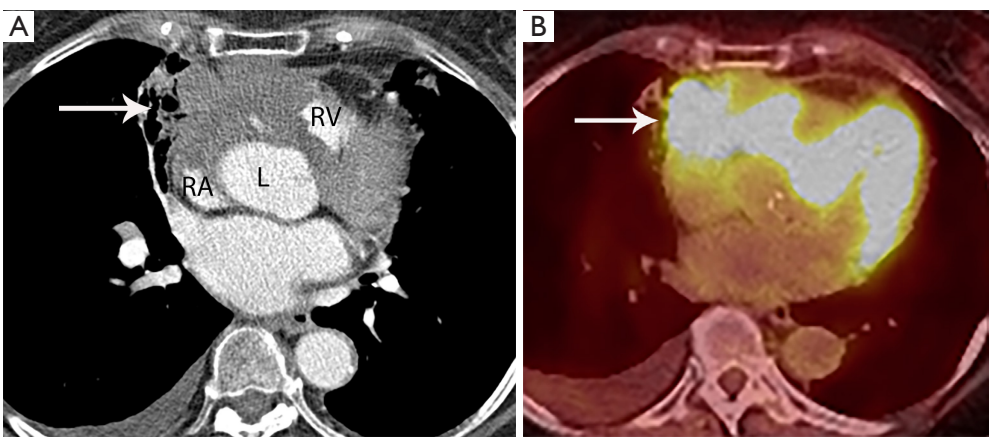

Figure 2 Adenosquamous thymic carcinoma. (A) Contrast-enhanced CT shows a right prevascular mediastinal tumor (arrow) invading the pericardium between the RA, ascending aorta (A) and RV. (B) PET/CT shows the tumor is markedly FDG avid (arrow). RA, right atrium; RV, right ventricle; CT, computed tomography; PET/CT, positron emission tomography/computed tomography; FDG, fluorodeoxyglucose.

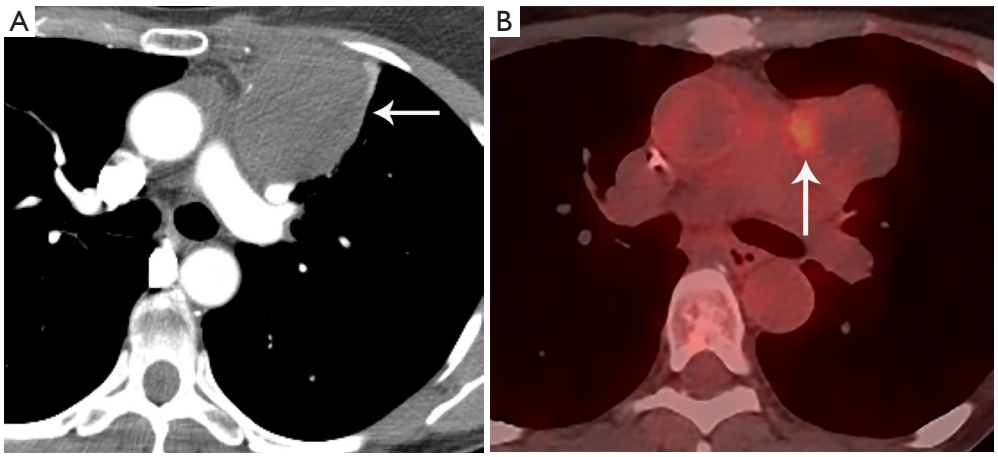

Figure 3 Thymoma. (A) CT shows the left prevascular mediastinal mass (arrow) is mostly homogeneous, with low attenuation measuring 10 HU suggesting a cystic component yet has a denser component of 48 HU along the medial peripheral aspect suggesting some solid component. (B) PET/CT shows FDG uptake with SUVmax of 3.4 along the medial peripheral aspect of the mass (arrow). At resection, pathology showed thymoma with cystic component and no invasion of the pericardium or lung. CT, computed tomography; HU, Hounsfield units; PET/CT, positron emission tomography/computed tomography; FDG, fluorodeoxyglucose; SUVmax, maximum standard uptake value.

in thymic mass evaluation is incompletely defined. False-positive studies can be seen with FDG uptake in non-neoplastic masses, such as in the setting of infection, thymic hyperplasia, or fibrosing mediastinitis. False-negative studies can be seen in certain histological types of thymic malignancy with lower metabolic activity. Additionally, there is lack of technique standardization which results in quantitative variability between studies (8). Given that other prevascular masses such as malignant germ cell tumor and lymphoma are often FDG avid, the presence of a hypermetabolic prevascular mass cannot distinguish between various tumors. There are studies that report that FDG uptake can help predict tumor invasiveness and prognosis. Other studies report FDG uptake as useful in differentiating low-grade from high-grade thymic malignancies; however, other studies report these observations as controversial due to overlapping imaging findings and FDG uptake between low-grade and high-grade thymic tumors (9). Overlapping findings are less common in more aggressive tumors, such as thymic carcinoma, due to higher overall tumor metabolism, with studies reporting that a maximum standard uptake value (SUVmax) of 6 can serve as a cutoff between thymic carcinoma and lower grade thymic tumors (10) (*Figures 2,3*). However, this threshold cannot differentiate thymic carcinoma from other malignancies such as lymphoma or non-seminomatous germ cell tumor. Finally, PET/CT clearly has a role to detect occult metastasis in hypermetabolic tumors.

Staging

A variety of thymic tumor staging systems have been utilized over the years. For decades, the predominant staging system, was the Masaoka-Koga staging system as it did correlate with survival (11-13). Masaoka-Koga was based on gross and microscopic pathologic tumor properties. Stage 1 tumors were completely encapsulated. Stage II tumors demonstrating microscopic invasion through the capsule (IIa) or into surrounding fat (IIb). Stage III tumors invade into adjacent structures such as lung, vessels, or pericardium. Finally, stage IV tumors demonstrate pleural or pericardial dissemination (IVa) or lymphatic-hematogenous metastasis (IVb) (1). There were issues with Masaoka-Koga staging, however, such as reliance on an initial small series of 96 patients from one institution and sometimes incomplete or absent capsule limiting stage II evaluation.

Given the need of accurate pre-treatment staging, greater consistency at pathologic examination, and a prognostic determinant on a large patient population from multiple institutions, the International Association for the Study of Lung Cancer (IASLC), the International Thymic Malignancies Interest Group (ITMIG), the European Society of Thoracic Surgeons, the Chinese

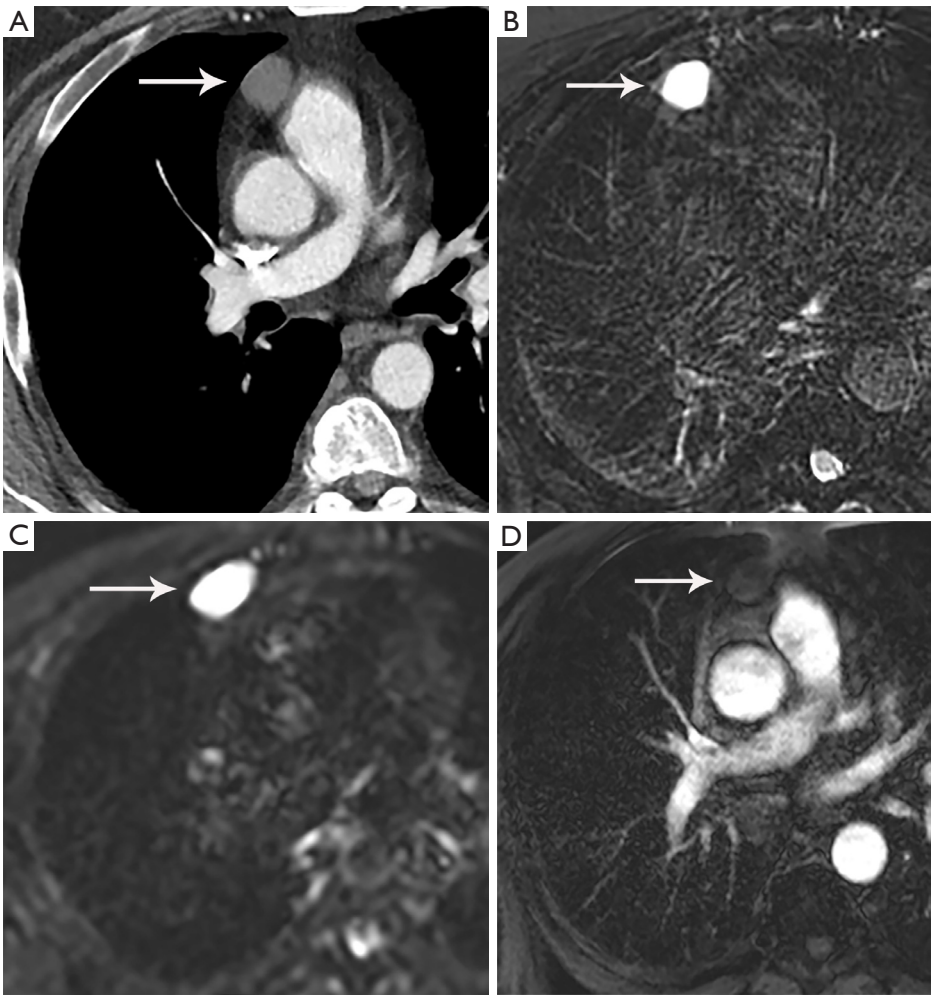

Figure 4 Thymic cyst. (A) Contrast-enhanced CT shows a right prevascular mediastinal 2.2 cm lesion (arrow) measuring 34 HU, which can represent solid or cystic lesion with proteinaceous material or hemorrhage. (B-D) MRI is useful to determine that this is a simple thymic cyst (arrows) with high signal intensity on T2 weighted (B) and STIR (C) and no enhancement on the post contrast image (D). CT, computed tomography; HU, Hounsfield units; MRI, magnetic resonance imaging; STIR, short tau inversion recovery.

Alliance for Research on Thymomas, and the Japanese Association of Research on Thymus partnered together to develop a tumor-node-metastasis (TNM) staging system for thymic tumors. While the Masaoka-Koga staging system was derived from retrospective series of 96 patients, the thymic tumor retrospective database included nearly 10,000 patients (14,15). This eighth edition of the TNM classification for malignant tumors has now been adopted by the American Joint Committee on Cancer and the Union for International Cancer Control (16).

In TNM 8th edition, the T descriptor for thymic tumors describes local invasion, and not tumor size, as size was not found to be a prognostic factor. T1 tumors demonstrate invasion into the mediastinal fat (T1a) or mediastinal pleura (T1b), T2 tumors demonstrate invasion into the pericardium, T3 tumors demonstrate invasion into the lung, brachiocephalic vein, superior vena cava (SVC), chest wall, or phrenic nerve, and T4 tumors demonstrate invasion into the aorta, intrapericardial pulmonary artery, myocardium, trachea, or esophagus. The N descriptor distinguishes prevascular or perithymic lymph nodes as N1. Deep intrathoracic or cervical lymph nodes are N2. The M descriptor is divided into M1a disease such as pleural and pericardial nodules and M1b disease such as distant organ metastasis (17-19). While the ultimate assigned stage is often the same with Masaoka-Koga and TNM staging

systems, TNM allows for a more detailed breakdown and reporting of the extent of disease (16). A few differences between Masaoka-Koga and TNM will help compare and contrast the two systems. In TNM, capsular and mediastinal pleural invasion are T1 disease, and in the absence of nodal disease would be stage I disease; however, this would be stage II disease in Masaoka-Koga. Pericardial invasion is T2/stage II in TNM, however, in Masaoka-Koga it is stage III. Prevascular or perithymic nodal involvement has been downgraded from Masaoka-Koga stage IVb to TNM stage IVa.

Ried *et al.* compared the Masaoka-Koga staging system with the TNM staging system. They found that some of the Masaoka-Koga stage IIa and IIb tumors were reclassified to stage I in TNM. Additionally, they reported that the TNM system more accurately characterized Masaoka-Koga stage III disease to determine which patients were better surgical candidates. They concluded that TNM staging was clinically useful and applicable compared with Masaoka-Koga staging (20).

There are, however, limitations of this TNM staging system for thymic tumors. The number of patients evaluated in the initial data who had nonsurgical treatment was small. This could potentially hinder predictive ability with higher stage disease. The nodal map was primarily derived from Japanese practice patterns which are more empirically based with more consideration on feasibility of surgical sampling. Finally, due to the limited data available, differentiation between parenchymal nodules (M1b) and pleural/pericardial nodules (M1a) was an empiric decision lacking statistical validation (16). A revision of this TNM staging is slated to be completed in 2023, revalidating and refining it.

Treatment response assessment

The Response Evaluation Criteria in Solid Tumors (RECIST) version 1.1 is currently utilized to assess response to treatment. ITMIG recommends certain modifications and caveats to the use of RECIST version 1.1, however, in thymic tumors due to unique patterns of spread (8). ITMIG recommends pretreatment and posttreatment studies be read by the same radiologist experienced in thoracic imaging to decrease interobserver variability when assessing these often-large irregular tumors with vague borders and local infiltration (21,22). Because thymic tumors tend to spread along the pleura, ITMIG also recommends using the modification of RECIST 1.1 like that used for malignant pleural mesothelioma (MPM) (8,13).

RECIST 1.1, with the modification for MPM, involves measuring up to a maximum of two lesions per organ and five lesions in total, representing all involved organs, as baseline target lesions. Longest diameter measurements are used, with the exception that short axis measurements are obtained of the pleura and lymph nodes. When the pleura is a target organ, short axis (perpendicular to the pleura) measurements are taken at two locations at three separate CT levels separated by at least 1 cm. The sum of these pleural measurements (up to a maximum of 6) becomes the overall pleural measurement, which is added to non-pleural target lesions up to a total of five (8,23).

The National Comprehensive Cancer Network (NCCN) recommends a surveillance regimen of thoracic CT every 6 months for 2 years, then annually for 10 years in thymoma and annually for 5 years in thymic carcinoma. ITMIG, however, recommends surveillance thoracic CT frequency for patients after resection of any thymic tumor as annually for 5 years following resection. From years six to eleven, alternating yearly radiograph and CT is performed, with yearly radiographs thereafter. For resected stage III or IVa thymoma, any stage thymic carcinoma, incomplete resection, or other high-risk tumors, an additional thoracic CT is recommended every six months for the first three years with consideration of CT one to three months after surgery serving as a new baseline after post-surgical changes have resolved (13,24).

CT is the primary modality used for tumor reassessment given that it is the most reproducible (25). When trying to avoid ionizing radiation and in those who cannot be given CT intravenous contrast due to allergy or diminished renal function, MRI can alternatively be used for tumor reassessment. Kerpel *et al.* evaluated 187 patients after resection for thymic epithelial tumors to assess the accuracy of MRI compared with CT for tumor assessment. MRI was demonstrated to be an adequate alternative to CT for reassessment. One caveat was that due to MRI artifact related to sternotomy wires, alternating CT with MRI was recommended (24).

In patients with microscopically margin negative resection (RO), or in patients who demonstrate complete radiologic response to therapy, local recurrence in the prevascular mediastinum is defined as: tumor in the thymic bed, pericardial, pleural, or pulmonary parenchymal tumor that is immediately adjacent to the thymic bed, lymph nodes immediately adjacent to thymic bed, or in the site of previous noncontiguous metastasis. Regional

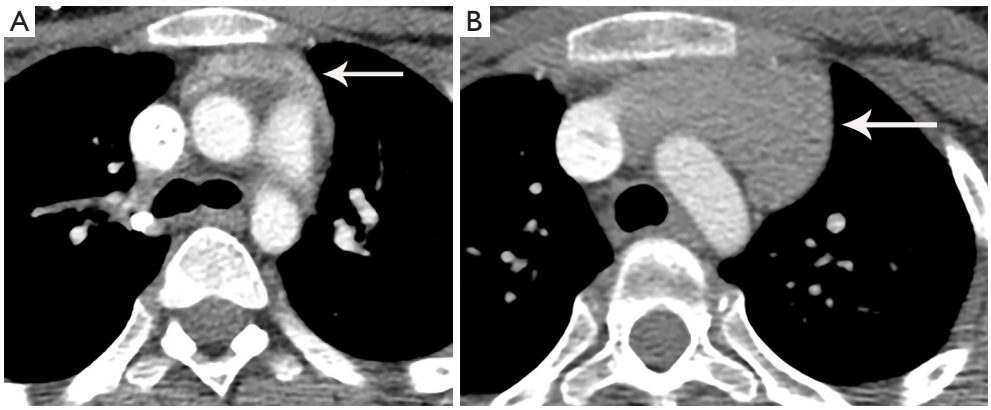

Figure 5 Thymic hyperplasia. Chondroblastic osteosarcoma of the femur, treated with methotrexate, doxorubicin, cisplatin. (A) CT shows the normal thymus for age (arrow) at baseline. (B) CT 4 months later shows increase in size of the thymus consistent with rebound hyperplasia (arrow). Enlargement of the thymus gland due to hyperplasia during the recovery phase from physical stress such as after chemotherapy or recovering from burns, does not displace or change the contour of vessels surrounding it. In the appropriate clinical context of thymic hyperplasia, CT is adequate for diagnosis and MRI is not needed for confirmation. CT, computed tomography; MRI, magnetic resonance imaging.

recurrence is defined as intrathoracic recurrence that is not contiguous with the thymic bed such as: parietal pleural nodules, pericardial nodules, visceral pleural nodules, and lymph nodes not contiguous with the thymic bed. Distal recurrence is defined as: extrathoracic recurrence or intraprenchymal pulmonary nodules that are not contiguous with the thymic bed (13).

Routine imaging characteristics of thymic tumors

Normal anatomic thymus appears as a triangular shaped structure in the prevascular space; however, a variety of normal variants may be seen. Benign and malignant pathologic processes can alter the size or shape of the thymus which can pose a diagnostic dilemma. Generally, benign processes can be easily distinguished based on imaging characteristics. A brief review of benign entities will serve as a comparison to malignant thymic tumors.

Benign

Thymic cysts

Congenital thymic cysts can occur anywhere along the course of the thymic descent, but most often occur in the prevascular mediastinal space (26). Congenital thymic cysts arise from remnants of the thyropharyngeal duct. Acquired thymic cysts are more common, often multi-locular and complex, associated with neoplasm (such as thymoma, lymphoma, or germ cell tumors), radiation therapy, aplastic anemia, systemic lupus erythematosus, myasthenia gravis, Sjogren syndrome, after tumor resection, an in the setting of acquired immune deficiency syndrome (AIDS) in children (26,27). In general, thymic cysts present as well circumscribed round or oval lesions in the prevascular space with fluid density Hounsfield units (HU) less than 20. They most commonly have no wall thickening, irregularity, or enhancement. If CT findings are indeterminant, MRI can be used for further evaluation. On MRI, simple thymic cysts demonstrate increased T2 signal, variable T1 signal depending on protein content, and no wall nodularity or enhancement (*Figure 4*).

Thymic hyperplasia

True thymic hyperplasia (or "rebound" hyperplasia) is present when the thymic volume is increased by more than 50%, commonly after infection, surgery, burns, chemotherapy, radiation therapy, or steroid therapy (*Figure 5*). Alternatively, lymphoid (or follicular) hyperplasia is seen when there is an increase in the number of lymphoid follicles, commonly associated with autoimmune diseases such as myasthenia gravis (*Figure 6*) or human immunodeficiency virus infection (27-30). There is generally smooth symmetric thymic

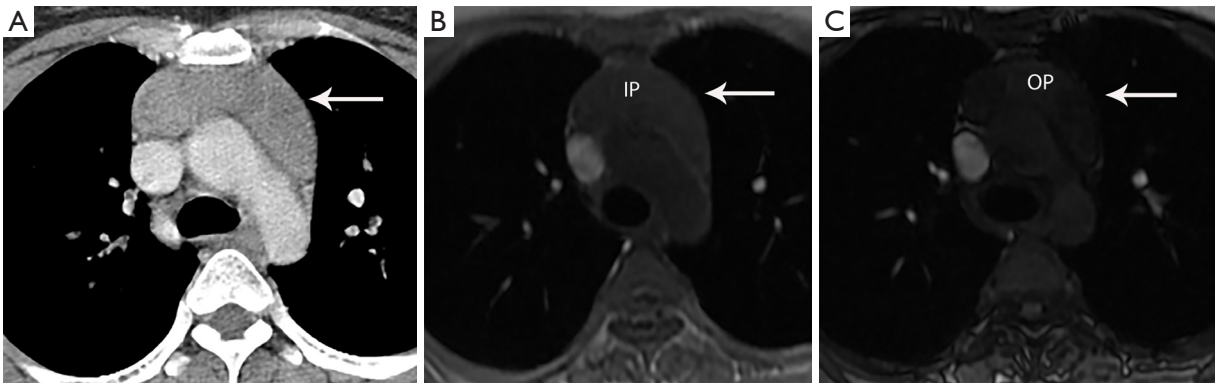

Figure 6 Lymphoid thymic hyperplasia with Grave's disease. (A) Contrast-enhanced CT shows mass-like thymic enlargement (arrow). With such an appearance, thymic hyperplasia, a thymic epithelial neoplasm or lymphoma involvement of the thymus are all considerations. (B,C) MRI with IP and OP imaging shows drop in signal intensity consistent with thymic hyperplasia (arrows), obviating the need for further investigation or biopsy. IP, in-phase; OP, out-of-phase; CT, computed tomography; MRI, magnetic resonance imaging.

enlargement in hyperplasia; however, nodular or bulky appearance can be seen which is difficult to distinguish from malignancy. Again, in equivocal cases, MRI can be used in a problem-solving function. In-phase and out-of-phase gradient-echo sequences can identify thymic hyperplasia. Thymic signal drop out during out-of-phase imaging corresponds with microscopic (or intravoxel) fat, which confirms thymic hyperplasia (31) (*Figure 6*).

Thymolipoma

Thymolipoma is a generally large, benign, slow growing tumor arising from the thymus. Thymolipomas are composed predominantly of adipose tissue with minimal scattered soft tissue and thymic tissue interposed (32,33). The classic appearance is a very large predominantly fat density mass in a cardiophrenic angle, most commonly on the left (*Figure* 7). Symptoms are overall rare but can be present related to compression or displacement of adjacent structures or in association with Graves' disease, myasthenia gravis, and hematological disorders (4,30).

Malignant

Thymic epithelial tumors

Thymic epithelial tumors include thymoma, thymic neuroendocrine tumor (carcinoid), and thymic carcinoma. These tumors are predominantly seen in the prevascular mediastinum with a myriad of imaging findings. Thymic epithelial tumors can be homogeneous or heterogeneous, solid or cystic, and have well-circumscribed or irregular borders. There is unfortunately significant imaging overlap between various World Health Organization (WHO) types of thymoma as well as between thymoma and thymic carcinoma. There are, however, clinical and imaging patterns that help in differentiation, but the differentiation usually requires histological proof. Malignant thymic tumors have a median age at presentation in the sixth decade. More benign tumors have a median age at presentation in the fourth to fifth decades (34-36). The more aggressive thymomas and malignant tumors are more likely to have clinical symptoms such as pain or shortness of breath (36). Benign tumors are more likely to have intralesional fat, be midline, and retain normal thymic shape. Malignant tumors are more likely to be larger and locally invasive (37-39). Common imaging findings and techniques utilized to more accurately differentiate various thymic tumors will now be reviewed.

Thymoma

Thymoma typically presents as a smooth or lobular mass involving one lobe of the thymus, although bilateral involvement can occur (39). Most thymomas demonstrate homogeneous enhancement, although, approximately one third can be heterogeneous due to areas of hemorrhage, necrosis, cystic change, or calcification (1) (*Figures 8*,*9*). Imaging characteristics can vary according to WHO histological classification, with vascular invasion and pleural/pericardial involvement more common with more aggressive histology (*Figure 2*). The thymomas with the

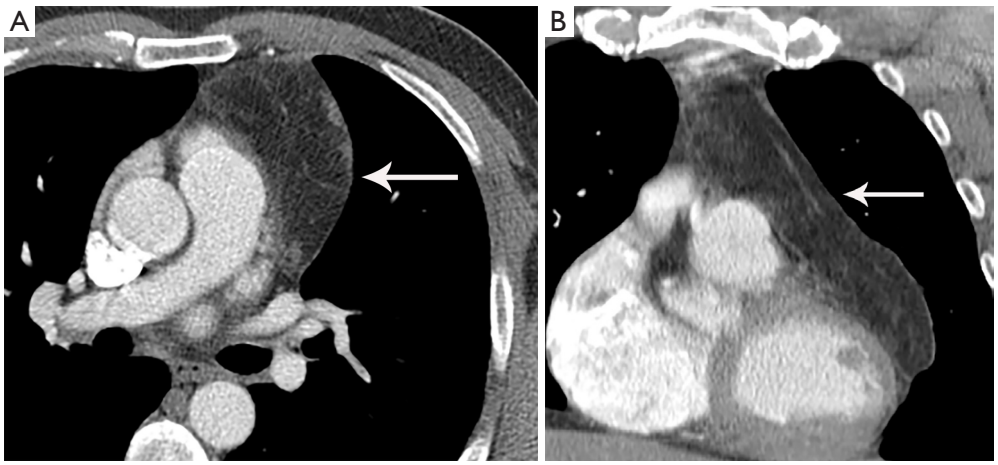

Figure 7 Thymolipoma. (A,B) Axial and coronal contrast-enhanced CT shows large left prevascular mediastinal lesion with fat attenuation (arrows). CT, computed tomography.

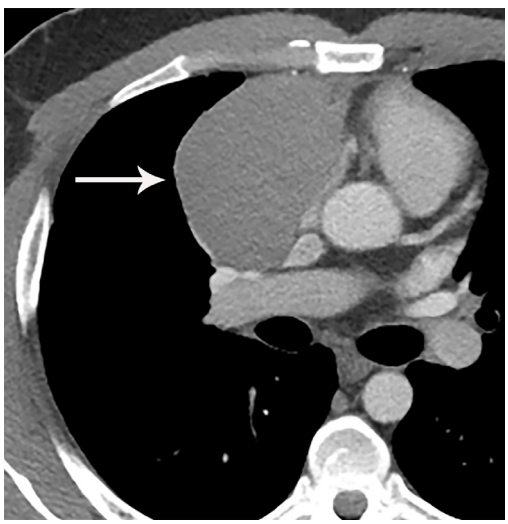

Figure 8 Thymoma and myasthenia gravis. Contrast-enhanced CT shows right prevascular mediastinal mass (arrow). CT, computed tomography.

more aggressive histologies tend to be larger, more lobular or irregular, have cystic or necrotic change, areas of calcification, or evidence of infiltration into surrounding fat (40-42) (*Figure 10*).

On MRI, thymomas have low to intermediate signal intensity on T1 weighted images and high signal intensity on T2 weighted images. If areas of cystic change or necrosis are present, these have decreased T1 signal intensity and increased T2 signal intensity. Fat suppression imaging can delineate thymomas from mediastinal fat which facilitates more exact measurements and enhancement evaluation. MRI is more limited than CT for calcification detection. MRI strengths include identifying nodules, thickened septae, and/or thickened capsule in cystic thymoma and differentiating cystic thymomas from benign prevascular thymic or pericardial cysts. Because of its superior contrast resolution, MRI also excels in identifying direct cardiac involvement compared to CT (43).

The role of FDG PET/CT in thymoma imaging is limited. Given the presence of FDG uptake in the normal and hyperplastic thymus, especially in younger adults and children, false-positive results can occur. In fact, physiologic uptake has been reported in 28% of patients under 40 years of age and up to 73% in children less than 13 years of age (44). PET/CT has not been shown to differentiate different WHO histological classifications of thymic tumors, although the more aggressive histologies tend towards higher FDG uptake (45,46) (*Figures 2,3*). Indium^{111} octreotide nuclear medicine scans have now been replaced by ^{68}Ga-labeled somatostatin analogues because ^{68}Ga-labeled somatostatin analogues, such as ^{68}Ga-DOTATATE, are used for PET/CT, and thus provide better resolution.

Thymic carcinoma and neuroendocrine tumor/carcinoid

Thymic carcinoma and thymic neuroendocrine tumors have similar imaging characteristics which may often overlap with the more aggressive histologies of thymoma, such as B3 thymoma. Thymic carcinomas and neuroendocrine

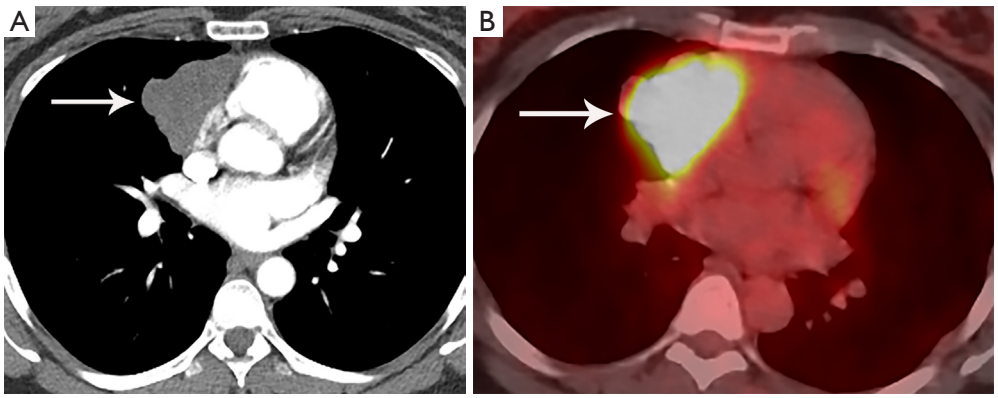

Figure 9 Thymoma. (A) Contrast-enhanced CT shows right prevascular lobular mediastinal mass (arrow). (B) FDG PET/CT shows FDG avid thymoma (arrow) with SUV of 16. Presence of intense FDG uptake suggests more aggressive type thymoma or thymic carcinoma. CT, computed tomography; FDG, fluorodeoxyglucose; PET/CT, positron emission tomography/computed tomography; SUV, standard uptake value.

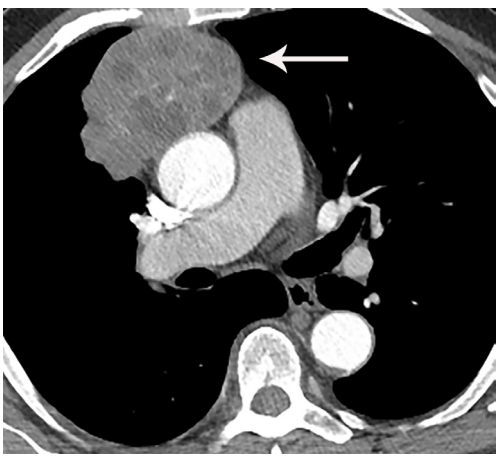

Figure 10 WHO type B3 thymoma. Contrast-enhanced CT shows right prevascular mediastinal mass with heterogeneous attenuation, lobular contours and areas of necrosis (arrow), consistent with more aggressive WHO subtype identified pathologically. WHO, World Health Organization; CT, computed tomography.

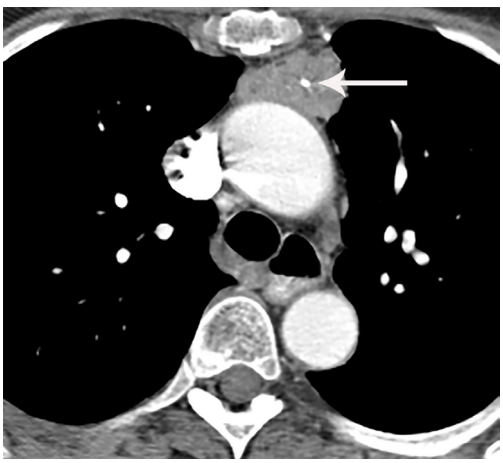

Figure 11 Thymic carcinoma. Contrast-enhanced CT shows left prevascular mediastinal mass (arrow) with small calcific focus. CT, computed tomography.

tumors commonly present as large prevascular masses with irregular or poorly marginated borders, areas of necrosis or cystic change, and hemorrhage. Compared with thymomas, there is a greater incidence of local invasion (1) (*Figures 2,11*). Pleural or pericardial nodules, pleural effusion, and distant metastasis are more commonly seen with thymic carcinoma or thymic neuroendocrine tumor than thymoma (*Figure 12*). More aggressive thymic epithelial tumors can invade or compress the SVC resulting in SVC syndrome. This is a clinical syndrome marked by swelling of the neck, face, and upper extremities, with associated cough, headache, and shortness of breath. Pleural metastatic disease, which is more common in thymic carcinoma and thymic neuroendocrine carcinoma, generally consists of small enhancing pleural nodules or areas of enhancing pleural thickening. These are generally adequately assessed with thin-slice contrast-enhanced CT, although, contrast-enhanced MRI and PET/CT can be of additional benefit in questionable cases.

MRI imaging findings of thymic carcinoma and thymic neuroendocrine tumors are similar to thymomas. As already noted, on MRI thymic carcinomas more likely demonstrate

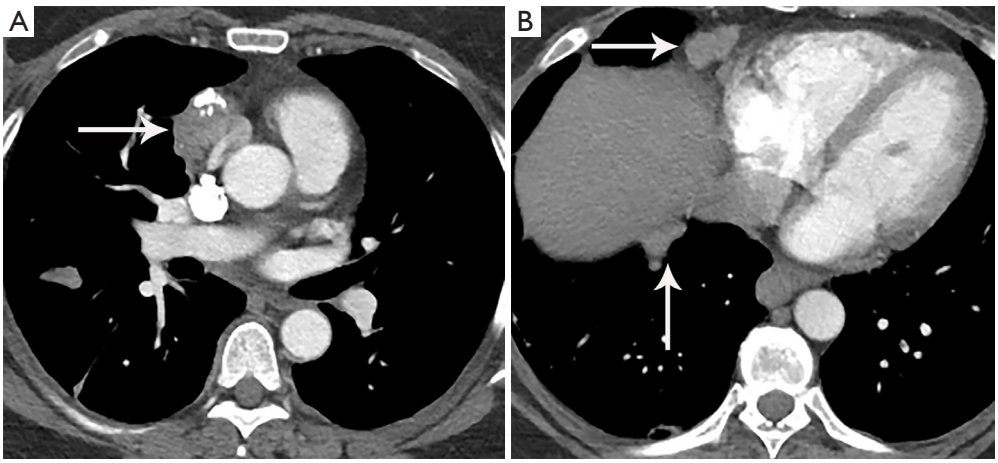

Figure 12 Thymic carcinoma with pleural metastases. (A) Contrast-enhanced CT shows a right prevascular lobular mediastinal mass with heterogeneous attenuation and calcifications (arrow). (B) CT shows nodular right diaphragmatic pleural metastases (vertical arrows) and right anterior diaphragmatic nodal metastasis (horizontal arrow). CT, computed tomography.

irregular contour; greater heterogeneity, hemorrhage, necrosis, and cystic change; greater degree of local vascular and mediastinal invasion; and lymphadenopathy (43,47,48).

As noted, FDG PET/CT does not reliably differentiate between the different histological types of thymoma. Several small studies, however, have suggested that FDG PET/CT can help differentiate thymoma from thymic carcinoma using various cutoffs of SUV max ranging between 4.6 and 6.3 (49,50). Since the more aggressive tumor histologies are FDG avid, FDG PET/CT can be useful in the assessment and follow-up of thymic carcinoma but is not routinely recommended (51). Thymic neuroendocrine tumors can additionally be evaluated with ^{68}Ga-DOTATATE PET/CT which may demonstrate improved sensitivity for lesion detection compared with FDG PET/CT which can help identify tumors that are candidates for peptide receptor radiotherapy (PRRT) with ^{177}Lutetium (51).

Primary thymic salivary gland tumors

Primary salivary gland tumors of the thymus are rare. It is important to differentiate these from more common metastasis by detailed radiologic and clinical evaluation (52). Only a few dozen cases of primary thymic salivary gland tumors, such as adenoid cystic carcinoma and mucoepidermoid carcinoma, have been reported (53-55). Imaging characteristics are like other thymic epithelial neoplasms with final diagnosis depending on histochemical evaluation.

Other prevascular mediastinal masses

Other prevascular lesions can have similar imaging features with thymic epithelial tumors such as lymphoma and germ-cell tumors. Lymphoma may differ though, as Hodgkin and non-Hodgkin lymphomas tend to present as a homogeneous smooth or lobulated soft tissue mass that may surround, but rarely invade adjacent structures.

Germ-cell tumors include a variety of benign and malignant tumors. The most common benign germ-cell tumor is a mature teratoma. Malignant germ-cell tumors include malignant embryonal carcinoma, yolk sac tumor, choriocarcinoma, and mixed germ cell tumor. Malignant germ-cell tumors often present as heterogeneously enhancing masses with areas of cystic change, necrosis, and calcification, which can have overlapping imaging features with thymic epithelial tumors.

Advanced imaging options

CT

To better distinguish various prevascular mediastinal masses, a variety of new CT techniques are being investigated. Functional CT imaging with CT perfusion provides quantitative data on tissue perfusion by acquiring specific graphs for tissue blood flow (BF), blood volume (BV), and permeability surface (PS). These parameters can be used to evaluate tumor angiogenesis, infiltration, and response to therapy (56). Bakan *et al.* found that CT perfusion values

were not significantly different between thymoma and thymic hyperplasia. There were significant differences in BF and BV values between thymomas and malignant prevascular lesions, however, such as thymic carcinoma. This demonstrates a possible role of CT perfusion imaging to aid in differentiation between thymoma and thymic carcinoma (57).

Dual-energy computed tomography (DECT) has also been evaluated to define a role in the differentiation of prevascular masses. Malignant tumors reveal higher iodine concentrations (IC) as compared to benign tumors (58). In a study of 37 patients, Chang *et al.* found that iodine related Hounsfield units (IHU) and IC could be helpful to differentiate low-risk thymomas, high-risk thymomas, and thymic carcinomas. Lower values were noted in higher grade tumors, presumably due to the presence of necrosis. They concluded that DECT, using iodine concentration measurement derived quantitative analysis, could aid in the ability to differentiate between low-risk thymoma, high-risk thymoma, and thymic carcinoma (59).

MRI

It has been reported that routine MRI cannot reliably differentiate low-risk from high-risk thymic epithelial tumors (48). Non-invasive functional MRI techniques such as diffusion-weighted imaging (DWI) and apparent diffusion coefficient (ADC) values are techniques that allow for quantitative evaluation of thymic epithelial tumors. Razek *et al.* reported that an ADC cutoff value of 1.22×10^3 mm^2/sec could be used to differentiate low-risk thymoma from high-risk thymoma and thymic carcinoma with an 87% sensitivity, 85% specificity, and 86% accuracy (60). Most commonly hot-spot regions of interest (ROI) are utilized for DWI/ADC measurements. Given concern for errors in sampling, however, several studies have shown that histogram analysis of ADC maps are more accurate and may aid in differentiation between low-risk thymomas, high-risk thymomas, and thymic carcinomas (61,62).

Functional MRI imaging with dynamic contrast enhanced (DCE) MRI has also been studied in relation to prevascular mediastinal tumor evaluation. In a study comparing thymic epithelial tumors, lymphoma, and malignant germ cell tumors, Yabuuchi *et al.* found that thymic epithelial tumors demonstrated a washout pattern, possibly due to high tumor cellularity and limited stroma, as compared to other tumor types (63,64). In a study evaluating the ability of DCE-MRI to differentiate thymic carcinoma from thymic lymphoma, Shen *et al.* reported that reflux rate constant from the extracellular extravascular space (EES) to the blood plasma (k_{ep}) was lower in thymic carcinoma and that the volume fraction of the EES (v_e) was higher in thymic carcinoma as compared to thymic lymphoma (65). While these results are interesting and promising, because of limited study sizes, further research is needed to clarify the role of DCE-MRI to help differentiate between various thymoma types and between thymoma and thymic carcinoma. Finally, early work suggests that quantitative features derived from MRI related to biologic behavior with various radiomics models (advanced mathematical analysis of existing data) may facilitate predictions of pathologic classification and staging of thymic epithelial tumors (66).

Conclusions

Imaging plays an integral role in patients with thymoma and thymic carcinoma. Imaging is used for initial diagnosis and staging, detection of locally invasive disease and distant metastasis, stratification of patients for therapy, and prognostication. Following medical and surgical therapy, imaging helps assess treatment response and to detect recurrent disease. While imaging findings overlap, combining clinical and imaging characteristics of CT, MRI, and PET/CT can help differentiate thymoma and thymic carcinoma, with new CT and MRI techniques currently being evaluated showing potential.

Acknowledgments

Funding: None.

Footnote

Peer Review File: Available at https://med.amegroups.com/article/view/10.21037/med-22-58/prf

Conflicts of Interest: All authors have completed the ICMJE uniform disclosure form (available at https://med.amegroups.com/article/view/10.21037/med-22-58/coif). EMM reports an honorarium for a lecture from each of the following companies: Boehringer Ingelheim, AstraZeneca, Merck Sharp and Dohme. The other authors have no conflicts of interest to declare.

Ethical Statement: The authors are accountable for all aspects of the work in ensuring that questions related

to the accuracy or integrity of any part of the work are appropriately investigated and resolved.

References

1. Benveniste MF, Rosado-de-Christenson ML, Sabloff BS, et al. Role of imaging in the diagnosis, staging, and treatment of thymoma. Radiographics 2011;31:1847-61; discussion 1861-3.
2. Regnard JF, Zinzindohoue F, Magdeleinat P, et al. Results of re-resection for recurrent thymomas. Ann Thorac Surg 1997;64:1593-8.
3. Ströbel P, Bauer A, Puppe B, et al. Tumor recurrence and survival in patients treated for thymomas and thymic squamous cell carcinomas: a retrospective analysis. J Clin Oncol 2004;22:1501-9.
4. Carter BW, Okumura M, Detterbeck FC, et al. Approaching the patient with an anterior mediastinal mass: a guide for radiologists. J Thorac Oncol 2014;9:S110-8.
5. Tomiyama N, Honda O, Tsubamoto M, et al. Anterior mediastinal tumors: diagnostic accuracy of CT and MRI. Eur J Radiol 2009;69:280-8.
6. Ackman JB. MR Imaging of Mediastinal Masses. Magn Reson Imaging Clin N Am 2015;23:141-64.
7. Ackman JB, Wu CC. MRI of the thymus. AJR Am J Roentgenol 2011;197:W15-20.
8. Benveniste MF, Korst RJ, Rajan A, et al. A practical guide from the International Thymic Malignancy Interest Group (ITMIG) regarding the radiographic assessment of treatment response of thymic epithelial tumors using modified RECIST criteria. J Thorac Oncol 2014;9:S119-24.
9. Lococo F, Cesario A, Okami J, et al. Role of combined 18F-FDG-PET/CT for predicting the WHO malignancy grade of thymic epithelial tumors: a multicenter analysis. Lung Cancer 2013;82:245-51.
10. Benveniste MF, Moran CA, Mawlawi O, et al. FDG PET-CT aids in the preoperative assessment of patients with newly diagnosed thymic epithelial malignancies. J Thorac Oncol 2013;8:502-10.
11. Falkson CB, Bezjak A, Darling G, et al. The management of thymoma: a systematic review and practice guideline. J Thorac Oncol 2009;4:911-9.
12. Filosso PL, Ruffini E, Lausi PO, et al. Historical perspectives: The evolution of the thymic epithelial tumors staging system. Lung Cancer 2014;83:126-32.
13. Huang J, Detterbeck FC, Wang Z, et al. Standard outcome measures for thymic malignancies. J Thorac Oncol 2010;5:2017-23.
14. Huang J, Ahmad U, Antonicelli A, et al. Development of the international thymic malignancy interest group international database: an unprecedented resource for the study of a rare group of tumors. J Thorac Oncol 2014;9:1573-8.
15. Masaoka A, Monden Y, Nakahara K, et al. Follow-up study of thymomas with special reference to their clinical stages. Cancer 1981;48:2485-92.
16. Ahmad U. The eighth edition TNM stage classification for thymic tumors: What do I need to know? J Thorac Cardiovasc Surg 2021;161:1524-9.
17. Bhora FY, Chen DJ, Detterbeck FC, et al. The ITMIG/IASLC Thymic Epithelial Tumors Staging Project: A Proposed Lymph Node Map for Thymic Epithelial Tumors in the Forthcoming 8th Edition of the TNM Classification of Malignant Tumors. J Thorac Oncol 2014;9:S88-96.
18. Kondo K, Van Schil P, Detterbeck FC, et al. The IASLC/ITMIG Thymic Epithelial Tumors Staging Project: proposals for the N and M components for the forthcoming (8th) edition of the TNM classification of malignant tumors. J Thorac Oncol 2014;9:S81-7.
19. Nicholson AG, Detterbeck FC, Marino M, et al. The IASLC/ITMIG Thymic Epithelial Tumors Staging Project: proposals for the T Component for the forthcoming (8th) edition of the TNM classification of malignant tumors. J Thorac Oncol 2014;9:S73-80.
20. Ried M, Eicher MM, Neu R, et al. Evaluation of the new TNM-staging system for thymic malignancies: impact on indication and survival. World J Surg Oncol 2017;15:214.
21. Erasmus JJ, Gladish GW, Broemeling L, et al. Interobserver and intraobserver variability in measurement of non-small-cell carcinoma lung lesions: implications for assessment of tumor response. J Clin Oncol 2003;21:2574-82.
22. Schwartz LH, Ginsberg MS, DeCorato D, et al. Evaluation of tumor measurements in oncology: use

of film-based and electronic techniques. J Clin Oncol 2000;18:2179-84.
23. Byrne MJ, Nowak AK. Modified RECIST criteria for assessment of response in malignant pleural mesothelioma. Ann Oncol 2004;15:257-60.
24. Kerpel A, Beytelman A, Ofek E, et al. Magnetic Resonance Imaging for the Follow-up of Treated Thymic Epithelial Malignancies. J Thorac Imaging 2019;34:345-50.
25. Eisenhauer EA, Therasse P, Bogaerts J, et al. New response evaluation criteria in solid tumours: revised RECIST guideline (version 1.1). Eur J Cancer 2009;45:228-47.
26. Quint LE. Imaging of anterior mediastinal masses. Cancer Imaging 2007;7 Spec No A:S56-62.
27. Shahrzad M, Le TS, Silva M, et al. Anterior mediastinal masses. AJR Am J Roentgenol 2014;203:W128-38.
28. Juanpere S, Cañete N, Ortuño P, et al. A diagnostic approach to the mediastinal masses. Insights Imaging 2013;4:29-52.
29. Nasseri F, Eftekhari F. Clinical and radiologic review of the normal and abnormal thymus: pearls and pitfalls. Radiographics 2010;30:413-28.
30. Nishino M, Ashiku SK, Kocher ON, et al. The thymus: a comprehensive review. Radiographics 2006;26:335-48.
31. Inaoka T, Takahashi K, Mineta M, et al. Thymic hyperplasia and thymus gland tumors: differentiation with chemical shift MR imaging. Radiology 2007;243:869-76.
32. Gaerte SC, Meyer CA, Winer-Muram HT, et al. Fat-containing lesions of the chest. Radiographics 2002;22 Spec No:S61-78.
33. Molinari F, Bankier AA, Eisenberg RL. Fat-containing lesions in adult thoracic imaging. AJR Am J Roentgenol 2011;197:W795-813.
34. de Jong WK, Blaauwgeers JL, Schaapveld M, et al. Thymic epithelial tumours: a population-based study of the incidence, diagnostic procedures and therapy. Eur J Cancer 2008;44:123-30.
35. Engels EA, Pfeiffer RM. Malignant thymoma in the United States: demographic patterns in incidence and associations with subsequent malignancies. Int J Cancer 2003;105:546-51.
36. McErlean A, Huang J, Zabor EC, et al. Distinguishing benign thymic lesions from early-stage thymic malignancies on computed tomography. J Thorac Oncol 2013;8:967-73.
37. Jeong YJ, Lee KS, Kim J, et al. Does CT of thymic epithelial tumors enable us to differentiate histologic subtypes and predict prognosis? AJR Am J Roentgenol 2004;183:283-9.
38. Jung KJ, Lee KS, Han J, et al. Malignant thymic epithelial tumors: CT-pathologic correlation. AJR Am J Roentgenol 2001;176:433-9.
39. Rosado-de-Christenson ML, Strollo DC, Marom EM. Imaging of thymic epithelial neoplasms. Hematol Oncol Clin North Am 2008;22:409-31.
40. Marom EM, Milito MA, Moran CA, et al. Computed tomography findings predicting invasiveness of thymoma. J Thorac Oncol 2011;6:1274-81.
41. Priola AM, Priola SM, Di Franco M, et al. Computed tomography and thymoma: distinctive findings in invasive and noninvasive thymoma and predictive features of recurrence. Radiol Med 2010;115:1-21.
42. Tomiyama N, Müller NL, Ellis SJ, et al. Invasive and noninvasive thymoma: distinctive CT features. J Comput Assist Tomogr 2001;25:388-93.
43. Sadohara J, Fujimoto K, Müller NL, et al. Thymic epithelial tumors: comparison of CT and MR imaging findings of low-risk thymomas, high-risk thymomas, and thymic carcinomas. Eur J Radiol 2006;60:70-9.
44. Jerushalmi J, Frenkel A, Bar-Shalom R, et al. Physiologic thymic uptake of 18F-FDG in children and young adults: a PET/CT evaluation of incidence, patterns, and relationship to treatment. J Nucl Med 2009;50:849-53.
45. Endo M, Nakagawa K, Ohde Y, et al. Utility of 18FDG-PET for differentiating the grade of malignancy in thymic epithelial tumors. Lung Cancer 2008;61:350-5.
46. Sung YM, Lee KS, Kim BT, et al. 18F-FDG PET/CT of thymic epithelial tumors: usefulness for distinguishing and staging tumor subgroups. J Nucl Med 2006;47:1628-34.
47. Han J, Lee KS, Yi CA, et al. Thymic epithelial tumors classified according to a newly established WHO scheme: CT and MR findings. Korean J Radiol 2003;4:46-53.
48. Inoue A, Tomiyama N, Fujimoto K, et al. MR imaging of thymic epithelial tumors: correlation with World Health Organization classification. Radiat Med 2006;24:171-81.
49. Nakagawa K, Takahashi S, Endo M, et al. Can (18)F-FDG PET predict the grade of malignancy in thymic epithelial tumors? An evaluation of only resected tumors. Cancer Manag Res 2017;9:761-8.
50. Shibata H, Nomori H, Uno K, et al. 18F-fluorodeoxyglucose and 11C-acetate positron emission tomography are useful modalities for diagnosing the histologic type of thymoma. Cancer 2009;115:2531-8.
51. Hephzibah J, Shanthly N, Oommen R. Diagnostic Utility of PET CT in Thymic Tumours with Emphasis on 68Ga-DOTATATE PET CT in Thymic Neuroendocrine Tumour - Experience at a Tertiary Level Hospital in India.

J Clin Diagn Res 2014;8:QC01-3.
52. Woo WL, Panagiotopoulos N, Gvinianidze L, et al. Primary mucoepidermoid carcinoma of the thymus presenting with myasthenia gravis. J Thorac Dis 2014;6:E223-5.
53. Nonaka D, Klimstra D, Rosai J. Thymic mucoepidermoid carcinomas: a clinicopathologic study of 10 cases and review of the literature. Am J Surg Pathol 2004;28:1526-31.
54. Wu SG, Li Y, Li B, et al. Unusual combined thymic mucoepidermoid carcinoma and thymoma: a case report and review of literature. Diagn Pathol 2014;9:8.
55. Yasuda M, Yasukawa T, Ozaki D, et al. Mucoepidermoid carcinoma of the thymus. Jpn J Thorac Cardiovasc Surg 2006;54:23-6.
56. Trojanowska A, Trojanowski P, Bisdas S, et al. Squamous cell cancer of hypopharynx and larynx - evaluation of metastatic nodal disease based on computed tomography perfusion studies. Eur J Radiol 2012;81:1034-9.
57. Bakan S, Kandemirli SG, Dikici AS, et al. Evaluation of anterior mediastinal solid tumors by CT perfusion: a preliminary study. Diagn Interv Radiol 2017;23:10-4.
58. Lee SH, Hur J, Kim YJ, et al. Additional value of dual-energy CT to differentiate between benign and malignant mediastinal tumors: an initial experience. Eur J Radiol 2013;82:2043-9.
59. Chang S, Hur J, Im DJ, et al. Volume-based quantification using dual-energy computed tomography in the differentiation of thymic epithelial tumours: an initial experience. Eur Radiol 2017;27:1992-2001.
60. Abdel Razek AA, Khairy M, Nada N. Diffusion-weighted MR imaging in thymic epithelial tumors: correlation with World Health Organization classification and clinical staging. Radiology 2014;273:268-75.
61. Guo Y, Kong QC, Zhu YQ, et al. Whole-lesion histogram analysis of the apparent diffusion coefficient: Evaluation of the correlation with subtypes of mucinous breast carcinoma. J Magn Reson Imaging 2018;47:391-400.
62. Zhang W, Zhou Y, Xu XQ, et al. A Whole-Tumor Histogram Analysis of Apparent Diffusion Coefficient Maps for Differentiating Thymic Carcinoma from Lymphoma. Korean J Radiol 2018;19:358-65.
63. Moran CA, Weissferdt A, Kalhor N, et al. Thymomas I: a clinicopathologic correlation of 250 cases with emphasis on the World Health Organization schema. Am J Clin Pathol 2012;137:444-50.
64. Yabuuchi H, Matsuo Y, Abe K, et al. Anterior mediastinal solid tumours in adults: characterisation using dynamic contrast-enhanced MRI, diffusion-weighted MRI, and FDG-PET/CT. Clin Radiol 2015;70:1289-98.
65. Shen J, Xue L, Zhong Y, et al. Feasibility of using dynamic contrast-enhanced MRI for differentiating thymic carcinoma from thymic lymphoma based on semi-quantitative and quantitative models. Clin Radiol 2020;75:560.e19-25.
66. Xiao G, Rong WC, Hu YC, et al. MRI Radiomics Analysis for Predicting the Pathologic Classification and TNM Staging of Thymic Epithelial Tumors: A Pilot Study. AJR Am J Roentgenol 2020;214:328-40.

doi: 10.21037/med-22-58
Cite this article as: Strange CD, Truong MT, Ahuja J, Strange TA, Patel S, Marom EM. Imaging evaluation of thymic tumors. Mediastinum 2023;7:28.

Case Series

Robotic resection of anterior mediastinal masses >10 cm: a case series

Obada Alqudah[1], Rhusmi Purmessur[1], John Hogan[1], Haisam Saad[1], Joana Fuentes-Warr[2], Jonathon Francis[3], Santosh Thandayuthapani[3], Vasileios Kouritas[1]^

[1]Department of Thoracic Surgery, Norfolk and Norwich University Hospital, Norwich, UK; [2]Department of General Surgery, Norfolk and Norwich University Hospital, Norwich, UK; [3]Department of Anaesthetics, Norfolk and Norwich University Hospital, Norwich, UK

Contributions: (I) Conception and design: V Kouritas, O Alqudah, J Hogan, H Saad; (II) Administrative support: V Kouritas; (III) Provision of study materials or patients: V Kouritas; (IV) Collection and assembly of data: V Kouritas, O Alqudah; (V) Data analysis and interpretation: V Kouritas, O Alqudah; (VI) Manuscript writing: All authors; (VII) Final approval of manuscript: All authors.

Correspondence to: Mr. Vasileios Kouritas, MD, PhD, CTh. Department of Thoracic Surgery, Norfolk and Norwich University Hospital, Colney Lane, Norwich NR4 7UY, UK. Email: vasileios.kouritas@nnuh.nhs.uk.

Background: Robot-assisted thoracic surgery (RATS) for intrathoracic pathology and especially for mediastinal mass resection has been increasingly accepted as an alternative method to open sternotomy and video-assisted thoracic surgery (VATS). However, the utilization of this approach for complex and advanced in size cases needs more clinical evidence. We are presenting a series of 4 patients who had resection of >10 cm mediastinal masses via RATS.

Cases Description: The mean age was 76.25±10.3 years and 3 were males (75%). All masses were positron emission tomography (PET) positive, and 1 patient had positive Acetyl-cholinesterase antibodies and myasthenia gravis (MG). All patients underwent RATS resection via DaVinci® X system. The dissections were conducted with spatula and/or Maryland bipolar forceps. In 2 cases, the resection was done with bilateral docking, and in 1 case, a drain was not inserted at the end. In 1 patient, pericardial resection was necessitated. All masses were thymomas with 1 dimension measured >10 cm on pathology. All patients were discharged on day 1 or 2 postoperatively with uneventful recoveries. There was no in-hospital, 30- or 90-day mortality. All patients were found to be without issues on follow-up.

Conclusions: This report shows that RATS is safe and can be offered in the management of >10 cm anterior mediastinal masses. The previous size limit of the tumor for minimally invasive and especially RATS approach of 5 cm should be challenged.

Keywords: Robotic; thymoma; thymectomy; case series

Received: 14 September 2022; Accepted: 17 April 2023; Published online: 26 April 2023.

doi: 10.21037/med-22-41

View this article at: https://dx.doi.org/10.21037/med-22-41

Introduction

Surgical resection is the treatment modality of choice for a significant number for anterior mediastinal tumours (1). Although imaging plays a crucial role in staging and in the establishment of the local invasion, on many occasions this is not possible to be totally clarified preoperatively (2). Moreover, these lesions are mostly symptomatic when they become large enough to compress or invade other organs (3).

Since the introduction of the minimally invasive approaches to the management of the anterior mediastinal tumours, there has been increasing volume of data showing better surgical results, and comparable oncological

^ ORCID: 0000-0002-6046-7476.

Table 1 Demographics and preoperational data of N=4 patients

Case	Age (years)	Gender	Co-morbidities	CT mass size (mm)	MG and treatment	CT findings of invasion	SUV	Ab (nmol/L)†
1	68	Male	Asthma, IDDM, HT	105×40×36	Yes, steroids, pyridostigmine, ICU stay	Pericardium	3.4	>20
2	81	Male	NIDDM, HT	102×63×76	No, none	None	3.2	negative
3	82	Male	COPD, CAD	80×56×101	No, none	None	3.5	negative
4	74	Female	Diarrhea	130×101×57	No, none	Pericardium, multilobulated	3.7	negative

†, negative if <0.5 nmol/L as per our institute's laboratory. CT, computed tomography; MG, myasthenia gravis; SUV, standardized uptake value; Ab, acetyl-cholinesterase receptor antibodies; IDDM, insulin dependent diabetes mellitus; HT, hypertension; ICU, intensive care unit; NIDDM, non-insulin dependent diabetes mellitus; COPD, chronic obstructive pulmonary disease; CAD, coronary artery disease.

outcomes in the short and long-term, when compared with open surgery (4-8). Robotic surgery more specifically has been implemented in the armamentarium of the minimally invasive procedures the last decade and has been shown to provide comparable outcomes with the traditional video-assisted thoracic surgery (VATS) (9,10).

In complicated anterior mediastinal masses cases in which either the mass is bigger than 5 cm, or it is infiltrating the pericardium or other structures, most surgeons would prefer to proceed to a sternotomy rather than pursue a VATS or a robotic-assisted thoracic surgery (RATS) resection in order to ensure safe and complete resection (11,12).

Herein, we report a case series of >10 cm and complicated anterior mediastinal masses, which were resected successfully and safely via RATS. We present this article in accordance with the AME Case Series reporting checklist (available at https://med.amegroups.com/article/view/10.21037/med-22-41/rc).

Highlight box

Key findings

- Anterior mediastinal masses >10 cm are successfully resectable with robotic surgery.

What is known and what is new?

- Surgeons treating patients with mediastinal masses >5 cm usually avoid minimally invasive surgery and perform sternotomy.
- Robotic systems allow the resection of mediastinal masses >10 cm, resulting in better postoperative outcomes, quicker recovery and similar to sternotomy oncological results.

What is the implication, and what should change now?

- Robotic systems allow the resection of increased size mediastinal masses via minimally invasive approach, previously not feasible with traditional thoracoscopic techniques. Patients with such masses should be offered robotic resection over sternotomy.

Case presentation

Study design

The present study is a case series of RATS resection of >10 cm and complicated anterior mediastinal masses performed in our institute. The study is retrospective, single-center including non-consecutive cases.

Setting and time-frame

The case series were performed at a tertiary university hospital with a high volume referral Thoracic Surgery department. The time-frame of the cases performed was over a period of 1.5 years (January 2021–June 2022).

Follow-up of patients ranges from 2–17 months and was done for all of them face to face at the outpatient department.

Patients

Four patients are herein reported. The mean age was 76.25±10.3 years and 3 were males (75%). Patients were referred to our department after diagnosing the lesions. Two of the patients were investigated initially for cough and 1 because of myasthenia gravis (MG). In 1 case the mass was found incidentally during a chest X-ray (CXR) for a usual check-up. The demographics of each of the patients and their co-morbidities are reported in *Table 1*. All patients had a positron emission tomography (PET) scan performed before surgery and all masses were found to be PET

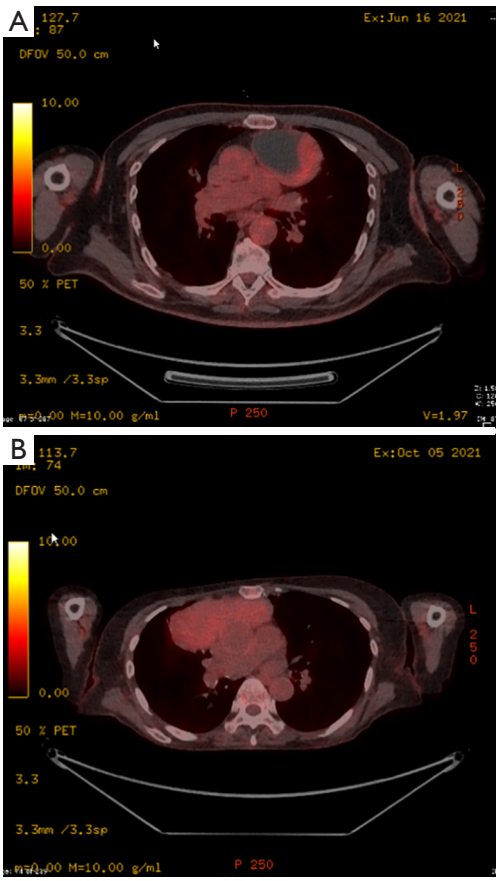

Figure 1 PET imaging of patients undergoing surgery. (A) PET scan from patient with a mass measuring 102×63×76 showing a partial cystic photopenic component and a solid lateral PET positive component. (B) PET scan from patient with a mass measuring 130×101×57 and which was homogenously PET positive. PET, positron emission tomography.

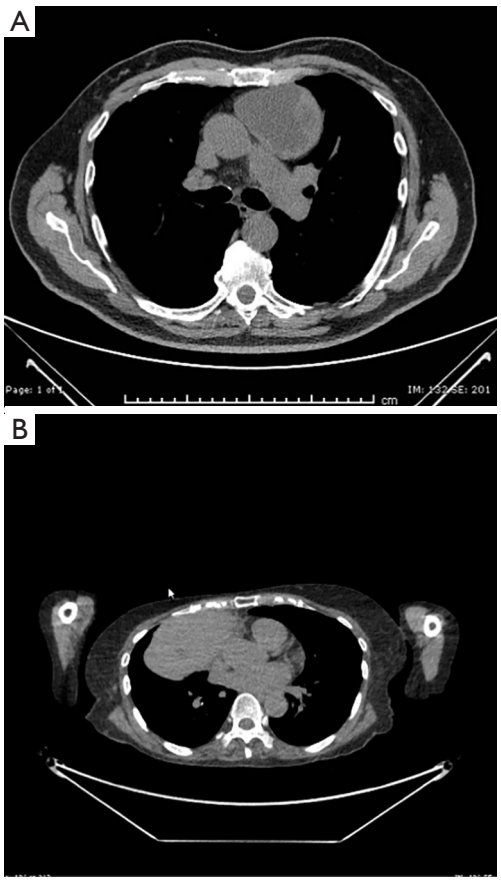

Figure 2 CT scans from the same patients showing the masses in the anterior mediastinum. (A) The mass is depicted to be cystic with a lateral solid part. (B) The mass is multilobulated and was considered to be involving the pericardium. CT, computed tomography.

positive [mean standardized uptake value (SUV): 3.45±1.23, range SUV 3.2–3.7, *Figure 1A*,*1B*]. They also had their acetyl-cholinesterase receptor antibodies determined which were positive in 1 case with MG (*Table 1*).

The measured computed tomography (CT) scan size of the masses was found to be above 10 cm at one of the measured axis (*Table 1*, *Figure 2A*,*2B*).

Anonymity of patients was ensured by using anonymized images and hospital numbers and age in years rather than names of the patients and dates of birth.

Surgical technique

Procedures were performed by 1 board certified surgeon, with adequate experience in robotic surgery previously signed off by the proctors as per the Intuitive™ training schedule.

Single lung ventilation was achieved with a double lumen tube while an arterial line was used in all cases for invasive monitoring during the procedure. A urine catheter was inserted in 2 cases.

All patients were placed with 30-degree right chest up, with the right arm tacked adducted below the body level as all procedures were started from the right aspect of the mediastinum. Draping included both sides for possible double docking or conversion to open.

All procedures were performed with the DaVinci X Intuitive® system either with single docking using 3 ports

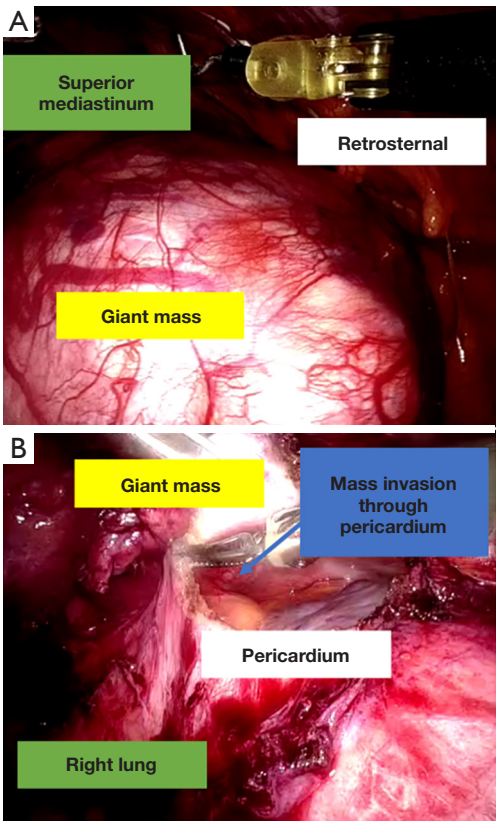

Figure 3 Pictures taken during surgery. (A) 15 cm anterior mediastinal mass. (B) Mass is pushed superiorly, the pericardium has been opened and lesions are found to be infiltrating through the pericardium.

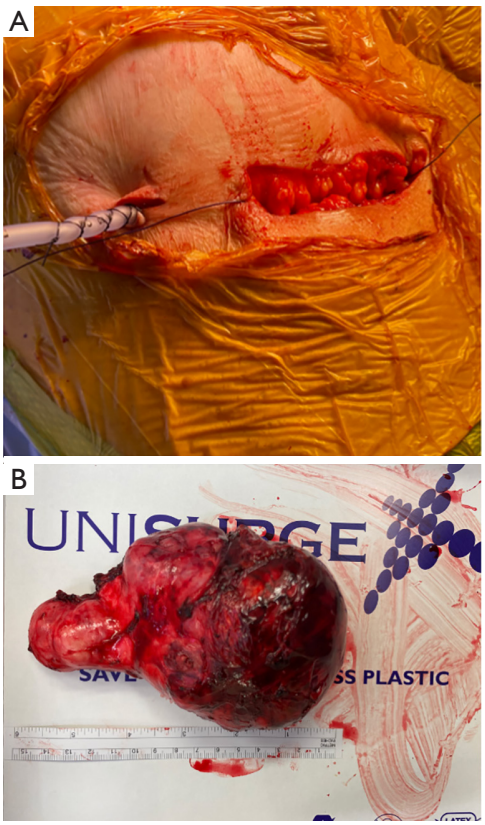

Figure 4 Pictures taken from the resection of 15 cm anterior mediastinal mass. (A) The 12 mm port was elongated up to 4 cm in order to facilitate the removal of the mass and this was used in all cases up to an extend. (B) One of the masses measured bigger than anticipated from imaging i.e., 15 cm in this case.

on the right (2×8 mm: 4th intercostal space mid-axillary line, 6th intercostal space anterior axillary line and 1×12 mm parasternally 5th intercostal space) or double docking with 2 extra ports on the left (2×8 mm: 6th intercostal space anterior axillary line and 4th intercostal space mid-axillary line) to achieve visualization of the left phrenic nerve, skeletonization of the left side of the mediastinum and for retraction of the specimen.

The CO_2 insufflation pressure range used was 8–10 mmHg with a flow of 5–20 mLs/min.

Dissection usually started from the diaphragmatic area (*Figure 3A*) towards the phrenic nerve and along it, dissecting the mediastinal fat/mass off it with Maryland bipolar forceps, in order to avoid damaging the nerve. Dissection with a spatula continued towards the left pleura medially to the internal mammary vessels which were preserved. The left pleura at this point was usually opened. Dissection then continued along the superior vena cava medially to the phrenic nerve towards the confluence with the right innominate vein. At this point, the left innominate vein was identified, and mediastinal fat/thymus/mass was dissected off it with sharp dissection either with spatula or with Maryland forceps. In all cases full thymectomy was performed (in 1 case was additionally necessitated because of MG) apart from resection of the mass. Ligation of thymic tributaries was performed using hem-o-lok clips. In 1 case, pericardial resection was necessitated (*Figure 3B*) of a 4×4 cm area superiorly and above the ascending aorta, without the need of a reconstruction.

The specimens were removed into an endobag through the 12 mm port which was accordingly extended up to 4 cm laterally as was needed for instance in the case of the 15 cm mass (*Figure 4A*). In 1 case and because the mass was partially cystic in nature, the mass was drained with the suction inside

Table 2 Intraoperative data of N=4 patients

Case	Docking	Duration of surgery (min)	Blood loss (mL)	Intraoperative events	No. of 8 mm ports	No. of 12 mm ports	Chest drain insertion	Thymectomy
1	Double	345	50	Resection of pericardium 4×4 cm	4	1	20 Fr	Yes
2	Single left	90	50	None	2	1	No	Yes
3	Single right	120	50	None	2	1	20 Fr	Yes
4	Double	120	100	Fibrotic tissues, pericardium not involved	4	1	20 Fr	Yes

Fr, French.

Table 3 Postoperative and histology data of N=4 patients

Case	Size (mm)	Pathology of mass	Stage	R0	Drain stay (days)	LOS (days)	Morbidity	In-hospital/30-day mortality
1	138×50	Thymoma	B2	Yes	1	2	No	No
2	100×60	Thymoma	AB	Yes	N/A	2	No	No
3	110×45	Thymoma	AB	Yes	1	1	No	No
4	150×70	Thymoma	AB	Yes	1	2	No	No

R0, resection status; LOS, length of stay; N/A, not available.

the endobag and was removed inside it intact.

A single chest tube was inserted in all but 1 case, from the right anterior axillary port site heading towards the superior mediastinum.

All patients were extubated after surgery and were admitted to High Dependency Unit for observation under the fear of myasthenic crisis.

The intraoperative details are summarized in *Table 2*.

Outcomes

All patients had satisfactory CXR after surgery and the chest drain was removed on postoperative day (POD) 1. Recovery was uneventful for all patients and 3 of them were discharged home on POD 2 with one discharged late on POD 1 after being discharged from high dependency unit (HDU). There was no in-hospital, 30- or 90-day mortality.

All masses were diagnosed by histopathology to represent thymomas, as summarized in *Table 3*, all measuring above 10 cm with the biggest measuring 15 cm in the long axis (*Figure 4B*). R0 resection was achieved in all cases. The cases were discussed at the multidisciplinary team (MDT) meeting and the oncologist present decided to offer adjuvant radiotherapy because of the size of the tumor under the fear of recurrence despite the R0 resection and the absence of capsular invasion (*Table 3*).

On follow-up, all patients reported no important issues from surgery and are under follow-up with CT scan without any reported recurrences up to now.

This case series has been reported in line with the AME Case Series Guideline (13).

All procedures performed in this study were in accordance with the ethical standards of the institutional and/or national research committee(s) and with the Helsinki Declaration (as revised in 2013). Written informed consent was obtained from the patients for publication of this case report and accompanying images. A copy of the written consent is available for review by the editorial office of this journal.

Discussion

We herein present a series of 4 cases, all above 10 cm, with one of them additionally requiring pericardial resection, which were all successfully removed via RATS. All patients recovered quickly from their procedure without adverse events and are well on follow-up. The size of an anterior mediastinal mass should not preclude pursuing minimally invasive surgery and especially RATS resection.

The anatomic boundaries of the narrow mediastinum with its various vital structures, makes it a challenging place to access and to safely dissect and/or resect tumours, especially the bigger in size ones. The open surgical approach i.e., sternotomy or thoracotomy, was notoriously the standard approach for surgical interventions to this region. When facing cases which necessitate resection of big masses, most surgeons would prefer to proceed to an open procedure or convert to one, in order to resect them safely and completely (11,12). It has been reported that a mass is perceived as "big" if it is bigger than 5 cm (14-16). This study shows that perseverance with RATS resection in cases of masses >10 cm can be easily and safely performed, without the necessity of a sternotomy or a thoracotomy. The most important tip for a safe and complete resection is patience and perseverance. Also, bilateral docking is very helpful to achieve more angles and safely identify the important structures in the mediastinum for example big vessels, the phrenic nerves etc. Finally, we used contralateral ports for traction inferiorly of the mass which will allow better access to the superior mediastinum structures for example the left innominate vein, the thymic horns etc.

Minimally invasive approaches are shown to be better in terms of recovery from the open ones offering amongst others shorter duration of surgery, shorter postoperative drainage and decreased blood loss, with comparable oncological outcomes (4,9,17,18). RATS resections and/or thymectomies are specifically shown to have superior outcomes in terms of recovery and safety versus transsternal ones and more specifically are shown to produce less intraoperative blood loss, lower incidence of postoperative complications, less risk of wound infection, fewer transfusions, shorter length of stay (LOS), and better quality of life after surgery, without compromising the oncological outcomes (6,8,10). All these were shown in our case series as all patients had minimal blood loss during surgery, had their drains removed the next day (in 1 case the surgeon decided not even to leave a drain in the chest) and all were discharged home within 2 days without issues. Despite all these, however, RATS resection of such big masses should not be offered at the beginning of the robotic learning curve because in inexperienced hands it could lead to harm, for example from injury to adjacent structures such as great vessels, or to oncological outcome issues, for example R1 resection or capsular rupture before removal etc.

Apart from these, in some cases, avoiding an open approach is very crucial as for example in one of our cases in which the patient had insulin dependent diabetes mellitus and difficult to control MG with high doses of steroids. In this specific case, proceeding to a sternotomy would cause additional issues to the recovery of the patient for example prolonged hospitalization and stay in intensive care unit, wound issues and others.

Comparing RATS with conventional VATS, these were shown to be comparable (9,18), but VATS is technically more challenging, due to its limited handling angles, and the suboptimal 2D vision screen, which makes it difficult to be used for giant masses resection. This case series shows that RATS can provide a wider range of maneuverability of instruments and 3D vision, which make the resection of masses in the mediastinum >10 cm, both safe and successful.

As it would make sense that size does matter in choosing the proper approach of surgery, the biggest size of an anterior mediastinal mass to our knowledge is reported via VATS to be 14 cm (14), although in 1 of our cases the resected mass was 15 cm. Literature is scanty with regards to this and very few cases of big masses have been reported to have been resected via minimally invasive approaches and RATS more specifically. To our knowledge, 9 cm is the biggest mass resected via RATS that has been reported (19).

Apart from the size, another important factor which needs careful consideration is the complexity of the mass to be resected i.e., the need for pericardial resection, invasion of big vessels or proximity to them, resection of lung parenchyma etc. (20). Resection of pericardium is the most common complexity a surgeon can face and there are reports showing efficiency of minimally invasive surgery and RATS in resecting such masses, en block with the pericardium, followed by pericardial patch reconstruction (21). This however was not necessitated in our case because the pericardium resected was on top of the aortic root towards the superior mediastinum.

Another consideration faced by the surgeons is the removal of the big specimen. In the cases of cystic components once the specimen is within the endobag then it can be punctured and hence removed easily via one of the ports which will need to be slightly enlarged (14). In solid masses though, extraction of the specimen is an issue, and consequently this can lead to a mini thoracotomy. In our cases though, we tackled this issue by enlarging the 12 mm port to 4 cm and with slight spreading of the ribs with retractors, the masses, including the 15 cm one, were removed without issues.

Conclusions

In conclusion, we report a series of 4 cases of >10 cm

anterior mediastinal masses, with 1 needing pericardial resection, which were all resected successfully and uneventfully via RATS, irrespectively of their size or complexity. Although RATS is not offered routinely by all institutes, its use in cases of >10 cm anterior mediastinal masses is safe and beneficial for the patients and as such they should be considered and attempted should this technology be available.

Acknowledgments

Funding: None.

Footnote

Reporting Checklist: The authors have completed the AME Case Series reporting checklist. Available at https://med.amegroups.com/article/view/10.21037/med-22-41/rc

Peer Review File: Available at https://med.amegroups.com/article/view/10.21037/med-22-41/prf

Conflicts of Interest: All authors have completed the ICMJE uniform disclosure form (available at https://med.amegroups.com/article/view/10.21037/med-22-41/coif). VK serves as an unpaid editorial board member of *Mediastinum* from August 2022 to July 2024. The other authors have no conflicts of interest to declare.

Ethical Statement: The authors are accountable for all aspects of the work in ensuring that questions related to the accuracy or integrity of any part of the work are appropriately investigated and resolved. All procedures performed in this study were in accordance with the ethical standards of the institutional and/or national research committee(s) and with the Helsinki Declaration (as revised in 2013). Written informed consent was obtained from the patients for publication of this case report and accompanying images. A copy of the written consent is available for review by the editorial office of this journal.

References

1. Almeida PT, Heller D. Anterior Mediastinal Mass. [Updated 2021 Aug 14]. In: StatPearls [Internet]. Treasure Island (FL): StatPearls Publishing, 2022. Available online: https://www.ncbi.nlm.nih.gov/books/NBK546608/
2. Juanpere S, Cañete N, Ortuño P, et al. A diagnostic approach to the mediastinal masses. Insights Imaging 2013;4:29-52.
3. Duwe BV, Sterman DH, Musani AI. Tumors of the mediastinum. Chest 2005;128:2893-909.
4. Chetty GK, Khan OA, Onyeaka CV, et al. Experience with video-assisted surgery for suspected mediastinal tumours. Eur J Surg Oncol 2004;30:776-80.
5. Melfi F, Fanucchi O, Davini F, et al. Ten-year experience of mediastinal robotic surgery in a single referral centre. Eur J Cardiothorac Surg 2012;41:847-51.
6. Azenha LF, Deckarm R, Minervini F, et al. Robotic vs. Transsternal Thymectomy: A Single Center Experience over 10 Years. J Clin Med 2021;10:4991.
7. Kang CH, Na KJ, Park S, et al. Long-Term Outcomes of Robotic Thymectomy in Patients With Thymic Epithelial Tumors. Ann Thorac Surg 2021;112:430-5.
8. Kang CH, Hwang Y, Lee HJ, et al. Robotic Thymectomy in Anterior Mediastinal Mass: Propensity Score Matching Study With Transsternal Thymectomy. Ann Thorac Surg 2016;102:895-901.
9. O'Sullivan KE, Kreaden US, Hebert AE, et al. A systematic review of robotic versus open and video assisted thoracoscopic surgery (VATS) approaches for thymectomy. Ann Cardiothorac Surg 2019;8:174-93.
10. Balduyck B, Hendriks JM, Lauwers P, et al. Quality of life after anterior mediastinal mass resection: a prospective study comparing open with robotic-assisted thoracoscopic resection. Eur J Cardiothorac Surg 2011;39:543-8.
11. Burt BM, Yao X, Shrager J, et al. Determinants of Complete Resection of Thymoma by Minimally Invasive and Open Thymectomy: Analysis of an International Registry. J Thorac Oncol 2017;12:129-36.
12. Yang CJ, Hurd J, Shah SA, et al. A national analysis of open versus minimally invasive thymectomy for stage I to III thymoma. J Thorac Cardiovasc Surg 2020;160:555-67.e15.
13. AME Case Series checklist 2020. Available online: https://cdn.amegroups.cn/static/public/20-AME-Case-Series-Checklist.pdf

14. Hughes BD, Okereke IC. Giant mediastinal mass: one port video assisted thoracoscopic surgery. J Surg Case Rep 2017;2017:rjx178.
15. Hess NR, Sarkaria IS, Pennathur A, et al. Minimally invasive versus open thymectomy: a systematic review of surgical techniques, patient demographics, and perioperative outcomes. Ann Cardiothorac Surg 2016;5:1-9.
16. Gossot D, Izquierdo RR, Girard P, et al. Thoracoscopic resection of bulky intrathoracic benign lesions. Eur J Cardiothorac Surg 2007;32:848-51.
17. Ye B, Tantai JC, Ge XX, et al. Surgical techniques for early stage thymoma: video assisted thoracoscopic thymectomy versus transsternal thymectomy. J Thorac Cardiovasc Surg 2014;147:1599-603.
18. Manoly I, Whistance RN, Sreekumar R, et al. Early and mid-term outcomes of trans-sternal and video-assisted thoracoscopic surgery for thymoma. Eur J Cardiothorac Surg 2014;45:e187-93.
19. Kodia K, Nguyen DM, Villamizar NR. A 9 cm robotic thymectomy and pericardial repair case report. Mediastinum 2020;4:38.
20. Kuo SW, Huang PM, Lin MW, et al. Robot-assisted thoracic surgery for complex procedures. J Thorac Dis 2017;9:3105-13.
21. Yang HC, Coyan G, Vercauteren M, et al. Robot-assisted en bloc anterior mediastinal mass excision with pericardium and adjacent lung for locally advanced thymic carcinoma. J Vis Surg 2018;4:115.

doi: 10.21037/med-22-41
Cite this article as: Alqudah O, Purmessur R, Hogan J, Saad H, Fuentes-Warr J, Francis J, Thandayuthapani S, Kouritas V. Robotic resection of anterior mediastinal masses >10 cm: a case series. Mediastinum 2023;7:29.

Case Report

Thoracoscopic resection of a cavernous haemangioma of anterior mediastinum: case report and literature review

Junrui Xu^, Yuefeng Xu, Renquan Zhang^

Department of Thoracic Surgery, First Affiliated Hospital of Anhui Medical University, Hefei, China

Contributions: (I) Conception and design: J Xu; (II) Administrative support: R Zhang; (III) Provision of study materials or patients: R Zhang; (IV) Collection and assembly of data: Y Xu; (V) Data analysis and interpretation: J Xu, Y Xu; (VI) Manuscript writing: All authors; (VII) Final approval of manuscript: All authors.

Correspondence to: Renquan Zhang, MD. Department of Thoracic Surgery, First Affiliated Hospital of Anhui Medical University, 218 Jixi Road, Hefei 230022, China. Email: zhangrenquan@live.cn.

Background: Mediastinal haemangioma is a rare type of tumour and accounts for ≤0.5% of all mediastinal tumours. Mediastinal haemangioma is often nonspecific upon examination by imaging. Mediastinal haemangioma diagnosis is difficult to confirm before surgery because the characteristic features of diagnostic imaging are poor, and these lesions are extremely rarely encountered in clinical practice.

Case Description: We herein report a case of thoracoscopic resection of a cavernous haemangioma in the anterior mediastinum. A 40-year-old man was referred to our hospital for a health examination. A chest computed tomography scan showed a mass with irregular contrast enhancement and a smooth surface. Using video-assisted thoracoscopic surgery, the tumour was completely extirpated and confirmed histologically to be a cavernous haemangioma. The patient recovered well, was discharged, he has since had no recurrences, and continues to be closely monitored as an outpatient.

Conclusions: Mediastinal haemangiomas, a rare type of mediastinal tumour, are typically benign and located in the anterior mediastinum, and lack specific symptoms and relevant imaging features. We found that minimally invasive thoracoscopic resection provided a satisfactory view and facilitated correct handling of a mediastinal cavernous haemangioma. Although such tumours are mostly benign and the prognosis is good, we recommend aggressive surgical management to avoid missing malignant lesions.

Keywords: Mediastinal haemangioma; case report; diagnosis; video-assisted thoracoscopic surgery (VATS)

Received: 01 January 2023; Accepted: 07 April 2023; Published online: 09 May 2023.

doi: 10.21037/med-23-1

View this article at: https://dx.doi.org/10.21037/med-23-1

Introduction

Mediastinal haemangiomas are rare tumours, and some reports indicate that they account for 0.5% or less of all mediastinal tumours (1). Given its nonspecific imaging manifestations, preoperative diagnosis is difficult, and surgery is the main treatment. We herein report a case of cavernous haemangioma in the anterior mediastinum that was successfully treated by video-assisted thoracoscopic surgery (VATS). We present this case in accordance with the CARE reporting checklist (available at https://med.amegroups.com/article/view/10.21037/med-23-1/rc).

Case presentation

A 40-year-old patient underwent chest computed tomography (CT) during a routine medical examination, and an anterior mediastinal mass was detected. The patient had undergone fracture fixation one year earlier for a right

^ ORCID: Junrui Xu, 0000-0002-6234-2335; Renquan Zhang, 0000-0001-5342-8498.

calcaneal fracture, and the internal fixation in the calcaneus was not removed. Otherwise, the patient had no other past medical history, his physical examination and laboratory data were normal, he had no history of chronic or genetic disease, and a chest radiograph showed no abnormalities. A CT scan revealed that a mediastinal mass was located in the anterior mediastinum. The mass range was approximately 9.2 cm × 3.9 cm × 3.6 cm. The CT scan also showed that the mass had a smooth surface and heterogeneous contents. The upper border of the tumour was from the sternal angle and the inferior border of the tumour was at the aortic outflow. The contrast-enhanced CT scan revealed uneven delayed enhancement shadows with multiple punctate calcifications (*Figure 1*). The patient was unable to undergo magnetic resonance imaging (MRI) due to the internal fixation in the right calcaneus. According to preoperative examinations and imaging reports, we suspected that the mass in the anterior mediastinum was a haemangioma. Mediastinal haemangiomas require differentiation from mediastinal cysts, neurogenic tumours, teratomas, and lymphomas. For diagnosis and treatment, we performed a minimally invasive thoracoscopic mediastinal tumour resection and sent the resected tumour for postoperative pathological examination. After the patient received general anaesthesia and a double lumen endotracheal tube was placed, we introduced a thoracoscope using a trocar in the seventh intercostal space at the posterior axillary line. We placed two other working trocars in the third and sixth intercostal spaces at the anterior axillary line in order to insert the dissecting instruments. The mass was located in the anterior mediastinum encased in a vascular cluster (*Figure 2*). We opened the mediastinal pleura with an electrocoagulation hook, and the anterior mediastinal haemangioma was resected along the mediastinal adipose tissue. We found that the tumour adhered closely to the superficial pericardium vessels and likely served as a source of vascular supply for the tumour; therefore, these vessels were carefully removed by dissection and the total thoracoscopic resection of the suspected mediastinal haemangioma was complete.

The resected specimen measured 15.0 cm × 6.0 cm × 1.4 cm and was surrounded by pericardial adipose tissue and haemorrhagic and transparent thrombosis (*Figure 3*). A large number of thick, sponge-like vascular sinuses were found during the mirror-image inspection of the tumour. Based on these findings, the tumours were diagnosed as mediastinal sponge haemangiomas. The patient recovered without postoperative complications and was discharged post-operative day four. The patient was examined one month later, with follow-up visits scheduled every 6 months thereafter. At present, 24 months after surgery, no recurrence has been observed and the individual continues to be carefully monitored as an outpatient. The patient has recovered well and is able to perform heavy physical work without reporting any adverse effects or complications. All procedures performed in this study were in accordance with the ethical standards of the institutional and/or national research committee(s) and with the Helsinki Declaration (as revised in 2013). Written informed consent was obtained from the patient for publication of this case report and accompanying images. A copy of the written consent is available for review by the editorial office of this journal.

Highlight box

Key findings

- We found that a mediastinal haemangioma can be completely resected under minimally invasive thoracoscopy, which is a safe and reliable procedure relative to traditional open surgery and accelerates patient recovery without postoperative recurrence or metastasis.

What is known and what is new?

- Mediastinal haemangiomas are a rare type of mediastinal tumour, typically benign, are located anterior mediastinum, and lack of specific symptoms and relevant imaging features.
- We herein report a case of thoracoscopic resection of cavernous haemangioma in the anterior mediastinum that was completely resected by thoracoscopy. Although such tumours are mostly benign and the prognosis is good, we recommend aggressive surgical management to avoid missing malignant lesions.

What is the implication, and what should change now?

- We recommend surgical treatment for mediastinal haemangioma to prevent compression symptoms caused by excessive tumour size. Thoracoscopic surgery is minimally invasive, safe and reliable, and should be the first choice of surgical approach.

Discussion

Mediastinal haemangioma is a rare type of mediastinal tumour. The first case was reported by Shennan in 1914 (2), and fewer than 100 cases were reported by the 1980s. The widespread use of CT and MRI technologies has led to an increasing number of cases being identified and reported. However, an up-to-date account of the total number of cases has not been reported in the literature. Instead,

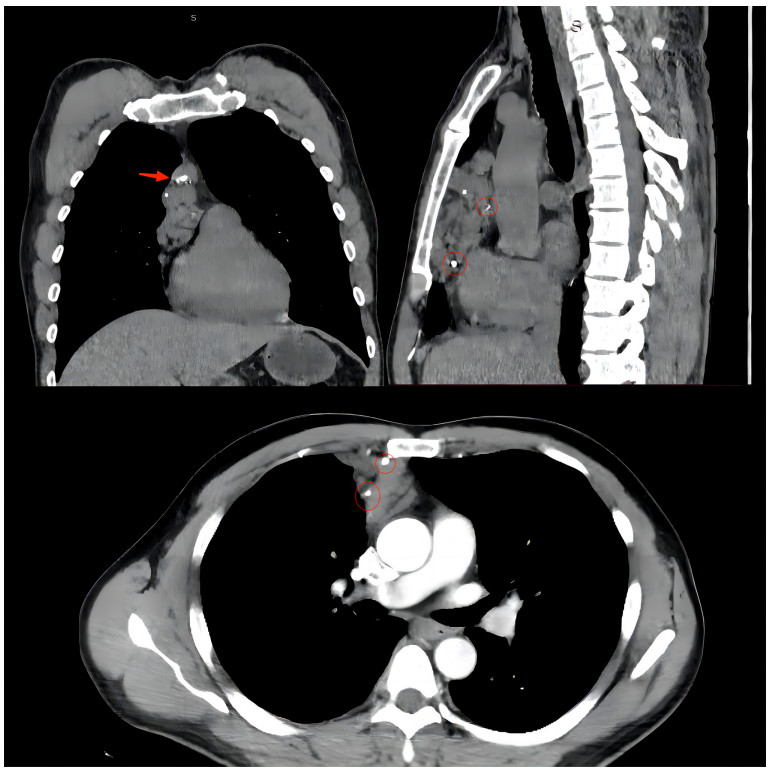

Figure 1 The contrast-enhanced CT scan showed a mass with an uneven delayed enhancement shadow that had multiple punctate calcifications. The vessel was pointed by red arrow and punctate calcifications were circled.

Figure 2 The mass was found in the anterior mediastinum, and its surface was covered with a vascular cluster.

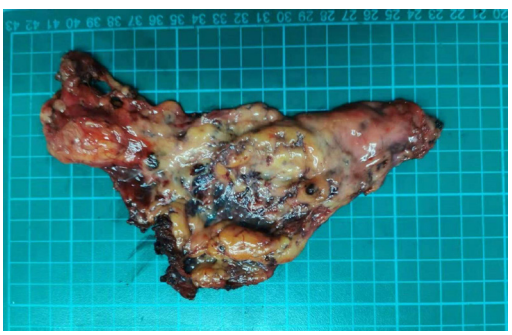

Figure 3 Tumour tissue specimens after surgery. We observed that the tumour was surrounded by pericardial adipose tissue and haemorrhagic and transparent thrombosis.

several single clinical centre case reports or single centre summaries in different countries and regions have been published. The total number and incidence of mediastinal haemangiomas remain rare compared with other types of mediastinal tumours. Mediastinal haemangiomas are mostly benign and are mainly classified as cavernous or capillary haemangiomas, followed by rarer benign types, including fibroangioma, angiolipoma, fibroangiolipoma, angiolymphangioma, venous haemangioma, arteriovenous fistula and angioleiomyoma (3,4).

Mediastinal haemangiomas are common in the anterior or posterior mediastinum and rarely occur in the middle mediastinum. Approximately 68% of mediastinal haemangiomas are located in the anterior mediastinum, 22% in the posterior mediastinum, and less than 10% are found in the middle mediastinum (5). Patients with mediastinal haemangioma do not present with specific clinical symptoms, and approximately 1/2–1/3 of lesions are discovered incidentally during physical examination by chest X-ray or CT. If symptoms are reported, tumour compression or the invasion of surrounding organs or tissues are often noted, with common symptoms including cough, wheezing, dyspnoea (6), chest pain, hoarseness, superior vena cava obstruction, Horner syndrome or dysphagia caused by the compression of the oesophagus (7), and tumour invasion of the spinal canal (8), which may present with neurological symptoms related to spinal cord compression.

Mediastinal haemangioma is often nonspecific on X-ray and CT imaging. The chest X-ray showed that the haemangioma was a round or lobulated mass. The presence of phleboliths in the lesion was found to be diagnostic, since this feature appears in 10% of patients with mediastinal haemangiomas (3). Moreover, thrombus in the haemangioma, venous inflammation and calcification form phleboliths that appear as rings or spotty calcifications on chest radiography. If the haemangioma is adjacent to the ribs, manifestations of erosion are observed in the ribs. Malignant mediastinal haemangiomas, which show ill-defined and peripheral invasion, can also erode the chest wall. A haemangioma typically appears as a heterogeneous lesion on an unenhanced CT scan, while the degree of internal enhancement of mediastinal haemangioma is heterogeneous on examination with contrast-enhanced chest CT. The degree of central enhancement is significantly higher than that at the edge, which may be a specific manifestation of haemangioma (9). Significant draining veins with local dilatation or venous aneurysm can be found on contrast-enhanced CT. The walls of the draining veins and feeding arteries in the lesion are smooth and regular, which may help to identify other blood-rich malignant tumours that are invading the blurred and irregular vascular wall. Blood supply arteries and draining veins are the main factors that increase the significant risk of bleeding and blood loss (10), and preoperative contrast-enhanced CT reveals draining veins, which are very important for surgical planning. In this case, the feeding artery and drainage vein of the haemangioma were clearly visible by preoperative chest enhanced CT, which allowed thoracoscopic surgery to proceed smoothly.

Chest MRI examination is helpful for imaging-based diagnosis of mediastinal haemangioma, and the findings obtained through magnetic resonance are similar to those of hepatic haemangioma. These lesions have a low to moderate signal intensity on T1-weighted images and high signal intensity on T2-weighted images (11). These characteristics can be attributed to the high vascular space content of haemangiomas. Haemangiomas exhibit three enhancement patterns on postcontrast images: homogeneous enhancement and peripheral nodular enhancement with or without centripetal enhancement. Mediastinal haemangiomas are mostly benign tumours with a low risk of recurrence and metastasis, so positron emission tomography-CT (PET-CT) is not recommended during routine examination unless there is a clear basis for malignancy or the presence of a high-risk factor for malignancy.

Diagnosing mediastinal haemangioma is difficult before surgery because the characteristic features of diagnostic imaging are poor, and these lesions are rarely encountered in clinical practice. Given the lack of specificity, benign haemangiomas are generally caused by congenital dysplasia, mediastinal haemangioma, and haemangioma in other parts of the body and are mainly associated with vascular neoplastic proliferation. Generally, fibrous adipose tissue is also observed to be associated with thymic remnants. Because mediastinal haemangioma is extremely rare in clinical practice and lacks specific clinical manifestations and imaging signs, it is often misdiagnosed as a common mediastinal disease, such as thymoma or neurogenic tumours (12). Imaging findings of significant enhancement and abundance may indicate the possibility of vasogenic tumours, but attention should be given to differentiating these lesions from giant lymphadenopathy, with diagnosis made on the basis of histopathological examination. The most reliable practice is to perform surgical resection and obtain pathological specimens. Because there are many vessels in mediastinal haemangiomas and some tumours are located in the posterior mediastinum or next to the great arteries, preoperative biopsy is not recommended, since this increases the risk of bleeding. For lesions that are difficult to identify, the vascular component should be identified and immunohistochemical assessment should be performed. To exclude lymphangioma and diagnose haemangioma, CD31 and CD34 show positive expression, and D240 shows negative expression (13).

Mediastinal haemangiomas are treated by surgical resection. The traditional surgical approach uses posterolateral, sternotomy or midline incision thoracotomy. In the current case study, preoperative chest CT and MRI examinations were routinely performed to assess the extent of tumour involvement and the course of tumour nutrient vessels in detail, and the appropriate surgical approach and steps were selected to avoid massive haemorrhage caused by blind operation. The development of VATS has led to the use of this technique as a treatment option. At present, there have been many reports on the use of VATS for the complete resection of anterior (posterior) mediastinal haemangiomas (14,15). Compared with the previous approach involving open surgery and resection (16), we achieved complete resection by thoracoscopy. The feeding vessels of the tumour were determined based on preoperative imaging and intraoperative exploration, which was helpful diagnosing and resecting the haemangioma. These observations help ensure proper management and prevent complications, such as bleeding. Thoracoscopic surgery facilitates the satisfactory observation of tumours and blood vessels and can safely remove mediastinal venous haemangiomas. In a retrospective analysis of 18 cases of mediastinal haemangioma (17), all cases were treated with surgical resection, 8 underwent VATS, and 9 underwent traditional posterolateral open surgery, all of which were completely resected without recurrence. This retrospective study confirms that the VATS technique is safe and reliable for performing surgical procedures for mediastinal haemangioma, enabling complete resection and reducing postoperative complications. VATS resulted in the complete resection of the anterior mediastinal haemangioma in this patient without bleeding or other complications. We suggest that, with a thorough preoperative examination and skilled operation, thoracoscopic complete resection is safe and feasible with less trauma to patients, rapid postoperative recovery and can reduce the occurrence of complications, such as bleeding. Several retrospective analyses (4,17) have reported that a very small number of patients with mediastinal haemangiomas experience recurrence after surgery due to incomplete resection or a higher degree of malignancy with an overall better prognosis. Although mediastinal haemangiomas are mostly benign and have a very low probability of recurrence, relevant research or guidelines are not available to indicate whether mediastinal haemangiomas require monitoring. We recommend that patients with mediastinal haemangioma undergo CT after surgery to prevent tumour recurrence, but further studies are required.

Conclusions

In summary, mediastinal haemangioma is a rare mediastinal tumour, most of which is benign, in the anterior mediastinum, and lacks specific symptoms and relevant imaging features. VATS is safe and reliable compared with the traditional thoracotomy approach. Although such diseases are mostly benign and the prognosis is good, we still recommend aggressive surgical management to avoid missing malignant lesions.

Acknowledgments

We thank the 2022 Chinese Congress on Oncology for its support and encouragement and for providing the authors with the opportunity to share this case. We thank the Mediastinal Committee of China Anti-Cancer Association for their guidance on this paper. Some content in this article has been presented in speech form by the authors at the 2022 Chinese Congress on Oncology Mediastinal Tumor Conference. This article was submitted to *Mediastinum* as a conference submission.
Funding: None.

Footnote

Reporting Checklist: The authors have completed the CARE reporting checklist. Available at https://med.amegroups.com/article/view/10.21037/med-23-1/rc

Peer Review File: Available at https://med.amegroups.com/article/view/10.21037/med-23-1/prf

Conflicts of Interest: All authors have completed the ICMJE uniform disclosure form (available at https://med.amegroups.com/article/view/10.21037/med-23-1/coif). The authors have no conflicts of interest to declare.

Ethical Statement: The authors are accountable for all aspects of the work and will ensure that questions related to the accuracy or integrity of any part of the work are appropriately investigated and resolved. All procedures performed in this study were in accordance with the ethical standards of the institutional and/or national research committee(s) and with the Helsinki Declaration (as revised in 2013). Written informed consent was obtained from the

patient for publication of this case report and accompanying images. A copy of the written consent is available for review by the editorial office of this journal.

References

1. Wada H, Teramatsu T. Mediastinal tumors--a statistical nationwide report of 1,546 cases between July, 1975 and May, 1979 in Japan (author's transl). Nihon Kyobu Geka Gakkai Zasshi 1982;30:374-8.
2. Shennan T. Histologically non-malignant angioma with numerousmetastases. J Pathol Bacteriol 1914;19:139-54.
3. Davis JM, Mark GJ, Greene R. Benign blood vascular tumors of the mediastinum. Report of four cases and review of the literature. Radiology 1978;126:581-7.
4. Yasuda A, Mizuno A, Mishima A, et al. Posterior mediastinal angioleiomyoma: report of a case. J Thorac Imaging 2007;22:363-5.
5. Yoshino N, Okada D, Ujiie H, et al. Venous hemangioma of the posterior mediastinum. Ann Thorac Cardiovasc Surg 2012;18:247-50.
6. Deepak J, Babu MN, Gowrishankar BC, et al. Mediastinal hemangioma: Masquerading as pleural effusion. J Indian Assoc Pediatr Surg 2013;18:162-4.
7. Odaka M, Nakada T, Asano H, et al. Thoracoscopic resection of a mediastinal venous hemangioma: Report of a case. Surg Today 2011;41:1455-7.
8. Callahan WJ, Simon AL. Posterior mediastinal hemangioma associated with vertebral body hemangioma. J Thorac Cardiovasc Surg 1966;51:283-5.
9. McAdams HP, Rosado-de-Christenson ML, Moran CA. Mediastinal hemangioma: radiographic and CT features in 14 patients. Radiology 1994;193:399-402.
10. Li JL, Liu HJ, Cui YH, et al. Mediastinal hemangiomas: Spectrum of CT and MRI findings - retrospective case series study and systematic review of the literature. Eur J Radiol 2020;126:108905.
11. Park JW, Jeong WG, Lee JE, et al. Pictorial Review of Mediastinal Masses with an Emphasis on Magnetic Resonance Imaging. Korean J Radiol 2021;22:139-54.
12. Zeyaian B, Soleimani N, Geramizadeh B. Posterior mediastinal capillary hemangioma misdiagnosed as neurofibromas: a rare case report and review of the literature. Rare Tumors 2015;7:5639.
13. Kahn HJ, Bailey D, Marks A. Monoclonal antibody D2-40, a new marker of lymphatic endothelium, reacts with Kaposi's sarcoma and a subset of angiosarcomas. Mod Pathol 2002;15:434-40.
14. Maeda S, Takahashi S, Koike K, et al. Preferred surgical approach for dumbbell-shaped tumors in the posterior mediastinum. Ann Thorac Cardiovasc Surg 2011;17:394-6.
15. Chan AP, Wong RH, Wan IY, et al. Video-assisted thoracic surgery excision of mediastinal hemangioma. Asian Cardiovasc Thorac Ann 2009;17:522-4.
16. Cohen AJ, Sbaschnig RJ, Hochholzer L, et al. Mediastinal hemangiomas. Ann Thorac Surg 1987;43:656-9.
17. Xu X, Qin X, Yang B, et al. Surgical management of mediastinal hemangioma: a report of 18 cases. Chinese Journal of Thoracic and Cardiovascular Surgery 2018;34:818-21.

doi: 10.21037/med-23-1
Cite this article as: Xu J, Xu Y, Zhang R. Thoracoscopic resection of a cavernous haemangioma of anterior mediastinum: case report and literature review. Mediastinum 2023;7:30.